New Research Methods for the Analysis of Fossil Anura Ilia and their Utility for Reconstructing the Palaeoenvironment of Swartkrans Cave

Ruan Brand

Supervised by Assoc. Prof. Deano Stynder and Dr Thalassa Matthews

Dissertation submitted in fulfilment of the requirements for the degree of Master of Science (MSc) in Archaeology

Department of Archaeology

University of Cape Town

February 2023

Name: Ruan Brand

Student Number: BRNRUA002

Course: AGE5000W

Declaration

I know that plagiarism is wrong. Plagiarism is to use another's work and pretend that it is one's own.

I have used the …*South African Archaeological Bulletin (SAAB)*… convention for citation and referencing. Each contribution to, and quotation in, this …*Masters dissertation*… from the work(s) of other people has been attributed and has been cited and referenced.

This… *Masters dissertation*… is my own work.

I have not allowed, and will not allow, anyone to copy my work with the intention of passing it off as his or her own work.

Signature Signed by candidate

Date 13-02-2023

Dedication

This dissertation is dedicated to Carol Joy Morris.

Thank you for always lending an ear and genuinely being interested in my peculiar research passions, which in this case were centred around frogs! I wish that I could have completed this project before losing you and getting to call you mom. Your absence will forever be felt, but so will the joy, support, and love that you provided. The lessons that you taught me throughout this process will live with me forever.

Acknowledgements

To my supervisors, Deano and Thalassa, for sticking through with me despite the numerous hurdles. Thank you for having my best interests at heart and for being there for me. I cannot thank you both enough for your input, guidance, and general mentorship throughout this arduous journey. It has been a rough one, but we got there!

To my dearest Ash, my mom, my dad, and my sister. You have all sacrificed so much for me along the way. I am ever grateful for having such a strong support system. Thank you all so much, especially Ash, for being my compass during these times of rough seas. I look forwarding to spending more time with you all, having now gained many new perspectives on what is important in life.

To Lesa and Briege, thank you both for always being there to assist me with my work duties whenever I needed to give more attention to my studies. I could not have asked for better colleagues and am incredibly excited about what lies ahead with us as a team at SAHRA.

To Louisa, thank you so much for always being ready to help me out at the last minute. Your friendship, mentorship, and support over not just this project, but also these last few years, has been amazing.

To Tim, thank you for not only sharing the images of the extra specimens with me, but also for all the late-night e-mails about this weird phase of life that we have found ourselves in.

To Kathy, thank you for providing a workspace for me at Wits and for your support at the start of this study. Your kindness, intelligence, and passion are something remarkable that I am still in awe of.

To Ron, thank you for giving me a unique and intimate view of the hominins of the Cradle.

To the SPRP team and all the students involved in the excavations, thank you for excavating the microfauna material so meticulously. Those careful excavations were critical in making this project possible.

To Vincent and Kerryn, thank you both for your great guidance on my results and the quantitative side of the project.

To Christine, thank you for always dealing with my funding related worries.

To the examiners for their insightful feedback which ultimately improved the quality of how I presented this research, thank you so much for your feedback!

To anybody who played any part in this project, no matter how minor, I apologize if I have not addressed you directly, but I am still ever grateful for the contributions that you have made.

Lastly, I herewith acknowledge the financial support for the first two years of this project from Genus: DST-NRF Centre of Excellence in Palaeosciences.

Abstract

Anura fossils are relatively common amongst microfauna assemblages but remain largely unanalysed because of a lack of expertise. This is unfortunate since Anura are effective indicators of environmental conditions as their life cycles and breeding patterns are integrally linked with temperature and rainfall. These factors, alongside having small home ranges and fast generation turnover, make Anura useful indicators of local climatic/environmental conditions. It has been hypothesized that areas with remnants of woodlands may have played an important role in human evolution by acting as refugia during periods of regional aridity and resource scarcity during the Pleistocene in Africa. In order to test this hypothesis, it is important to develop proxies that can detect these remnants. The archaeological site of Swartkrans Cave, located in the Cradle of Humankind, has yielded many samples of unanalysed Anura fossils, and has also produced the largest known sample of fossils belonging to the early Pleistocene hominin *Paranthropus robustus*, as well as a handful of early *Homo* fossils. In this study, the fossil Anura community of Swartkrans Cave is reconstructed in order to determine whether local environmental conditions were consistent with the idea of a refugium as per results of other studies of the Cradle of Humankind. Fossil assemblages from the Oldowan (Member 1, 2.2 Ma) and Acheulean (Member 3, 960 ka) deposits of Swartkrans Cave were analysed and compared as they provide snapshots of environmental conditions during periods covering the origin and extinction of *P. robustus*. The fossil Anura community indicates that a woodland-hydro-refugium persisted up to at least 960 ka, with the nearby Blaaubank river having been a more significant feature in the past. This analysis focuses on Anura ilia, which have several diagnostic features useful for taxonomic identification. A guide for identifying southern African Anura ilia was recently published, and this study (which presents the first application of this guide) explored the use of additional research methods,

including the application of geometric morphometrics. The guide for identifying southern African Anura ilia proved to be useful, with two specific measurements proving particularly relevant regarding their application to fossil assemblages. Furthermore, this study indicates that the use of Procrustes corrections alongside this guide will greatly assist future researchers with their identifications of southern Africa Anura ilia.

Table of Contents

List of Tables

List of Figures

List of Abbreviations, Acronyms, and Shortenings

Acetabular Breadth = Breadth of the acetabulum below the ilioschiatic junction

CAF = Central Analytical Facilities

cf. = Compare

CT = Computerized Tomography

DAE = Dorsal acetabular expansion

ESI = Evolutionary Studies Institute

H. = *Homo*

ka = Thousand years ago

K-S = Kolmogorov-Smirnov

M1 = Member 1

M1HR = Member 1 Hanging Remnant

M1LB = Member 1 Lower Bank

M1LBEE = Member 1 Lower Bank East Extension

M2 = Member 2

M3 = Member 3

Ma = Million years ago

MNI = Minimum number of individuals

NISP = Number of individual specimens

P. = *Paranthropus*

PAST = PAleontological STatistics

p-value = Probability value

SPRP = Swartkrans Paleoanthropology Research Project

STK = Sterkfontein Cave

SWK = Swartkrans Cave

The Cradle = The Cradle of Humankind

TPH = Turnover-pulse hypothesis

U-Pb = Uranium-lead

VAE = Ventral acetabular expansion

VSA = Angle between the VAE and the anterior margin of the ilial shaft

Wits = University of Witwatersrand

Note that some additional abbreviations, acronyms, and shortenings are used within figures, but these are explained in the titles of the figures.

Chapter One: Introduction

1.1 Using Anura for Paleoenvironmental Reconstructions

The scope of most paleoenvironmental studies is to reconstruct a region's environment, however, the nuances of small variations within that environment are frequently lost. This is especially pertinent with recent research starting to focus on the sheltering role that woodland-and-hydro-refugia may have played in human evolution during periods of high aridity in the Pleistocene in Africa (Caley *et al*. 2018; Cuthbert *et al*. 2017). Studies on Anura have focused on their use as palaeoclimatic proxies as they are found in a variety of habitats globally, have small home ranges, rapid population turnover, and are good indicators of climatic change as they are sensitive to fluctuations in moisture and temperature. Despite some notable exceptions, the majority of Anura also require some form of moisture to reproduce (Altig & Johnston 1989; Crump 2015; Gervasi & Foufopoulos 2008; Roelants *et al*. 2011; Zhang *et al*. 2013). They therefore make for excellent proxies for elucidating micro-environments, and for identifying areas of woodland-and-hydro-refugia. The Cradle of Humankind (the Cradle) reflects a generally desiccating African landscape during the Pleistocene and boasts several sites that have yielded hominin fossil and cultural remains. One such site is Swartkrans Cave (SWK), which has yielded the world's largest collection of *Paranthropus* fossils, some early *Homo* fossils, as well as an abundance of macro-and-microfaunal remains, including many unanalysed Anura fossils. This thesis attempts to use fossil Anura ilia to reconstruct the micro-environment that existed around SWK during the Oldowan (2.2 Ma) and Acheulean (960 ka) cultures, in an attempt to understand what might have drawn early hominins such as *Paranthropus* and *Homo* to the site.

This is achieved through the first application of Matthews *et al*.'s (2019) identification guide to the ilia of southern African Anura. Moreover, as this dissertation is the first application

thereof to a fossil assemblage, measurements used within the guide are evaluated, and suggestions are made for future researchers looking to make similar taxonomic identifications of fossil Anura assemblages. Geometric Morphometrics (GM) is applied to explore whether this analytical method might usefully be applied to future studies. As the evolutionary history of Anura in Africa remains poorly studied (Gardner & Rage 2016), this is important as it has the potential to support future fossil Anura studies.

1.2 Thesis Outline

The remainder of this dissertation is laid out as follows. In chapter two, the literature surrounding this topic is reviewed. Through an exploration of the link between hominin evolution and climate change, ongoing investigations into various aspects of human evolution are presented, highlighting the potential importance that woodland-and-hydro-refugia may have played in a desiccating African Pleistocene. Thereafter, an overview of current paleoenvironmental proxies is provided, with an emphasis placed on those useful for identifying such refugia. The potential for Anura fossils to elucidate palaeoenvironments is then demonstrated by a summary of pertinent, previous research in the area. Finally, a background to the Cradle and SWK is provided, highlighting results from research on other paleoenvironmental proxies.

In chapter three, the materials and methods employed in this dissertation are described, with chapter four summarising results obtained.

In chapter five, the results are placed in context with the background provided in chapter two. Here, an emphasis is placed on the palaeoenvironment surrounding SWK in relation to the rest of the Cradle. The application to the fossil record of some of the measurements suggested in

the new guide are evaluated, with suggestions being made for future researchers. The implications thereof for use on fossil Anura ilia is discussed, then future research implications are presented alongside limitations of this study. The dissertation concludes with a summary of key findings.

Chapter Two: Background

2.1 African Pleistocene Climate Change and Hominin Refugia

One of the most intriguing areas of research in the field of human evolutionary studies focuses on the reconstruction of climatic and environmental conditions under which our ancestors evolved (Potts 2013). Most evidence of early hominins are found in East Africa, which has been a focus of research as a result (Donges *et al*. 2011). In her seminal work, Vrba (1974, 1975) proposed that from 5 Ma onwards, Africa experienced aridification, which led to the spread of grasslands and the retraction of woodlands. Later, Vrba (1985 in 1993) proposed the turnover-pulse hypothesis (TPH), stating that during major global cooling 2.8 Ma, mammals, including hominins, would have gone through a period of expedited extinctions and radiations, resulting in rapid habitat change and hence turnover of species. There has been much debate in this regard, as more recent species lists and chronologies, shows a lack of overlap with the timing of the 'turnover-pulse' (Faith & Behrensmeyer 2013). Nevertheless, the TPH provides a theoretical framework with which to explain how climate change drove human evolution.

Geological evidence indicates that climate variability increased globally around 6 Ma, and by 3 Ma this variability became even more pronounced, with evidence from the Mediterranean suggesting that Africa was especially vulnerable to wet and dry cycling over that time (Peter 2004). Adaptations started to appear in the hominin fossil record from 6 Ma, starting with traits like bipedalism, then over the next millions of years, enlarged cranial capacity, increased omnivory, and improved manual dexterity, among others. Our genus, *Homo*, made its first appearance during the more pronounced climatic variability after 3 Ma in Africa, which is the time period that coincides with the first undisputed evidence of stone tools (Schick & Toth 2006).

By 3 Ma, the global climate cooled, the world became drier, and climate cycling experienced increased maxima and minima (Philander & Federov 2003). Generally, in Africa, grasslands thrived under these conditions and started expanding more rapidly, encroaching on, and reducing, the areas occupied by woodlands. It is also during this time that the hominin lineage diversified rapidly, with *Australopithecus garhi*, *Homo rudolfensis*, *H. habilis*, *Paranthropus robustus*, and *P. boisei* appearing in the fossil record (Asfaw *et al*. 1999; Carruthers 2019; Wood & Baker 2011; Wood & Constantino 2007). From a cultural perspective, the first undisputed stone tools (dated to 2.6 Ma and assigned to the Oldowan industry) were discovered, dating to just after the onset of this increased climate variability (Schick & Toth 2006). This time period therefore includes a dramatically fluctuating climate that also sees many new species of hominin evolving, and the first undisputed evidence of material culture.

By 2 Ma, the climate in South and East Africa became warmer and wetter, with woodlands expanding once more, and grasslands retracting slightly (Caley *et al*. 2018; Cerling *et al*. 2011). This period coincides with the deposition of many specimens of *P. robustus* in South Africa in the Cradle of Humankind (the Cradle), with these predominantly being found at SWK. These hominins exhibit morphological adaptations for eating hard foods, such as large teeth and sagittal crests, and had arched feet similar to those of modern humans (Peterson *et al*. 2018; Ryan *et al*. 2018). However, studies looking into the diets of *P. robustus* have shown that these probably varied seasonally between grassland and woodland resources (Constantino *et al*. 2018; Lee-Thorp *et al*. 2000; Sponheimer *et al*. 2006; Steininger 2011) with their pelvic structure favouring an arboreal lifestyle, like earlier *Australopithecines* (Grine & Susman 1991). Moreover, *Au. sediba*, from the Cradle of Humankind at Malapa, dated to 1.8 Ma, exhibits increased cranial capacity and well-articulated hands, also generally better adapted to an arboreal lifestyle (Churchill *et al*. 2018; Kivell *et al*. 2011). *H. ergaster* starts to appear in the fossil record as early as 1.9 Ma in East Africa, and spread throughout Asia, Eastern Europe

and southern Africa, existing intercontinentally for about 1.5 million years, with several *H. ergaster* fossils found in the Cradle (Ferring *et al*. 2011; Herries *et al*. 2020; Tattersall 2007; Zhu *et al*. 2018). They exhibit adaptations that are closer to those of *H. sapiens* than previous hominins, such as a large cranial capacity, obligate bipedalism, and intentional fire use by at least 1.7 Ma (as evidenced at Wonderwerk cave in South Africa [Beaumont 2011]). Lastly, as early as 1.6 Ma, they are linked to the onset of the Acheulean industry, which sees cleavers and classical biface hand axes appearing in the fossil record (Lycett & Gowlett 2008). This technological suite followed *H. ergaster*'s exodus from Africa, and in combination with *H. ergaster*'s ability to confront new environments, shows a level of adaptability very close to that of *H. sapiens*.

By 800 ka, the greatest climate fluctuations started occurring, with *P. robustus* and *H. ergaster* disappearing from the fossil record. The assumption is that *P. robustus,* being more adapted to an arboreal lifestyle, relied on the refugia provided by woodlands when grasslands expanded throughout Africa (Caley *et al*. 2018). There would be some reprieve during climatic fluctuations, when woodlands would expand and grassland retract, allowing regional spread, but eventually, the grassland pressure drove them into smaller, isolated pockets, most likely leading to extinction (Caley *et al*. 2018). This is in contrast to *H. ergaster,* which is believed to have eventually evolved into *H. heidelbergensis,* and like their ancestors, also spread across the globe, eventually expanding into the cold climate of north-western Europe (Stringer 2012). They are morphologically closer to humans than previous hominins and have a larger cranial capacity. Humans, as well as some of our more recent evolutionary cousins, such as *H. neanderthalensis*, are generally believed to have descended from *H. heidelbergensis* (Stringer 2012). By around 350 ka, the Earth experienced an elongated orbit which led to long periods of fluctuation between high aridity and high moisture. It is at this time, that the earliest members of our species, *H. sapiens*, start to appear in the fossil record (Campisano 2012).

It is therefore evident, that changing climatic conditions coincide with important times and possible 'pulses' in human evolution as proposed by Vrba (1985 in 1993) through her TPH. However, during periods of major pulses, when speciation of the hominin lineages occurred, smaller woodland refugia may have played a critical role in ensuring the survival of species like *P. robustus* (Caley *et al*. 2018). It is thus important to unpack what the climatic and resultant environmental conditions were in these refugia in order to ascertain if, and how, they supported some hominin lineages. This is especially important for understanding what conditions led to the extinction of some hominins, like the *Paranthropus* genus, yet the success of other hominins, such as our own genus, *Homo*. To deduce palaeoenvironments and trace palaeoclimatic change we require paleoenvironmental proxies.

2.2 Paleoenvironmental Proxies

Researchers utilise several proxies to reconstruct palaeoenvironments. Gornitz (2009) provides a broad overview of these and groups the indicators into three categories based on the proxy type utilised: Lithological/mineralogical, geochemical, and palaeontological. The method utilised when employing an indicator to reconstruct a palaeoenvironment is dependent on the scale and type of information required. For example, if a study's aim is to determine whether a deposit had a woodland (C_3 pathway) or grassland (C_4 pathway) type of environment at the time of deposition, then one possibly suitable paleoenvironmental proxy to utilise is the analysis of the isotope ratio of $\delta^{13}C$. However, preservation and availability of suitable material plays a pivotal role in determining which indicators to utilize (Gornitz 2009). It is therefore important to understand what proxies are available for researchers to employ, what their limitations are, and which have proven most successful in reconstructing palaeoenvironments that are relevant for tackling questions about human evolution.

Lithological and mineralogical indicators speak to what rock and mineral formations can reveal about paleoclimates and paleoenvironments. They are usually sedimentary-based and rely on having formed near the Earth's surface, capturing data on the environment and/or climate at their time of formation (Gornitz 2009). Geochemical indicators make use of isotope ratios, trace elements, as well as organic matter, providing a quantitative method for the purpose of paleoenvironmental reconstructions as different climate and/or environments would have different measurable amounts of certain chemicals (Gornitz 2009).

Palaeontological indicators make use of preserved faunal and/or floral remains through methods such as morphological adaptation analysis, but predominantly through the nearest living relative approach (Gornitz 2009). The nearest living relative approach stems from taxonomic uniformitarianism, which posits that a fossil taxon would have occupied the same habitat that its living counterpart would occupy today, be it an animal or a plant. This principle, although coming with certain provisions (which are unpacked later), provides a powerful framework for paleoenvironmental reconstruction (Reed 1998).

Indicators may overlap. For example, speleothems preserve data on $\delta\,^{18}O$ ratios which is a parameter that can be used as a proxy for palaeotemperatures, and they also preserve data on $\delta^{13}C$ ratios, a parameter that can be used as a proxy for vegetation shifts (Vaks *et al*. 2006; Wang *et al*. 2008). For a more comprehensive summary of the different indicators and parameters see Gornitz (2009). This dissertation focusses on the most relevant indicators pertaining to archaeological studies.

The earliest paleoenvironmental reconstructions employed in archaeological excavations involved the analysis of faunal remains through the nearest living relative approach. Early researchers relied on the Bovidae, as their fossil remains were often found in direct association with hominin remains, and/or cultural material, and their modern counterparts are found in a

variety of habitats. This means that they can be used to reconstruct a wide range of environments which are directly linked to snippets of time in human evolution (Reed 1998; Sponheimer *et al*. 1999). Faunal reconstructions expanded to include other faunal groups, mainly consisting of avian taxa, and small mammals (Avery 2007). A reliance on taxonomic uniformitarianism came under critique however, when research revealed that ecological preferences of taxa could change, meaning that the habitat occupied by a modern taxon might differ to the habitat occupied by its fossil counterpart. Moreover, unresolved taxonomic issues might result in the incorrect identification of fossil taxa, and the nearest living relative approach did not incorporate variations in behaviour, or take into account the inherent plasticity, and potential adaptations made by fossil counterparts (Matthews *et al*. 2020; Domínguez-Rodrigo & Musiba 2010; Semprebon & Rivals 2007).

There are, however, taxon-independent methods that seek to address behavioural change or adaptations in the fossil record, thereby overcoming this issue. The most prevalent of these include the analysis of dental micro-and-meso-wear (Merceron *et al*. 2006; Stynder 2011), the analysis of ecomorphological adaptations of limb bones (DeGusta & Vrba 2003), as well using isotope ratios in teeth enamel (Merceron *et al*. 2006). Although these methods have proven reliable and useful, they rely on long-term spatiotemporal averaging of environmental conditions. This is because, specifically for large animals, such as bovids, they have large home ranges and seasonal migration patterns (Sponheimer *et al*. 1999). Their indicators would therefore reflect a variety of environments, sampled over time, meaning that although the general environment may be gleamed from these proxies, the niche 'micro-paleoenvironments' that would have attracted a hominin to one area but not another, would not be reflected. This is especially important as research has shown that despite the onset of the rapid spread of grasslands in Africa 3 Ma, hominins most likely spent time in refugia, close to reliable water sources, particularly during arid periods (Cuthbert *et al*. 2017). These refugia would have

distinct environments that differ to those in the general region. As microfaunal taxa have considerably smaller home ranges, and higher generational turnover, researchers have used them to reconstruct the palaeoenvironments of such refugia as they assist in giving a spatio-temporal snapshot of these 'micro-paleoenvironments' (Avery 2007; Williams *et al*. 2020).

The analysis of micro-mammal teeth has received the most attention in this regard. To inform on paleoenvironmental conditions, the method involves additional analyses, such as the change in size over time of certain taxa's dental features, or changes in diversity of the micro-mammal taxa in the deposit (Avery 2001, 2007; 2021; Faith *et al*. 2019; Comay & Dayan 2018; Matthews *et al*. 2011, 2020; Nel *et al*. 2018). Other micro taxa-based methods rely on identification of the taxa, such as with avian-based studies (Olsen & Rasmussen 1986; Pavia 2020), or Anura-based studies (Blain *et al*. 2008, 2013, 2014; Delfino 2020; Matthews *et al*. 2015, 2016; Sampson 2003). These methods have provided useful paleoenvironmental information, however, they are susceptible to the above-mentioned issues that underlie taxonomic uniformitarianism. Moreover, taphonomic and taxonomic bias may result from the manner in which the microfaunal fossil assemblages originated, and accumulated, in the fossil deposits. If they originate as the result of predation, for example, they may initially become associated with the site in the form of a regurgitated owl pellet, and predator behaviour regarding issues such as prey selection (predator and prey size is related, and certain predators have strong taxonomic preferences), hunting behaviour, and so on, will influence the taxonomic composition of the assemblage, and this will also affect the degree of preservation of the bones or teeth at the time of their deposition, and their resistance to post-depositional damage (Comay & Dayan 2018; Matthews *et al*. 2011).

Furthermore, preservation is a major concern for many proxies. It is therefore important to understand that preservation bias might play a role in the taphonomy as some parameters may not be captured during deposition or may be destroyed before being studied. Pollen is an

example of a proxy that can be used to elucidate vegetation but is generally poorly preserved in humid environments (Meadows *et al*. 2010). The fossil record can, similarly, be incomplete, or sometimes contradictory, so it is imperative to use multiple indicators/proxies when researching palaeoenvironments.

This multiproxy approach has built on our understanding of the incomplete African paleoenvironmental record, with new and specialised proxies being developed, such as the use of *Hyrax* middens (Chase *et al*. 2009). The multidisciplinary and multi-proxy approach has been successfully utilized to elevate our understanding of human evolution in East Africa at the sites of Olduvai Gorge in Tanzania, and the Turkana Basin in Kenya/Ethiopia (Vincent 2021). Multiproxy approaches in southern Africa were comparatively rare in the past, with most site investigations usually relying on a single, or limited number of indicators to reconstruct the palaeoenvironment. Nevertheless, more recent research in southern Africa has made strides in improving this as multidisciplinary studies are becoming the norm, with multi-proxy approaches to reconstructing the palaeoenvironment occurring at most of the major archaeological and paleoanthropological sites (Jacobs *et al*. 2020; Marean *et al*. 2020; Sobol *et al*. 2022; Strobel *et al*. 2021; Wurz *et al*. 2018). Moreover, researchers are continually exploring potential new proxies towards this end, and one such proxy is the use of Anura.

2.3 Anura as Paleoenvironmental Proxies

2.3.1 Anura life history

The order Anura emerged sometime between the Permian and the early Triassic around 244 Ma (Zhang *et al*. 2013) and represents the most diverse group of amphibians, exhibiting adaptations based on geography, reproduction, and anatomy (Frost 2022). Today, Anura are

distributed on all continents except for Antarctica, although two fossils dating to the early Cenozoic, ca. 40 Ma, shows that they were, in the past, also found there (Mörs *et al*. 2020). Their habitats vary immensely today, ranging from arid deserts to wet rainforests, and they possess diverse and unique behavioural and morphological adaptations, allowing them to survive in a large variety of ecological niches (Roelants *et al*. 2011; Zhang *et al*. 2013).

Amphibians have a biphasic life history that begins with a free-living larval stage known as a 'tadpole'. This phase commences after their eggs hatch. The duration of the tadpole phase is dependent on a variety of factors that act to maximise growth while minimising mortality. Generally, the tadpole phase of Anura involves a short period of endotrophy (consuming nutrients from parental supplied yolk) and is followed by exotrophy (consuming nutrients found in the environment) wherein the larva utilises swimming as its main form of locomotion (Altig & Johnston 1989). They then metamorphose into the adult phase and are then referred to as frogs and/or toads (Altig & Johnston 1989; Crump 2015; Gervasi & Foufopoulos 2008; Roelants *et al*. 2011). There are however five notable exceptions to this. There are four taxa that give birth to live frogs, or tadpoles that do not feed; namely the critically endangered Puerto Rican species *Eleutherodactylus jasperi* (Drewry & Jones 1976), the east African genus *Nectophrynoides* (Wake 1980), the west African genus *Nimbaphrynoides* (Sandberger *et al*. 2010), and some members of the genus *Breviceps* of southern Africa (Minter 1999). The Indonesian species *Limnonectes larvaepartus*, is the only frog currently known to give birth to live tadpoles (Iskandar *et al*. 2014). For the majority of frog taxa, some form of moisture is required to enable the exotrophic larval phase to attain nutrients via swimming.

However, this moisture dependency is not unique to the tadpole phase. Most adult frogs and toads are bound to environments where they can access moisture because they require their skin to be moist in order to respire and inhibit desiccation, and/or it may be a necessity for breeding (Tracy *et al*. 2010). However, there are several species that require only a minimal

amount of moisture as they exhibit special adaptations to reduce water loss, and to cope with aridity. For example, the crucifix toad *Notaden bennettii* of eastern Australia (Heatwole *et al*. 1971) burrows into the ground to prevent desiccation, and only emerges when temporary ponds are available to breed, as does *Pyxicephalus*, the African bullfrog (Yetman & Fergusion 2011). The waxy monkey tree frog *Phyllomedusa sauvagii* of South America has secretions which reduces water loss considerably, and they breed during the rainy season with their hatching tadpoles dropping into water from eggs laid on leaves which overhang water (Archibald *et al*. 2015). In southern Africa the desert rain frog (*Breviceps macrops)* of Namibia, lives in a small, 2000km^2 stretch on the coastline, relying mainly on moisture from fog coming off the ocean to keep its skin moist (Channing 2011). Other special adaptations, such as laying eggs underground and secreting a special jelly to keep them moist, also aid in inhibiting desiccation (Minter 1999). Such specialised adaptations enable Anura to occupy a variety of different habitats, even in highly arid regions, such as southern Africa during the Pleistocene.

2.3.2 Anura in the global archaeological fossil record

A current understanding of Anura taxonomy is provided by Frost (2022). There are 56 families recognised worldwide, of which fourteen occur in the southern African region (that is Angola, Botswana, Eswatini, Lesotho, Malawi, Mozambique, Namibia, South Africa, Zambia, and Zimbabwe), comprising 45 genera, and 305 species (Frost 2022). Table 2.3.1 provides an overview of the habitats of 39 of the southern African genera which are the genera described in the work of Matthews *et al*. (2019). Although the Anura of this region appear in literature from as early as the 18th century, with Linnaeus (1758) describing some taxa, Gardner and Rage (2016) caution that our understanding of both Anura evolution and biogeography in this region still remains extremely poor. This is attributed to the small amount of Anura fossils that

predate the Pleistocene, as well as a shortage of both experts and comparative skeletal Anura collections (Matthews *et al*. 2019). Despite this, research pertaining to Anura, as well as the utilisation of Anura for reconstructing past environments and climates in southern Africa, is an ever-growing area of research (Delfino 2020; Matthews *et al*. 2015, 2016, 2019; Sampson 2003). This is especially becoming more accessible with Matthews *et al*. (2019) publishing an identification guide to southern African Anura ilia.

Table 2.3.1. *The modern habitats occupied by the 39 Anura genera of southern Africa utilised by Matthews et al. (2019).*

Family	Genus	Common name	Number of species in genus (Frost 2022)	Taxon coincides with this habitat*
Microhylidae	*Phrynomantis*	Rubber frogs	5	Dry savanna and grasslands/floodplains
Arthroleptidae	*Arthroleptis*	Leaf-litter frogs	49	Forests only
Arthroleptidae	*Leptopelis*	Tree frogs	54	Forests and southern African species tend towards subfossorial/dry savanna environments
Arthroleptidae	*Trichobatrachus*	Hairy frog	1	Forests only
Phrynobatrachidae	*Phrynobatrachus*	Puddle frogs	95	Highly varied
Hemisotidae	*Hemisus*	Shovelnose frogs	9	Subfossorial but mainly dry savanna and grasslands/floodplains
Breviceptidae	*Probreviceps*	Forest rain frogs	6	Forests only
Breviceptidae	*Breviceps*	Rain frogs	20	Generally subfossorial but highly varied
Ranidae	*Amnirana*	White-lipped frogs	11	Generally forests, but highly varied
Rhacophoridae	*Chiromantis*	Foam-nest frogs	4	Dry savanna and grasslands/floodplains and sometimes dry woodlands

Hyperoliidae	*Afrixalus*	Leaf-folding frogs	33	Generally forests, but highly varied as long as the environment has high ambient moisture levels
Hyperoliidae	*Cryptothylax*	Bush-frogs	2	Generally forests, but requires high ambient moisture levels
Hyperoliidae	*Hyperolius*	Reed frogs	145	Highly varied
Hyperoliidae	*Kassina*	Running frogs	15	Generally forests, but can be varied
Hyperoliidae	*Kassinula*	*K. wittei*	1	Moist savanna/grassland floodplain
Hyperoliidae	*Phlyctimantis*	Bush-frogs	5	Forests and moist savanna
Hyperoliidae	*Semnodactylus*	Weale's running frog	1	Grasslands and fynbos
Pyxicephalidae	*Amietia*	River frog	16	Anywhere that has running water (streams, rivers, etc.)
Pyxicephalidae	*Anhydrophryne*	Moss frogs	3	Forests and high ambient moisture level grasslands
Pyxicephalidae	*Arthroleptella*	Moss frogs	10	Fynbos
Pyxicephalidae	*Cacosternum*	Dainty frogs	16	Highly varied
Pyxicephalidae	*Microbatrachella*	Micro frog	1	Fynbos – specifically only around cape reeds (critically endangered)
Pyxicephalidae	*Natalobatrachus*	Natal diving frog	1	Forests and requires rivers
Pyxicephalidae	*Nothophryne*	Mongrel frogs	5	Forests and requires rocks around rivers/streams
Pyxicephalidae	*Poyntonia*	Montane Marsh frog	1	Only montane fynbos with high ambient moisture levels
Pyxicephalidae	*Pyxicephalus*	Bull frog	4	Subfossorial in dry savanna/grassland/ floodplains
Pyxicephalidae	*Strongylopus*	Stream frogs	10	Anywhere riparian (mainly fynbos/flooded grassland)
Pyxicephalidae	*Tomopterna*	Burrowing frogs	16	Anywhere with some wet soils -

Ptychadenidae	*Hildebrandtia*	Burrowing frogs	3	dry/moist savanna/grassland Subfossorial in dry savanna
Ptychadenidae	*Ptychadena*	Grass frogs	59	Highly varied, but generally grasslands and forest edges
Pipidae	*Xenopus*	Clawed frogs	35	Entirely aquatic, but highly varied as long as there is water
Heleophrynidae	*Hadromophryne*	Natal ghost frog	1	Needs permanent streams/rivers – generally forests and grasslands
Heleophrynidae	*Heleophryne*	Ghost frogs	6	Fynbos and permanent water required
Bufonidae	*Capensibufo*	Mountain toadlets	5	Fynbos
Bufonidae	*Mertensophryne*	Forest toads	14	Generally forests, but can be varied
Bufonidae	*Poyntonophrynus*	Pygmy toads	11	Generally grasslands
Bufonidae	*Schismaderma*	African red toad	1	Savanna and grasslands
Bufonidae	*Sclerophrys*	African true toads	44	Highly varied, but generally needs high ambient moisture levels
Bufonidae	*Vandijkophrynus*	Van Dijk's toads	6	Grasslands, some fynbos, but needs rocks near water

*The habitat information is sourced from Channing and Rödel (2019) and Carruthers and Du Preez (2017).

At the 5.1 Ma Early Pliocene paleontological site of Langebaanweg, on the west coast of South Africa, Matthews *et al*. (2015) analysed the fossils of 19 Anura taxa. These fossils contradicted the results of previous studies which suggested that aridification of the west coast had already begun at this time (Matthews *et al*. 2015, 2016). Moreover, one of the identified Anura genera, namely *Ptychadena*, allowed for a more detailed picture to be constructed of the seasonality of the rainfall pattern, since modern *Ptychadena* are only found in summer rainfall zones (Matthews *et al*. 2016). Up until this study, all other studies assumed that at the time of the formation of the Langebaanweg fossil site, the area had already developed its modern-day

winter rainfall regime (Franz-Odendaal *et al*. 2002; Rossouw *et al*. 2009) which the discovery of a *Ptychadena* fossil disputed. The presence of the frog fossils thus provided novel information on rainfall seasonality, something other faunal studies had been unable to do.

Additionally, this Anura based, high-resolution palaeo-freshwater proxy has been utilised to identify specific types of water bodies in southern Africa. On the west coast of South Africa, at the Middle Pleistocene archaeological site of Duynefontein 2 (DFT2), Sampson (2003) identified an Anura community that consisted predominantly of *Ranidae* and *Pipidae*. These taxa are only able to survive in freshwater bodies of approximately one meter deep. This observation, along with the low numbers of burrowing Anura taxa, and the presence of concentric bands of frog bones (possibly a result of surface wavelets) in the excavation, suggest that an interdunal pond existed at the locality at time of site formation. This is significant, as historically the area boasts no bodies of fresh water nearby, yet around 300 ka, the area managed to support several large animals, such as the extinct long horned buffalo (*Syncerus antiquus*) and African elephant (*Loxodonta africana*), as well as hominins, indicated by stone tools accumulated at the site (Cruz-Uribe *et al*. 2003). The presence of some form of perennial waterbody was noted through earlier studies via the identification of animals that would have required a large amount of water over a longer period of time to support them, such as hippopotamus (*Hippopotamus amphibius*) and southern reedbuck (*Redunca arundinum*) (Klein *et al*. 1976, 1999). However, these proxies lacked the higher resolution data that the Anura provided, because they could only indicate some form of waterbody, whereas the Anura contributed further details, such as the type and depth.

The strength of Anura in reconstructing paleoenvironments has been utilised in other parts of Africa as well. At the 4.1 Ma site of Kanapoi in Kenya, Delfino (2020) identified several Anura species, and used these to reconstruct the palaeoenvironment of the area at that time. With the predominant taxa being the head-first burrowing ‘shovel-nose’ frog genus, *Hemisus*, Delfino

(2020) identified the area as having been predominantly grassland or relatively dry, open low tree-shrub savanna. This contrasts with the only other study to have attempted to reconstruct the palaeoenvironment in the area for that time period. Schoeninger *et al*. (2003) used tooth-enamel isotope ratios of browsers and grazers at the nearby site of Allia Bay, which is dated to 3.9 Ma. They found the data to be consistent with a woodland environment, although Schoeninger *et al*. (2003) suggest the presence of grasslands alongside the woodlands, indicated by the presence of the grazing suid *Phacochoerus*. This area and time period is important as the early bipedal hominid, *Australopithecus anamensis*, was found at both sites (Schoeninger *et al*. 2003).

Anura have also been utilised for the reconstruction of palaeoenvironments of hominin bearing sites outside of Africa. Blain *et al*. (2014) analysed Anura, amongst other microfauna, to reconstruct the paleoclimate of the oldest 'Out of Africa' early Palaeolithic site of Dmanisi in Georgia. Dated to 1.8 Ma, the Dmanisi deposits have yielded over 40 hominin remains, as well as tools and other fossils. The question of what would have drawn early hominins to this area has prompted research into the area's palaeoclimate and environment. The work of Blain *et al*. (2014) suggested an arid environment with water stress events for early hominins living in the area. These reconstructions, which were initially based on Anura, were further refined by Blain *et al*. (2022), by adding Geographic Information System and occupied area distribution techniques to estimate monthly temperature and rainfall reconstructions. This allowed for a more precise reconstruction of the environment of the area, such as it being characterised by Mediterranean forests, woodlands, and shrubs and having a six-month dry period from May to October. This initial use of Anura, and then it being used to elucidate monthly conditions through multidisciplinary work, also reaffirms the notion of the spread of arid environments during the expansion of early *Homo* out of Africa.

Anura, amongst other herpetofauna, have been utilised to reconstruct the paleoenvironments of Barranco Leon, and Fuente Nueva 3 in Spain, sites which have yielded some of the earliest evidence of *Homo* presence in Western Europe around 1.4-1.2Ma (Sánchez-Bandera *et al*. 2020). These were analysed with the habitat weighting method (Blain *et al*. 2008), which relies on the modern-day distributions of taxa found in the deposits to reconstruct palaeoenvironments. The study showed that the Anura, amongst other herpetofauna, within the different deposits from both sites reflected the highly oscillating climatic conditions that became prevalent globally around that time. This shows the precision with which Anura may reflect palaeoclimatic changes between deposits from the same sites and areas.

Anura have also been utilised to support the notion that the decline of woodlands in Europe was a driver in the extinction of Neanderthals. Blain *et al*. (2013) studied Anura from Gorham's Cave in Gibraltar, which is a site known for preserving the last presence of Neanderthals on the Iberian Peninsula followed by the start of human presence there. The Anura were used to determine that there was a decrease in rainfall at the time, and to propose that this decrease in rainfall would have resulted in the decline of woodlands, making Neanderthals vulnerable to habitat loss.

As the above testifies, over the last decade, Anura have proven to be a powerful reconstruction tool for paleoenvironments and climates, including challenging Pliocene paleoenvironmental and climate reconstructions at Langebaanweg and Kanapoi, reaffirming the belief that arid environments were linked to the spread of early hominins, and potentially to the demise of the Neanderthals. Although Anura represent a relatively new method of tackling paleoenvironmental and climate reconstructions, they have proven to work in a variety of contexts and have provided valuable insights into the changing environmental conditions linked to human evolution.

2.4 The Cradle of Humankind and Swartkrans Cave

2.4.1 Palaeoenvironment of the Cradle

The Cradle yields one of the richest and most diverse hominid fossil concentrations in the world, spanning across at least 15 sites (Fig. 2.4.1). For hominin presence to have become embedded in the fossil record, the area must have consisted of an environment that would favour preservation, and also drew hominins to it. Much research in the Cradle has focused on trying to understand what these attractions were.

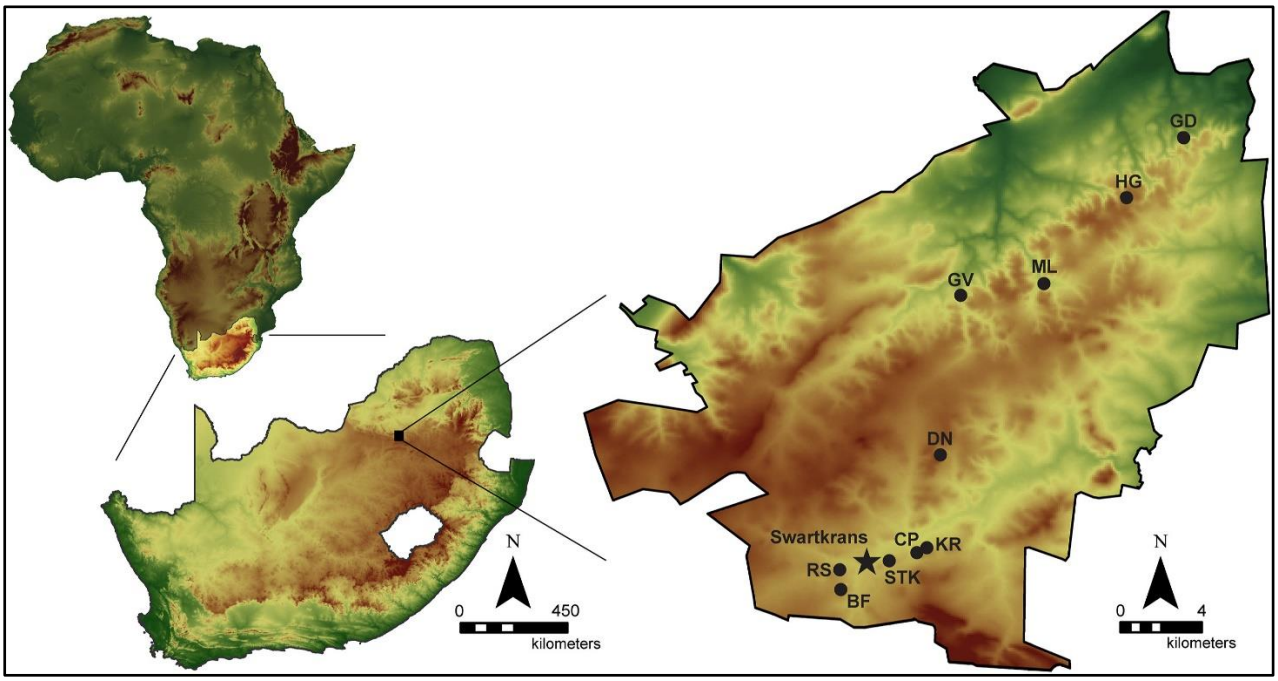

FIG. 2.4.1. *The location of SWK in South Africa in relation to some of the other archaeological sites in the Cradle. BF = Bolt's Farm; CP = Cooper's Cave; DN = Drimolen; GD = Gondolin; GV = Gladysvale; HG = Haasgat; KR = Kromdraai; ML = Malapa; STK = Sterkftontein; RS = Rising Star (sites not shown are Minnaar's Cave, Motsetse, Plover's Lake, and Wonder Cave). From Kuman et al. (2021, page 2, Fig. 1).*

The main problem with paleoenvironmental reconstructions based on deposits from the Cradle is that there have been issues with finding suitable material to date (Herries & Shaw 2011; Granger *et al*. 2015; Kramers & Dirks 2017) and there is thus still debate surrounding the depositional context of the karst cave systems. Pickering *et al*. (2019), through a Uranium-lead (U-Pb) isotope analysis of speleothems, claim that during wet periods, most of the cave sites in the Cradle would have been closed off, meaning no deposits would have accumulated during interglacial periods. This implies that sampled cave deposits would have accumulated during more arid, glacial periods, and that the faunal remains entombed in these deposits would derive mainly from animal communities adapted to open, arid environments. However, Stratford *et al*. (2020) have disputed this claim as they consider that it ignores important contexts, such as the omission of fossil evidence from Sterkfontein Cave (STK) indicating accumulation during wetter, interglacial periods, and this misrepresents the complexity of karst cave systems. Hopley *et al*. (2021) have also questioned the use of the Kernel Density Estimator tool utilised by Pickering *et al*. (2019) to identify six wet-phase peaks used in their argument, however, Pickering *et al*. (2021) claim that their argument still holds with the omission of the results of the Kernel Density Estimator tool. Despite the unresolved issue of the depositional context of the Cradle sites, and a seemingly ongoing debate, many paleoenvironmental studies have been carried out and serve as a baseline for reconstructing the environments of the Cradle over the last 3 million years.

To reconstruct the environments that existed over the time span during which hominins lived in the Cradle, researchers have utilised proxies, ranging from geochemical (Leichliter *et al*. 2017; Lee-Thorp *et al*. 1994, 2007; Sponheimer *et al*. 1999, 2006), to fossil fauna and flora (Avery 2001; Bamford 1999; Brophy 2004; Brophy *et al*. 2016; Pavia 2020; Reynolds & Kibii 2011; Sewell *et al*. 2019; Vrba 1974, 1975). Although there is some disagreement amongst the interpretations and results of these proxies, there is at the very least a general consensus.

Presently, the Cradle's environment consists of a predominantly highveld grassland with 650-750 mm of rainfall per annum (Avery 2001; Holland & Witthüser 2009). The palaeoenvironment of the Cradle differs from this, generally showing a slightly more humid environment from 3-2 Ma, and then the decline of woodlands and the spread of open grasslands and savannahs from 2 Ma to 800 ka (Sewell *et al*. 2019).

Avery's (2001) analysis of microfaunal taxa from STK and SWK suggested an annual precipitation of only 310-550 mm between 2 Ma and 1 Ma, as well as a widespread savanna-grassland environment. Avery (2001) also mentions a riverine habitat near the two sites and postulates that microfauna taxa differ between the sites potentially as a result of predation patterns being different with these two sites being on opposite sides of the Blaaubank river. Moreover, Avery (2001) states that the types of microfauna taxa observed would coincide with interglacial conditions. This contrasts with the interpretation of Pickering *et al*. (2019) that fossils only accumulated during glacial periods. There is however a cautionary note with reconstructing a greater region's environment using microfaunal taxa. Leichliter *et al*. (2017) explain that such taxa occupy smaller habitats within a larger habitat, and this can lead to inconsistencies when considering the broader environment. Leichliter *et al*. (2017) also investigated microfaunal taxa from the Cradle, but instead of employing a faunal based, nearest living relative approach, they employed a geochemical proxy by analysing the stable carbon isotope values on the enamel of small mammal teeth. They report that in the 1.8 Ma deposit of SWK, their results are skewed towards a closed woodland environment because of the dominance of a wetland specialist, *Otomys* (vlei rat). This contrasts with the results of Avery (2001), who also noted the presence of *Otomys*. These studies show that although the same type of material was used, different analytical methods resulted in different conclusions. This therefore reiterates the need for multiple palaeo-proxies to be used to establish a more comprehensive view. A good site to use in this regard is SWK.

2.4.2 Swartkrans Cave

SWK is located among the southern cluster of archaeological sites in the Cradle, around the Blaaubank river. The site lies on a hill and overlooks STK, which is just over 1km away (Fig 2.4.2). SWK has received much attention, starting with Robert Broom and John Robinson in the late 1940's, to Bob Brain systematically excavating the site for more than 20 years from 1965 to 1986 (Kuman *et al*. 2021). The most recent excavations started in 2005 with the Swartkrans Paleoanthroplogy Research Project (SPRP) and are still ongoing. The site is known for having shown that early *Homo* and *P. robustus* co-existed, with excavations also having yielded around 30 *P. robustus* bones and numerous unassigned hominin bones. Multiple stone tools from the Oldowan, as well as bone tools have also been excavated at SWK (Kuman *et al*. 2021).

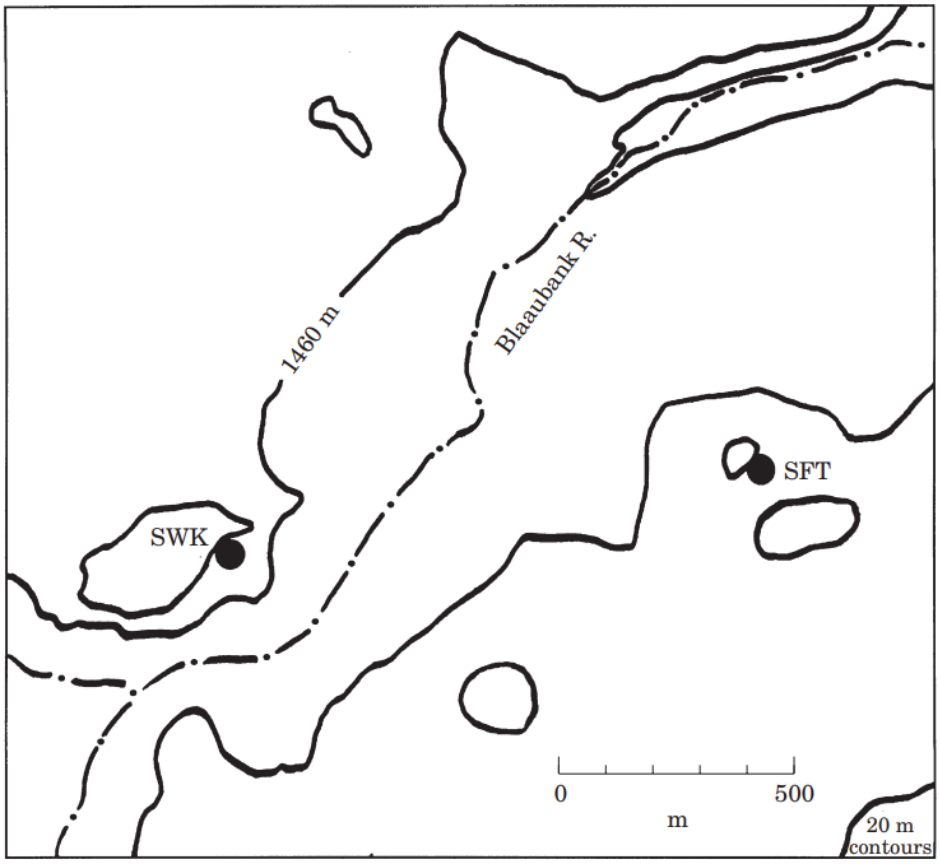

FIG. 2.4.2. *SWK in relation to STK (SFT in the image). From Avery (2001, page 115, Fig. 1).*

To understand what the human evolution implications of the paleoenvironmental reconstructions around SWK are, it is important to unpack the depositional history of the site. Although there are five members in the SWK formation, only Members 1, 2, and 3 are touched on here as Members 4, and 5 were deposited during the MSA and LSA respectively. The oldest member, Member 1 (M1), consists of three subunits, M1 Lower Bank (M1LB), M1LB East (M1LBEE), and M1 Hanging Remnant (M1HR). The former has the same depositional history and are only differentiated because M1LBEE was uncovered during much later excavations. These units consist of sandy silt, and contain fossils and artefacts. Dating of M1LB/M1LBEE started with rough estimates based on faunal composition (Vrba, 1985 in 1993) at 1.5-1.8 Ma but in recent times, this has seen greater refinement due to the improvement of dating techniques and technologies. M1LB/M1LBEE has been dated directly by cosmogenic nuclide burial to 1.8-2.2 Ma (Gibbon *et al*. 2014) and more recently using the Isochron method to 2.22 Ma (Kuman *et al*. 2021). Kuman *et al*. (2021) elaborate on this date, indicating that the M1LB/M1LBEE must have accumulated rapidly because of the proximity of the date to Pickering *et al*.'s (2019) U-Pb age of 2.25 Ma for the basal flowstone that underlies this layer.

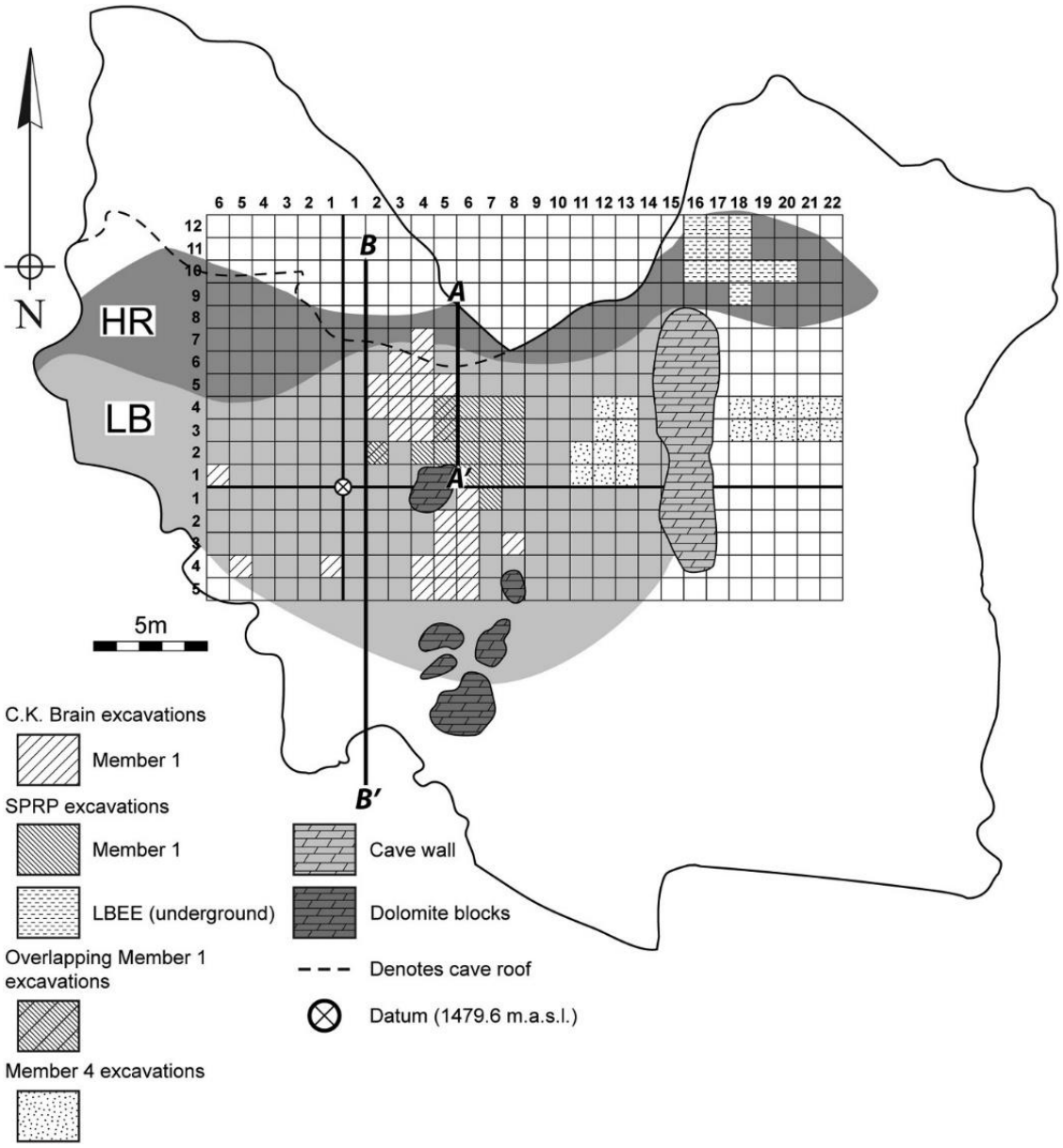

FIG. 2.4.3. *A plan of the excavation grid at SWK. From Kuman et al. (2021, page 3, Fig. 2).*

Eventually, M1HR filled the cave when the shafts that enabled M1LB/M1LBEE to accumulate became choked. M1HR consists of sandy sediments, like M1LB/M1LBEE, but differs in that it contains more inclusions of larger rocks and has thus far only yielded fossils and two bone tools, with no stone artefacts. Based on the principle of superposition, M1HR is therefore deemed to be slightly younger than M1LB/M1LBEE, and with a capping flowstone separating

it from Member 2, accumulated at its most recent 1.7 Ma (Pickering *et al*. 2011). It is possible that there was a hiatus between the choking of the M1LB/M1LBEE shafts and the opening of the M1HR shafts, based on the difference of 500 thousand years for the dating. This depositional history might allude to Pickering *et al*. (2019)'s claim of a hiatus of accumulation during intense, wetter interglacial periods, but there is currently no other research that has attempted to investigate this. Kuman *et al*. (2021) indicate that future research will attempt to date M1HR more absolutely, which should aid in understanding the accumulation history of M1 fully.

The second oldest layer, Member 2 (M2), consists of much finer sediment than those that make-up M1. Like M1, it contains many fossils and artefacts. Early age estimates based on fauna indicate an age around 1.5 Ma (Vrba, 1975). Although M2 has been targeted with more modern dating techniques, such as U-Pb on tooth enamel, placing it around 1.36 Ma+-0.2 Ma (Balter *et al*. 2008), M2 was not targeted for cosmogenic nucleide dating by Gibbon *et al*. (2014) because the little *in situ* remaining sediments from M2 did not yield good samples. It is however wedged between M1 and Member 3 (M3), and it therefore accumulated at its oldest 1.7 Ma, based on the capping flowstone U-Pb date of 1.7 Ma (Pickering *et al*. 2011), and was therefore possibly deposited somewhere in the age range indicated by Balter *et al*. (2008), between 1.56 Ma-1.16 Ma. M2 was however not directly targeted by this project because of the research question that focuses on the difference between the more established Oldowan and Acheulean deposits of SWK, which occur in M1 and M3 respectively, and the limited use of material from this layer stems from it being between these two layers. Moreover, with the uncertainty surrounding the age of M2, conclusions drawn based on a presumed age of the deposit would be tentative.

The youngest layer relevant to this project is, therefore, M3, which consists of more sub-angular rock sediments than the other layers, contains an abundance of fossils and artefacts, and bears evidence of fire use. The early faunal-based date estimates suggest that M3 accumulated about 1 Ma (Vrba 1975), with more recent dating using cosmogenic nucleide by Gibbon *et al*. (2014) placing M3 at 960 ka. This date coincides with the U-Pb tooth enamel date range given by Balter *et al*. (2008) of 830 ka+-210 ka.

It is important to note the Cradle as a general area most likely has had many kinds of smaller environments throughout the last 2.5 million years of depositional history. Some of these environments might vary drastically between sites, even for similarly aged deposits. Another cautionary note is that the environmental variation within the timespans might become lost in the 'time-averaging' of the environments. This could be especially true if most of the Cradle's deposits accumulated during arid glacial periods, as postulated by Pickering *et al*. (2019). Nevertheless, as a sum, and taking these reconstructions for what they represent, a rough picture of the Cradle's environment can be reconstructed, which ultimately speaks to the environment that persisted at SWK over the last 2.5 million years.

A cardinal point in paleoenvironmental reconstructions comes from Vrba's (1974, 1975) seminal bovid analyses. Vrba developed an '*Alcelaphini* and *Antilopini* criterion' (AAC) which states that when *Alcelaphini* and *Antiliponi* make-up more than 60% of the bovid population, an open, grassland environment existed, and where they made up less than 30% of the bovid population, a closed, forested environment existed. The use of AAC was employed at STK (Vrba 1974, 1975), SWK, as well as at Kromdraai (Vrba 1975), and generally showed that the earlier deposits had more closed environments than the more recent deposits. Importantly for SWK though, what Vrba (1985 in 1993) called STK Locality (recodified as STK Member 4 by Partridge [1978]), had an almost 50% AAC, indicating a mosaic environment, shifting from being closed and tending towards more openness. It became much more open by the time M1

of SWK (Partridge 1978) was deposited 1.8-2.2 Ma (Vrba's [1975] 'SWK Pink Breccia'), with an ACC of around 80%. During the deposition of M2 of SWK around 1.56-1.16 Ma (Vrba's [1975] 'SWK Brown Breccia') though, the open grasslands gave way to slightly more closed woodlands, but there was still a dominant grassland/savannah environment with an AAC of around 70% (Vrba 1975). However, it must be stressed that Vrba's work was at the early stages of taxa based paleoenvironmental reconstructions and that the AAC has been heavily criticized as it does not consider the plasticity of the diet of *Alcelaphini* and *Antilopini* (Lee-Thorp *et al*. 2007). Therefore, a more holistic picture needs to be constructed by looking at the results of other proxies, from more recent studies.

Bamford (1999) analysed fossilised wood from Member 4 of STK, which is wedged between two flowstones dated to 2.61 and 2.07 Ma respectively (Pickering & Herries 2020), which places it in a similar timespan as SWK M1. Two taxa were identified, with one of these being the tropical liana, *Dichapetalum mombuttense*, a species that grows in the forests of modern-day Congo, and the other, a pambati tree, *Anastrabe integerrima*, a shrub that grows in the forests along South Africa's south and east coasts today (Bamford 1999). This implies at the very least a presence of some form of woodland during the formation of Member 4 of STK. Bamford's (1999) analysed specimens were also strategically chosen within the deposit through spacing, meaning that this would hopefully sample the entire timeframe in which the deposit accumulated, which, with current dates, spans a timeframe of slightly more than 500 thousand years. However, as the Cradle environment is known for preserving pollen quite poorly, the fact that only fossilized woodland species are present does not mean that these species dominated the landscape (Bamford 1999). These trees may have existed as a small refugium of a gallery forest within a grassland/savannah environment, and further studies need to try and tease out the paleoenvironments in and around SWK.

For the accumulation of Malapa, dated to have occurred 2-1.7 Ma, there are very few proxies available to try and reconstruct what environment *Au. sediba* would have encountered. There is, however, a single coprolite, from the 1.95 Ma layer, which contains wooden fragments, pollen, and phytoliths that indicate a much higher rainfall in the cradle than what is present today (Bamford *et al*. 2010). This contrasts with Avery's (2001) analysis of micromammal taxa that indicates less rainfall for 2-1 Ma timespan at STK and SWK.

Furthermore, Pavia's (2020) analysis of avian faunal remains from Kromdraai Member 2 resulted in a paleoenvironmental reconstruction that indicates a grassland environment, with a large cliff or rocky outcrop, and a waterbody with a gallery forest nearby. Although this deposit is yet to be accurately dated, Kromdraai is close to SWK and STK, and contains *P. robustus* fossils, and thus probably coincides in date with SWK M1. Irrespective of the reasons underpinning the different paleoenvironmental reconstructions from these sites, the consensus seems to be that there was a slightly wetter, but mainly mosaic environment in the Cradle before about 1.7 Ma. This time coincides with the Earth experiencing intense precession changes, meaning the tilt-angle on which the Earth spin's is less stable. This has the effect of increased Walker Circulations, which resulted in humid low-pressure air being circulated further away from Africa and therefore Africa experienced a general increase in aridity (Trauth *et al*. 2007).

Studies looking at the environment that persisted at the Cradle from 1.7 Ma onwards are sparse. Some limited faunal lists from Member 5 from STK exist with Reed (1998) also having reported on the percentage of arboreal taxa to grazers at SWK. These lists seem to hint at an open savanna on the edge of a water source, with the decline of woodlands and spread of grasslands from M1 to M3. This general aridification is supported by Lee-Thorp *et al*. (2007) as they used existing $\delta^{13}C$ data from Makapansgat, SWK, and STK to suggest that the landscape became dominated by an open, grassy environment from 1.7 Ma onwards. However, in contrast to the results of Reed (1998), there is evidence to suggest that woodlands survived

for longer around SWK, with investigations by Steininger (2011) on the dietary profiles of Bovidae from M2 and M1 indicating more mixed feeders in M2, and more grazers in M1. It is evident that paleoenvironmental work in the Cradle has focused on the earlier deposits, and the younger deposits, like the 960 ka M3 of SWK, received less attention. Moreover, further research is needed to investigate inconsistencies between these multi-proxy paleoenvironmental reconstructions.

Chapter Three: Materials and Methods

3.1 Materials

The fossil material analysed in this study are Anura ilia excavated from SWK Member 1 (M1) (n=89, 48 left and 41 right) and Member 3 (M3) (n=61, 30 left and 31 right). Additional ilia were identified from Member 2 (M2) (n=15, 10 left and 5 right), but these were omitted from most analyses due to small sample size, and the problematic chronology of M2. All analysed ilia were extracted from two samples that were merged to form this project's total sample (n=165). The first, herein referred to as the 'Wits Sample' (n=87), was excavated in 2013 by the Swartkrans Palaeoanthropology Research Project (SPRP). The second sample, herein referred to as the 'Tim Campbell and Juan Daza Sample' (TCJD) (n=78) consists of high-resolution images of Anura ilia in lateral/acetabular view, at unknown magnification, excavated between 1979-1986 by Bob Brain, and photographed by Dr Tim Campbell of Baylor University and Dr Juan Daza of Sam Houston State University. A Minimum Number of Individual's (MNI) count was performed based solely on the number of left and right sided ilia. As the total sample was made up of unstandardised images from different sources, further analyses were based on the Number of Individual Specimen's (NISP) count as opposed to the MNI count.

The Wits Sample is housed at the Evolutionary Studies Institute (ESI), at the University of Witwatersrand (Wits) in Johannesburg. Ninety sieve find bags from the June 2013 excavation season were sorted through by the researcher, with the use of forceps, a 40x hand lens, and an auxiliary LED light. All Anura ilia were removed, individually placed into plastic zip-lock bags, and assigned a unique identification number. To reduce the chances of bone breakage, these were then bubble-wrapped, placed into two hard plastic boxes, and transported to the Iziko South Africa Museum, Cape Town for further analyses. Hereafter, 30 of the best-preserved specimens were selected after inspection using a light microscope at 200x

magnification and were then sent to the Central Analytical Facilities (CAF) at Stellenbosch University where the CAF team Computerized Tomography (CT) scanned the sample using a General Electric V TomeX L240 and processed into usable file formats with VGStudioMax. These CT scans were used to facilitate better identification, to carry out precise linear and angle measurements, and to explore the potential of GM.

3.2 Taxonomic Identification

The remaining material from the Wits sample that was not CT scanned (n=57), was analysed under 200x magnification with a light microscope. The photo-editing software Photoscape X was used to analyse and identify the TCJD sample (n=78). Comparative collections of southern African Anura fossils are scarce, and therefore most of the identifications utilised very little actual comparative material. Instead, CT scanned material available on Morphosource (www. https://www.morphosource.org/) and CT scanned material shared by Dr Thalassa Matthews of both extant and extinct taxa, aided in the confirmation of identifications. All specimens were identified to the level of genus, and in some rare cases, down to species level (n=45). Taxonomic classification followed Frost (2022).

To enable identification of fossil taxa, a unique southern African Anura ilia identification process flow (Fig 3.2.1) was developed, which uses the standardised ilia terminology of Gómez and Turazzini (2016) (Fig 3.2.2). This process flow was compiled based on the identification guide of Matthews *et al*. (2019), and from images and CT scans shared by Dr Matthews. In theory, this process flow can be used to identify other southern African Anura ilia samples down to genus level. It aims to rely as little as possible on distinctions based on the Ventral Acetabular Expansion (VAE), as this feature is rarely preserved in fossils (Matthews *et al*. 2019) and the analysed sample is no exception to this. However, use of the VAE cannot

currently be avoided for discriminating between certain genera within the same family (i.e., *Bufonidae* and *Heleophrynidae*) or for six other genera from three families that are morphologically very similar (i.e., in Arthroleptis and Leptopolis [*Arthroleptidae*]; *Amietia*, *Arthroleptella*, and *Strongylopus* [*Pxyicephalidae*]; *Hildebrandtia* [*Ptychadenidae*]; and *Phrynobatrachus* [*Phrynobatrachidae*]). Moreover, the TCJD sample relied on images that were captured in lateral/acetabular view only, and certain features that were considered good for identification by Matthews *et al*. (2019), were not present in this view (i.e., the interiliac tubercle and medial oblique ridge). This process flow therefore differs slightly from the identification suggestions made by Matthews *et al*. (2019) and should be read in conjunction with their guide.

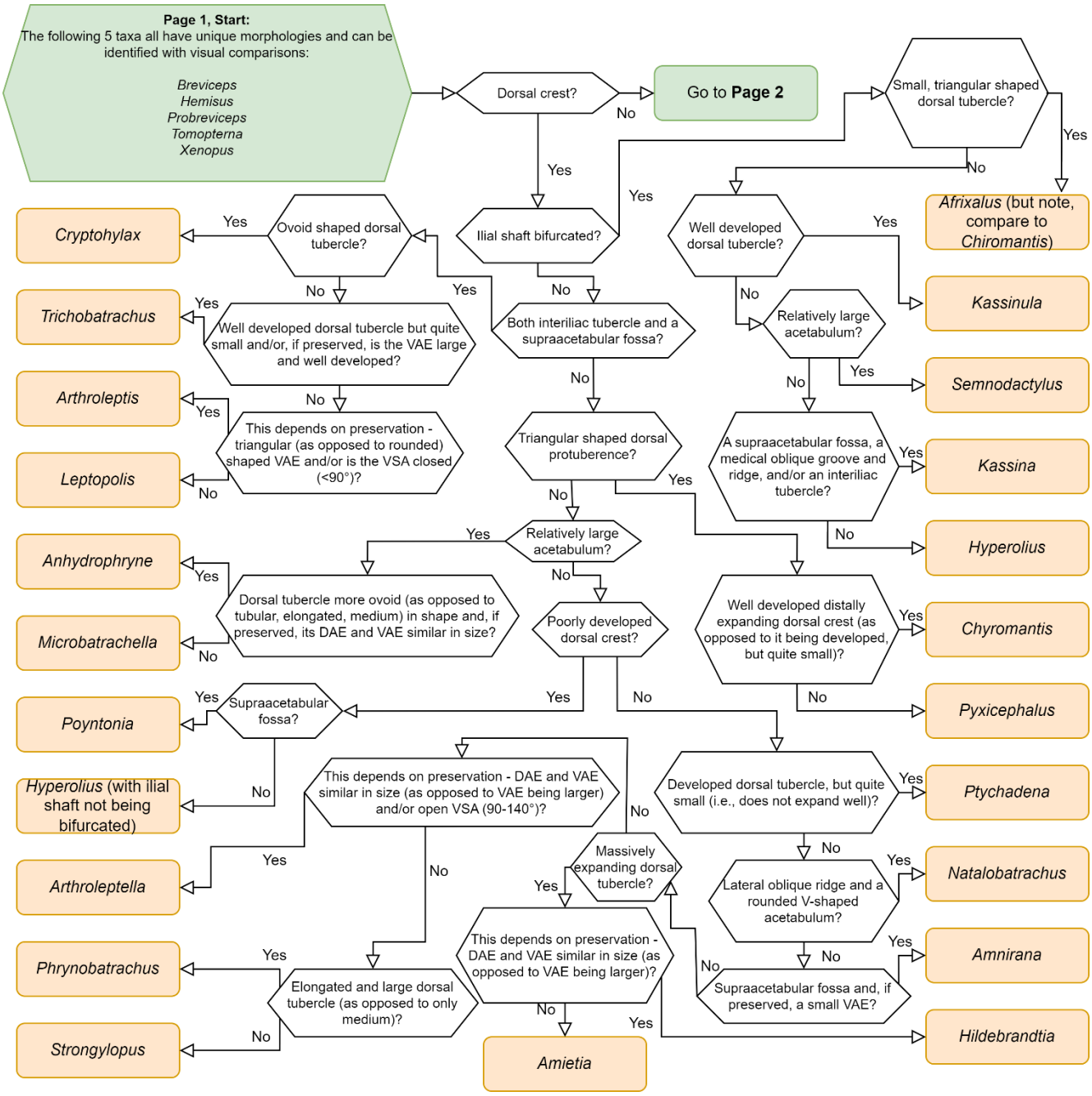
Page 1, Start:
The following 5 taxa all have unique morphologies and can be identified with visual comparisons:
Breviceps
Hemisus
Probreviceps
Tomopterna
Xenopus
Dorsal crest?
No
Go to Page 2
Yes
Small, triangular shaped dorsal tubercle?
Yes
No
Afrixalus (but note, compare to Chiromantis)
Ilial shaft bifurcated?
Yes
No
Well developed dorsal tubercle?
Yes
No
Kassinula
Ovoid shaped dorsal tubercle?
Yes
No
Cryptohylax
Both interiliac tubercle and a supraacetabular fossa?
Yes
No
Relatively large acetabulum?
Yes
No
Semnodactylus
Well developed dorsal tubercle but quite small and/or, if preserved, is the VAE large and well developed?
Yes
No
Trichobatrachus
Triangular shaped dorsal protuberence?
Yes
No
A supraacetabular fossa, a medical oblique groove and ridge, and/or an interiliac tubercle?
Yes
No
Kassina
This depends on preservation - triangular (as opposed to rounded) shaped VAE and/or is the VSA closed (<90°)?
Yes
No
Arthroleptis
Leptopolis
Relatively large acetabulum?
Yes
No
Hyperolius
Dorsal tubercle more ovoid (as opposed to tubular, elongated, medium) in shape and, if preserved, its DAE and VAE similar in size?
Yes
No
Anhydrophryne
Microbatrachella
Poorly developed dorsal crest?
Yes
No
Well developed distally expanding dorsal crest (as opposed to it being developed, but quite small)?
Yes
No
Chyromantis
Supraacetabular fossa?
Yes
No
Poyntonia
Pyxicephalus
This depends on preservation - DAE and VAE similar in size (as opposed to VAE being larger) and/or open VSA (90-140°)?
Yes
No
Developed dorsal tubercle, but quite small (i.e., does not expand well)?
Yes
No
Ptychadena
Hyperolius (with ilial shaft not being bifurcated)
Arthroleptella
Massively expanding dorsal tubercle?
Yes
No
Lateral oblique ridge and a rounded V-shaped acetabulum?
Yes
No
Natalobatrachus
This depends on preservation - DAE and VAE similar in size (as opposed to VAE being larger)?
Yes
No
Amnirana
Phrynobatrachus
Elongated and large dorsal tubercle (as opposed to only medium)?
Yes
No
Supraacetabular fossa and, if preserved, a small VAE?
Yes
No
Hildebrandtia
Strongylopus
Amietia

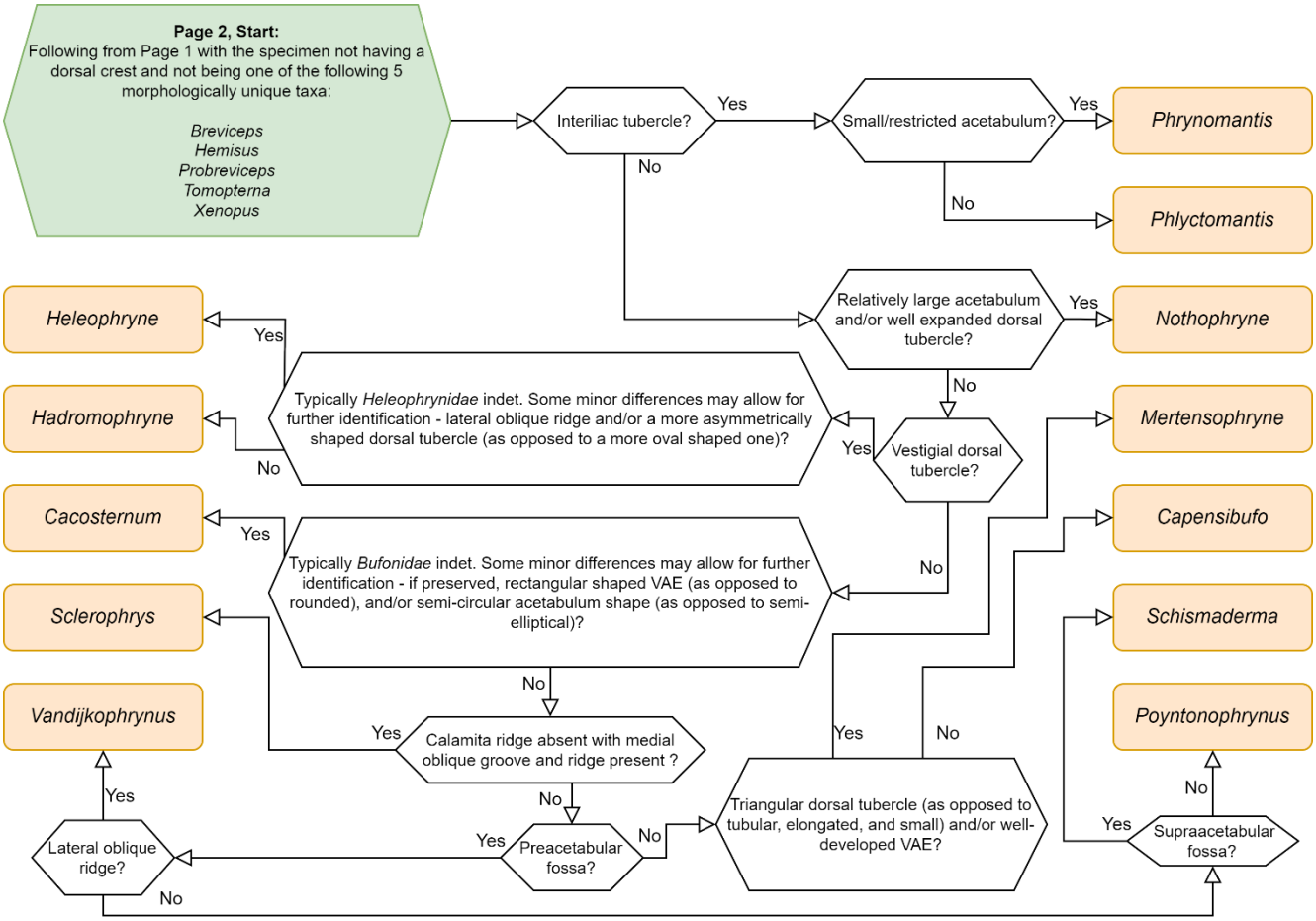

FIG. 3.2.1. *Southern African Anura Ilia Identification Guide Process Flow. Based on the work of Matthews et al. (2019). DAE = dorsal acetabular expansion; VAE = ventral acetabular expansion.*

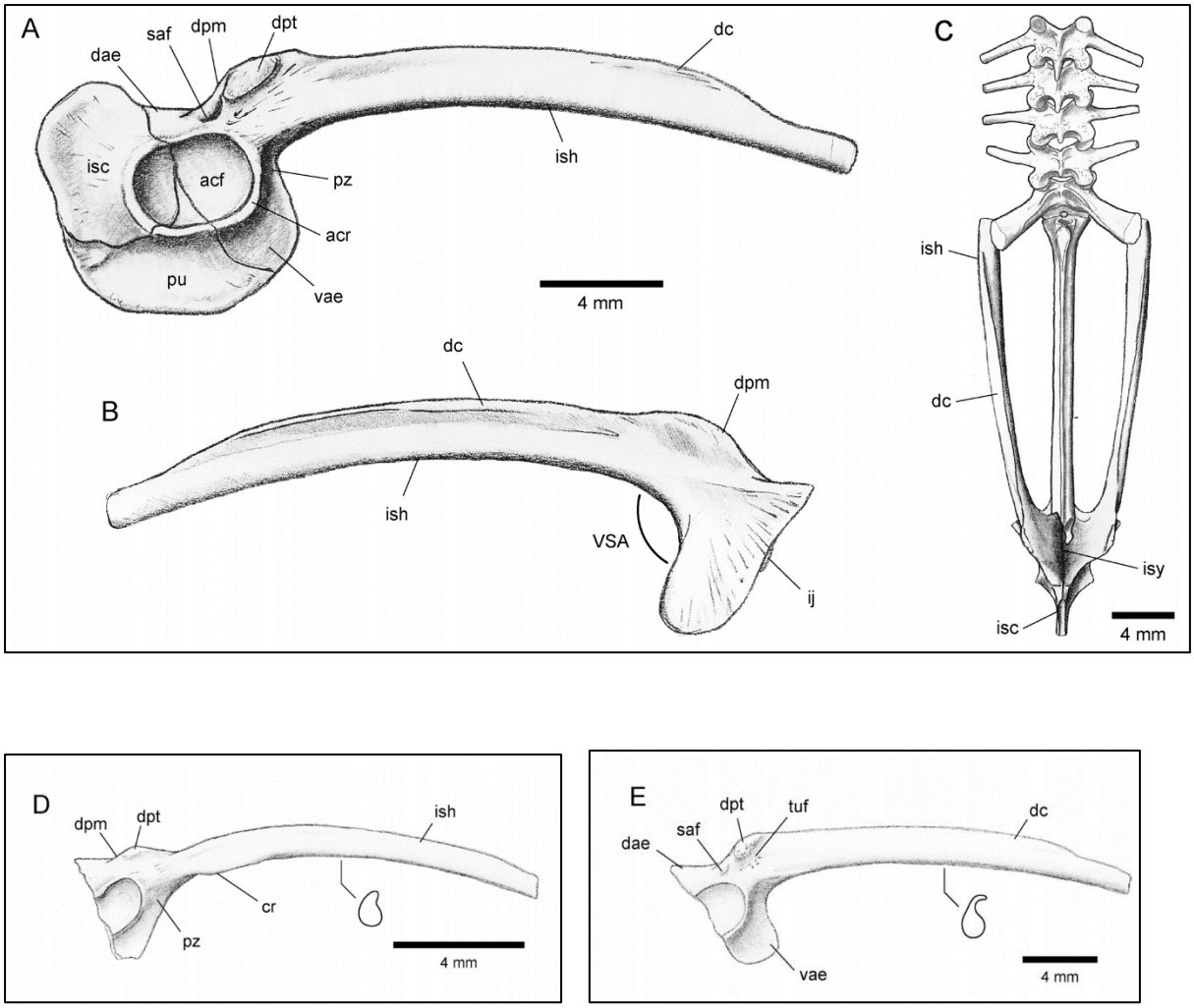

FIG. 3.2.2. *The location of the features referred to in the Southern African Anura Ilia Identification Guide Process Flow (Fig 3.2.1) and other common features of an Anura ilium, on an illustration of a Leptodactylus latrans ilium (A: lateral/acetabular view, B: medial view, and C: dorsal view in relation to the sacrum), a Nannophryne variegate ilium (D: lateral/acetabular view), and Rana temporaria ilium (E: lateral/acetabular view) adapted from Gómez and Turazzini (2016: pg. 2, Fig. 1; pg. 5, Fig. 4). For more information on these features, see Gómez and Turazzini (2016). The features specifically referred to in the process flow are* ***bolded*** *here: acf = acetabular fossa, acr = acetabular rim (together these two constitute the* ***acetabulum****); cr =* ***calamita ridge****; dae =* ***dorsal acetabular expansion****; dc =* ***dorsal crest****; dpm = dorsal prominence, dpt = dorsal protuberance (together these two constitute the* ***dorsal tubercle****); ij = ilioschiatic juncture; isc = ischium; ish =* ***ilial shaft****; isy*

= interiliac symphysis; pu = pubis; pz = preacetabular zone (the ***preacetabular fossa*** *is a fossa that occurs here); saf =* ***supraacetabular fossa****; tuf =* ***tubercular fossa****; vae =* ***ventral acetabular expansion****; VSA = the angle between the vae and the anterior margin of the ish.*

3.3 Linear and Angle Measurements

Of the 30 CT scanned specimens, six were *Pipidae* and were excluded from further analyses as they are morphologically distinct from all other Anura. The remaining 24 CT scanned specimens were imported into the software Meshlab. Using the measuring tool in Meshlab, two straight line measurements and one angle measurement was recorded for each specimen. These measurements stem from Matthews *et al*. (2019)'s suggested measurements. The first measurement was the Neck Width, the second the breadth of the acetabulum below the ilioschiatic junction (Acetabular Breadth), and the last was of the angle between the VAE and the anterior margin of the ilial shaft (VSA). It must be noted that the VAE is not well preserved in this sample and that the VSA measurements might be more inaccurate and unreliable. Because of the small sample size of 24, the measurements suggested by Matthews *et al*. (2019), that rely on features of the dorsal crest, were not used as this would have excluded the 11 *Tomopterna* specimens in the sample as this family does not have a dorsal crest. The length of the ilium was also excluded, as none of the CT scanned specimens had a full ilial shaft preserved.

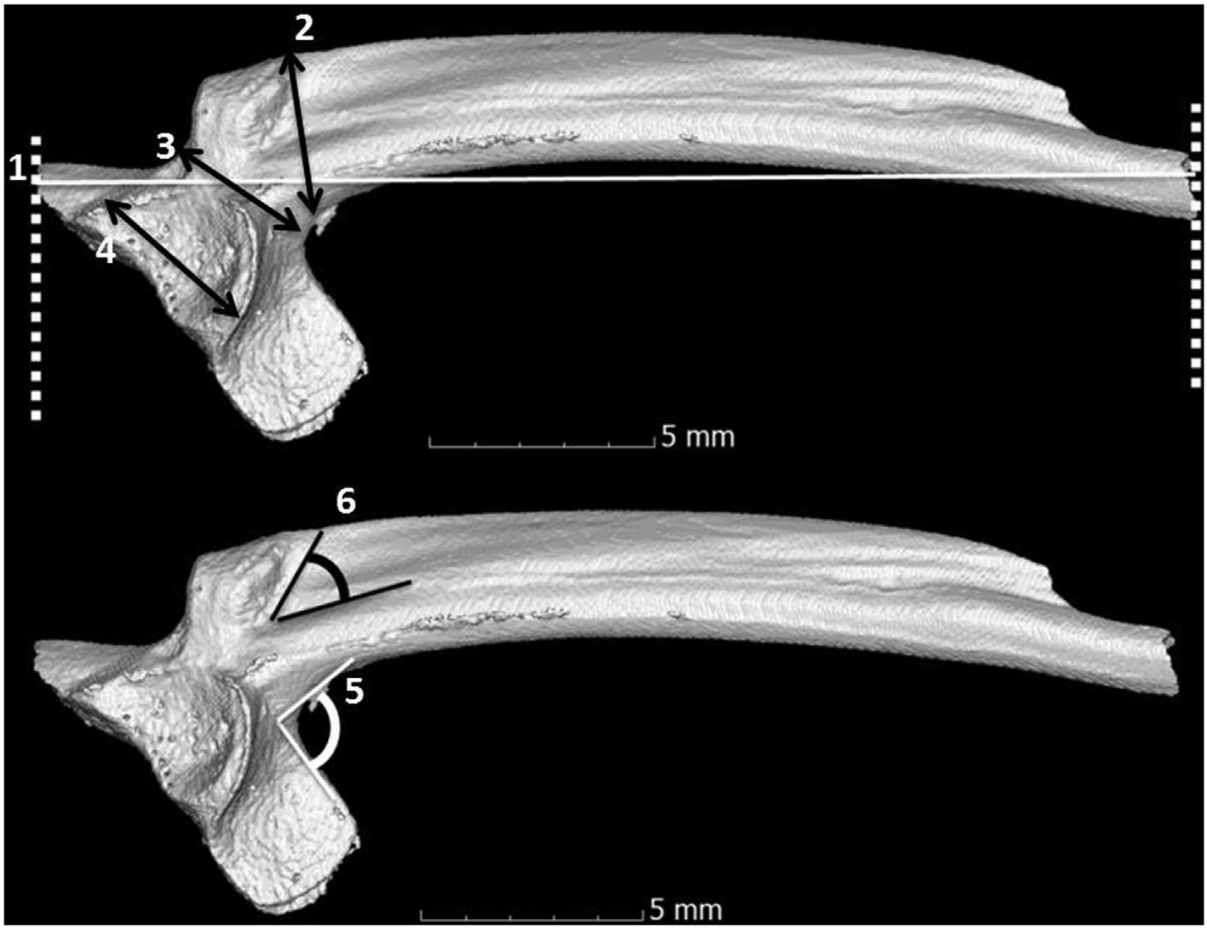

FIG. 3.3.1. *The measurements on the ilia of Matthews et al. (2019, pg. 48, Fig. 1). These are displayed on an Amietia vertebralis specimen with 1 = Length of ilium (excluded in this study), 2 = Height of dorsal crest at base of dorsal protuberance (excluded in this study), 3 = Neck depth, 4 = Breadth of the acetabulum below the ilioischiatic junction (Acetabular Breadth), 5 = VSA, 6 = Angle between the dorsal protuberance and the lateral oblique ridge (excluded in this study).*

3.4 Geometric Morphometrics and Interlandmark Distances

After measurement, the 24 CT scanned specimens were subjected to a basic geometric morphometrics (GM) analysis. Three of the CT scanned specimens did not have a dorsal acetabular expansion (DAE) preserved and were thus excluded, making the GM analysed

sample size 21. Nine landmarks were developed based on simulating the simplest way of showing the shape of the ilium without relying on semi-landmarks. The nine landmarks used for the GM analyses are described in Table 3.4.1 and illustrated in Figure 3.4.1. These landmarks were placed using Meshlab's PickPoints function.

Table 3.4.1. *The description of the placement of the nine landmarks used in this study.*

Landmark ID Number	Description
1	Middle of the acetabular fossa (lateral view).
2	Point where acetabular rim borders the VAE (lateral view).
3	Straight line from point **'2'** to the end of the VAE (lateral view).
4	Base of the ilial shaft where the VAE meets the ilial shaft (lateral view).
5	Straight line across the ilial shaft from point **'4'** to the top of the ISH (lateral view).
6	Centre of acetabular rim where it meets the ilial shaft (lateral view).
7	Centre of the supraacetabular fossa (lateral view).
8	Highest point of DAE (dorsal view).
9	Point where acetabular rim borders the DAE (lateral view).

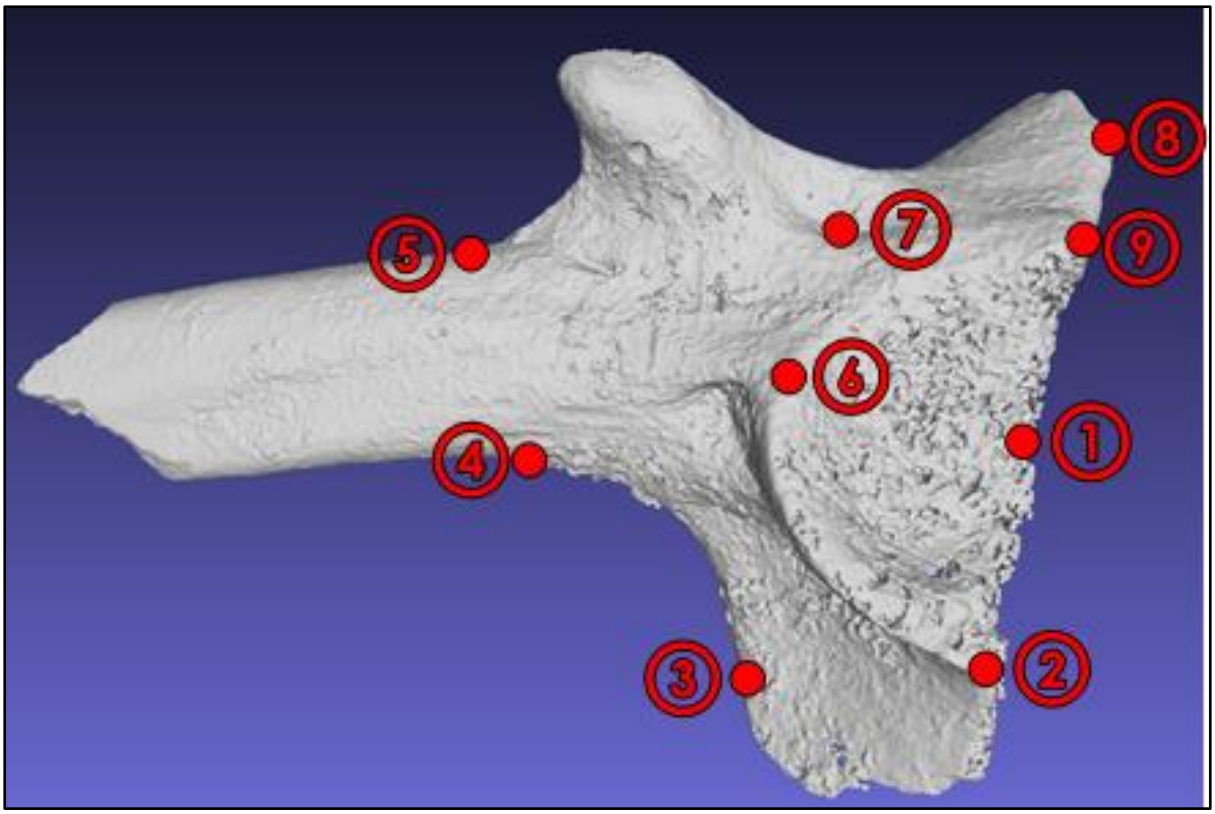

FIG. 3.4.1. *Example of the location of the landmarks on specimen SWK_M3_87-I08 (Tomopterna tandyi).*

The landmark data were then imported to MorphoJ where a Procrustes correction was performed which transforms the co-ordinate data to standardize information on size, location, and orientation (Savriama 2018). An outlier check was also performed, but no outliers were found.

Thereafter, Euclidean geometry was used on the nine landmarks to generate 12 new straight-line measurements (interlandmark distances) for the 21 GM analysed specimens. To eliminate the effects of size, location, and orientation on the interlandmark distances, the same interlandmark measurements were calculated on the Procrustes corrected specimens. Eleven of these distances are indicated on the wireframe diagram displayed in Fig 3.4.2., and the 12th distance is between points 2 and 9, which is the diameter of the acetabular rim.

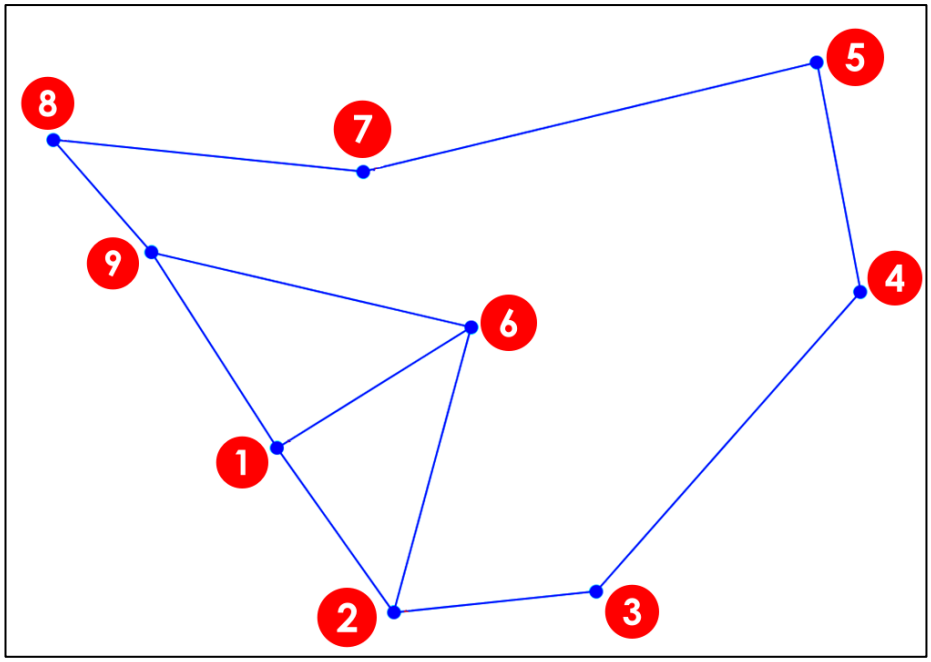

FIG. 3.4.2. *Wireframe diagram of a sample specimen (SWK_M3_87-I08, Tomopterna tandyi) showing the interlandmark distances analysed.*

3.5 Statistical Analyses

The software PAleontological STatistics (PAST) was used to run statistical tests, unless otherwise stated. To test whether the taxonomic composition of M1 and M3 differed statistically, a Fisher's Exact Test was performed on the total sample and tested for at the $p \leq 0.05$ level. This test was chosen over the more conventional Chi^2 test as the assumption that at least 80% or more of the expected values should be counts of 5 or more was not being met with only 36% of the expected value counts being 5 or more (Nowacki 2017).

The 24 CT scanned specimen's measurements were imported into the software PAST, alongside six further specimen's measurements, five of which were extracted from Matthews *et al*. (2019) and one which was shared by Dr Matthews. These were then grouped into the three genera that comprised the sample (*Amnirana*, *Tomopterna*, and *Strongylopus*). The distribution of the Neck Width, Acetabular Breadth, and VSA measurements were then plotted

to inspect the resultant distributions per taxa. To compare the three measurements between the three genera, pairwise Mann-Whitney U and Kolmogorov-Smirnov (K-S) tests were performed and tested for at the 0.05 level. These tests are deemed the most appropriate as they are non-parametric and can be used on the small sized samples (Özçomak *et al*. 2013).

A Principal Components Analysis (PCA) was run to visualise the variation of the most relevant measurements between the analysed genera and to see possible clustering within the genera that might have been alluded to in the distribution plots. Convex hulls were used to identify clusters as opposed to 95% confidence intervals because of the small sample size. In cases where there was noteworthy clustering, the specimens clustering from within that genus were grouped. This group was then subjected to Mann-Whitney U tests and K-S tests, with the remainder of the specimens from that genus, to test whether the two groups within that same genus might come from a different distribution based on those measurements. This test was also performed at the 0.05 level.

The GM analysed sample's 12 interlandmark measurements were then compared between the *Tomopterna* and *Amnirana* specimens using t-tests, F-tests, Mann-Whitney U tests, and K-S tests at the 0.05 level to see whether specific measurements might be good candidates for differentiating between these taxa. The same was done on the Procrustes corrected interlandmark distances. To unpack some of the within genus clustering identified by the earlier PCA, those identified groups' interlandmark and Procrustes corrected interlandmark distances were also subjected to t-tests, F-tests, Mann-Whitney U tests, and K-S tests at the 0.05 level. Each interlandmark distance for each taxon and group, was also tested for normal distribution using Shapiro-Wilks, Anderson-Darling, and a Lilliefors tests to ascertain whether they were normally distributed. This was done to determine which statistical test provided the most reliable results as both t-tests and F-tests assume that the underlying distribution is normally distributed (i.e., parametric), whereas the Mann-Whitney U tests and K-S tests do not (Field

2018). If that specific interlandmark distance was normally distributed, then the results of the t-test and F-test were interpreted in addition to the results of the Mann-Whitney U test and K-S test.

Chapter Four: Results

4.1 Taxonomic Identification

The taxonomic diversity varies marginally between M1 and M3 (see Table 4.1.1), with five families represented in each, and a sixth present in M2. Of the *Breviceptidae*, the genus *Probreviceps* is represented by one ilium in M1, and another one in M2, but is absent from M3. *Bufonidae* are represented by seven ilia, four of which were assigned to the genus *Sclerophrys*, and the other three as indeterminate *Bufonidae* (due to a lack of preserved identifying features). *Pyxicephalidae* is the most diverse family represented, comprising of three identifiable genera, including the best represented genus in the analysed sample, *Tomopterna* (n=67), as well as a few *Amietia* (n=6) and *Strongylopus* (n=8) specimens. The well preserved *Tomopterna* specimens could be identified down to species level with three species represented. It is noteworthy that there were a few specimens of *T. tandyi* which were considerably smaller than the others, but bar size, were morphologically indistinguishable. Seven *Strongylopus* specimens were identified down to genus level, with a single *Strongylopus* specimen from M2 sufficiently preserved to enable identification down to species level. Phrynobatrachids were absent from M1 and M3 and were only represented by two specimens in M2. Pipids are the third most well-represented family, with 37 *Xenopus* ilia present. The second most well-represented genus is the ranid *cf. Amnirana* (n=38).

Table 4.1.1. *Anura taxa recovered from Swartkrans Cave, Members 1, 2 and 3.*

Family	Genus	Species	No. Ilia/MNI in M1	No. Ilia/MNI in M2	No. Ilia/MNI in M3	NISP/MNI
Brevicipitidae	*Probreviceps*	*Indeterminate*	1/1	1/1	0	**2/2**
Bufonidae	*Indeterminate*	*Indeterminate*	2/2	0	1/1	**3/3**
	Sclerophrys	*Indeterminate*	1/1	0	3/3	**4/4**
Pyxicephalidae	*Amietia*	*Indeterminate*	4/2	0	2/2	**6/4**
	Tomopterna	*Indeterminate*	8/5	1/1	12/8	**21/14**
		T. delalandii	6/5	0	3/2	**9/7**
		T. krugerensis	2/1	0	1/1	**3/2**
		T. tandyi	14/11	4/3	14/8	**32/22**
	Strongylopus	*Indeterminate*	3/2	1/1	3/3	**7/6**
		S. grayii	0	1/1	0	**1/1**
Phrynobatrachidae	*Phrynobatrachus*	*Indeterminate*	0	2/1	0	**2/1**
Pipidae	*Xenopus*	*Indeterminate*	22/17	2/1	13/8	**37/26**
Ranidae	*cf. Amnirana*	*Indeterminate*	26/15	3/2	9/7	**38/24**
NISP/MNI			**89/62**	**15/11**	**61/43**	**165/116**

The outcome of the Fischer's Exact Test (F = 1.56, p = 0.57), comparing the two largest assemblages (M1 and M3) on a generic level, resulted in a p-value greater than 0.05. This indicates that the composition of the Anura community has remained largely unchanged through time from the deposition of M1 to M3.

4.2 Linear and Angle Measurements

4.2.1 Measurements

The linear and angle measurements on the 24 CT scanned specimens are provided in Table 4.2.1. Figures 4.2.1, 4.2.2, and 4.2.3 show the distributions of these three measurements respectively amongst the three Genera. Only the *Tomopterna* specimens had outliers, of which one specimen had an extremely small Neck Width (ZM046810 from Matthews *et al*. [2019]), and the other outliers stems from measurements from a single, extremely large specimen from

this study (SWK_M1_51-IO2) that had an abnormally large Neck Width and Acetabular Breadth. The Neck Width distribution plots hint at bimodal distributions for the *Strongylopus* and *Amnirana* specimens, and a slightly normal distribution for the *Tomopterna* specimens. A similar trend can be observed in the Acetabular Breadth measurements, except that the *Tomopterna* distribution seems to be skewed to the right. The VSA measurements again show a bimodal distribution for the *Strongylopus* specimens. The distribution for the *Tomopterna* specimens is skewed to the right again, and the distribution for the *Amnirana* specimens is skewed to the left. Most of these distributions deviate slightly from their normal curves.

Table 4.2.1. *Results of the linear and angle measurements.*

Family	Genus	Species	Specimen number.	Neck Width (mm)	Acetabular Breadth (mm)	VSA (°)	Source of Data (deposit if applicable)
Pyxicephalidae	*Strongylopus*	*Strongylopus grayii*	CAS211614	1.5	1.7	130.4	Dr Thalassa Matthews
Pyxicephalidae	*Strongylopus*	*Strongylopus indet.*	58-IO1	1.89	2.04	121.2	This study (M1)
Pyxicephalidae	*Strongylopus*	*Strongylopus indet.*	67-IO1	1.94	2.11	131.9	This study (M3)
Pyxicephalidae	*Strongylopus*	*Strongylopus springbokensis*	TM66787	1.41	1.57	138.08	Matthews *et al.* (2019)
Pyxicephalidae	*Tomopterna*	*Tomopterna delalandii*	77-IO5	2.45	2.29	133	This study (M3)
Pyxicephalidae	*Tomopterna*	*Tomopterna delalandii*	80-IO3	2.44	2.47	128.1	This study (M3)
Pyxicephalidae	*Tomopterna*	*Tomopterna delalandii*	ZM046810	1.45	2.08	110.42	Matthews *et al.* (2019)
Pyxicephalidae	*Tomopterna*	*Tomopterna krugerensis*	TM061058	1.81	2.12	122.58	Matthews *et al.* (2019)
Pyxicephalidae	*Tomopterna*	*Tomopterna tandyi*	09-IO1	2.36	2.3	110.5	This study (M1)
Pyxicephalidae	*Tomopterna*	*Tomopterna tandyi*	51-IO2	3.25	3.15	120.8	This study (M1)
Pyxicephalidae	*Tomopterna*	*Tomopterna tandyi*	64-IO1	2.48	2.38	103.6	This study (M2)

Pyxicephalidae	*Tomopterna*	*Tomopterna tandyi*	67-IO2	2.43	2.62	126	This study (M3)
Pyxicephalidae	*Tomopterna*	*Tomopterna tandyi*	68-IO3	2.24	2.24	105.8	This study (M3)
Pyxicephalidae	*Tomopterna*	*Tomopterna tandyi*	69-IO1	2.58	2.44	122.5	This study (M3)
Pyxicephalidae	*Tomopterna*	*Tomopterna tandyi*	75-IO2	2.73	2.72	112.8	This study (M3)
Pyxicephalidae	*Tomopterna*	*Tomopterna tandyi*	77-IO2	2.48	2.53	146.5	This study (M3)
Pyxicephalidae	*Tomopterna*	*Tomopterna tandyi*	87-IO8	2.44	2.35	113.2	This study (M3)
Pyxicephalidae	*Tomopterna*	*Tomopterna tandyi*	ZM052343	1.61	2.63	113.16	Matthews *et al*. (2019)
Ranidae	*Amnirana*	*Amnirana albolabris*	CAS202204	1.76	1.96	117.07	Matthews *et al*. (2019)
Ranidae	*Amnirana*	*Amnirana darlingi*	ZM181779	2.45	2.3	130.22	Matthews *et al*. (2019)
Ranidae	*Amnirana*	*Amnirana indet.*	07-IO1	2.2	2.29	98*	This study (M1)
Ranidae	*Amnirana*	*Amnirana indet.*	17-IO1	2.01	2.24	130	This study (M1)
Ranidae	*Amnirana*	*Amnirana indet.*	22-IO1	3.4	3.58	139.4	This study (M1)
Ranidae	*Amnirana*	*Amnirana indet.*	23-IO1	3.22	3.57	132.7	This study (M1)
Ranidae	*Amnirana*	*Amnirana indet.*	26-IO1	1.87	1.81	123.9	This study (M1)
Ranidae	*Amnirana*	*Amnirana indet.*	28-IO1	1.9	2.33	134.7	This study (M1)
Ranidae	*Amnirana*	*Amnirana indet.*	88-IO1	2.1	2.16	113.6*	This study (M1)
Ranidae	*Amnirana*	*Amnirana indet.*	90-IO1	3.47	3.3	114.3	This study (M1)
Ranidae	*Amnirana*	*Amnirana indet.*	66-IO1	2.73	3.13	115.5	This study (M2)
Ranidae	*Amnirana*	*Amnirana indet.*	84-IO1	2.84	2.57	125.4	This study (M3)
Ranidae	*Amnirana*	*Amnirana indet.*	87-IO2	3.24	3.37	125	This study (M3)

*poorly preserved VAE means that this measurement is probably an underestimation of the VSA.

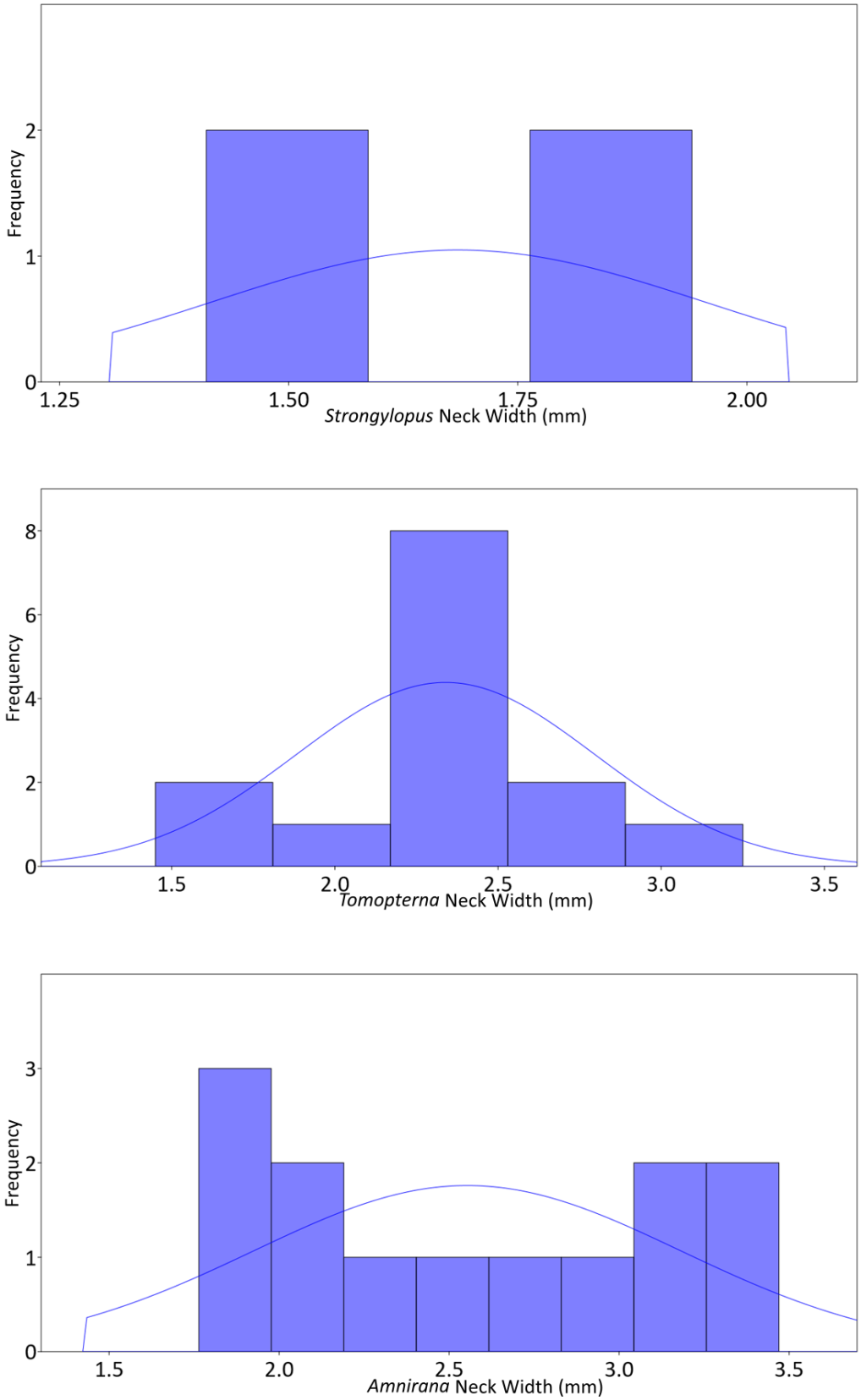

FIG. 4.2.1. *Distribution plots of the Neck Width measurements of the 4 Strongylopus specimens, the 14 Tomopterna specimens, and the 13 Amnirana specimens.*

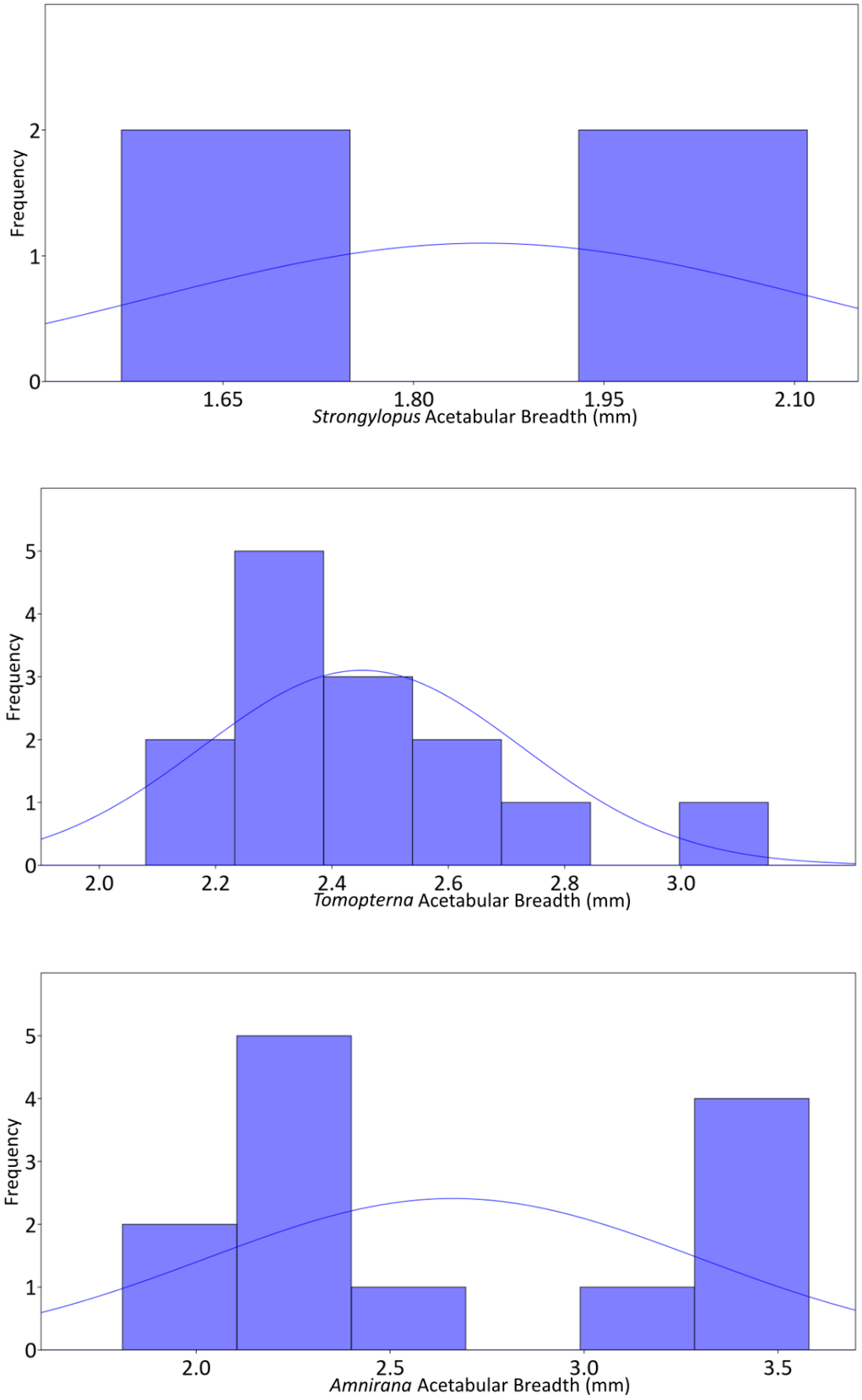

FIG. 4.2.2. *Distribution plots of the Acetabular Breadth measurements of the 4 Strongylopus specimens, the 14 Tomopterna specimens, and the 13 Amnirana specimens.*

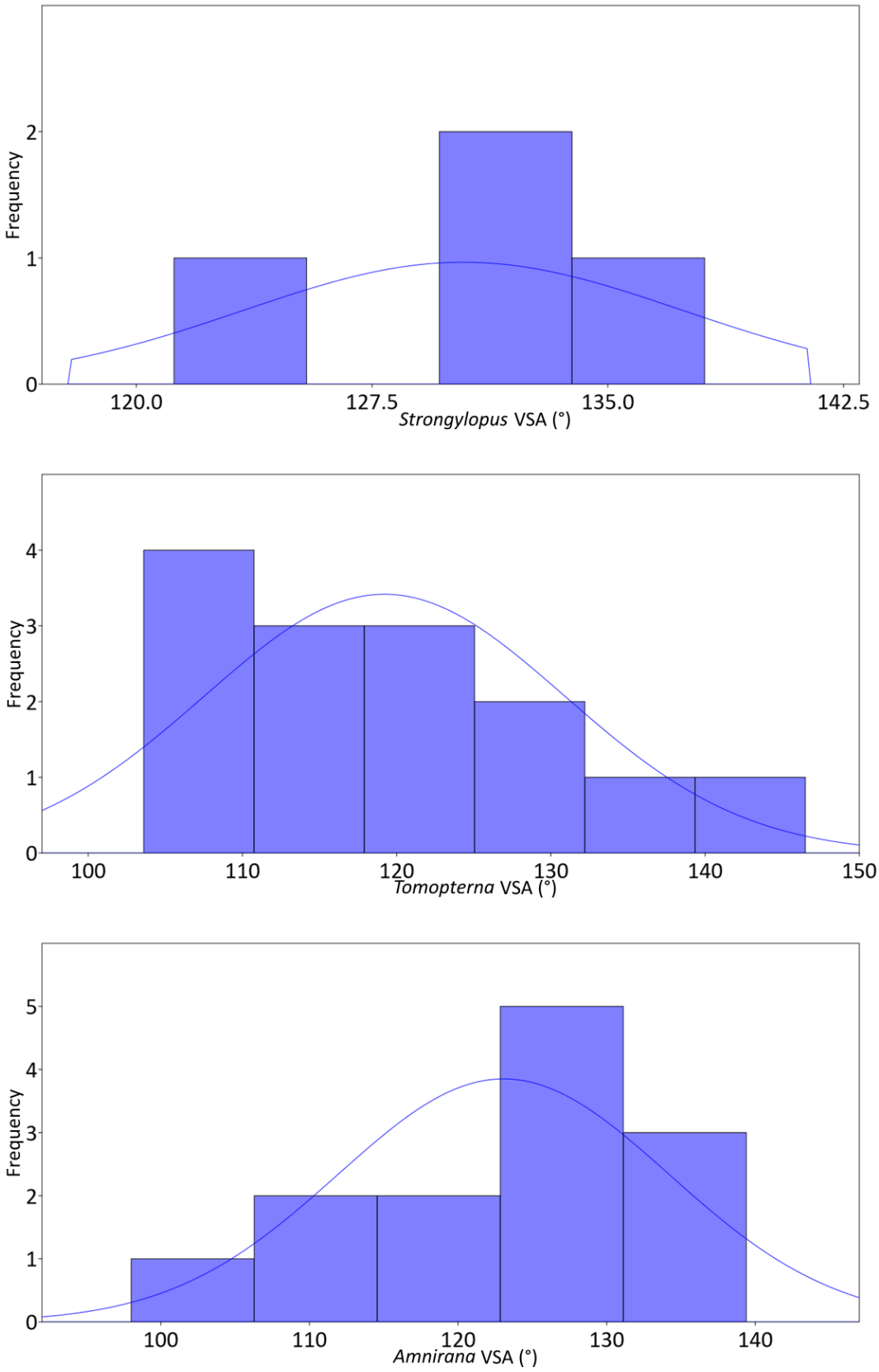

FIG. 4.2.3. *Distribution plots of the VSA measurements of the 4 Strongylopus specimens, the 14 Tomopterna specimens, and the 13 Amnirana specimens.*

The p-values for the Mann-Whitney U tests and K-S tests are presented in Table 4.2.2. None of the VSA measurements had a p-values less than or equal to 0.05, showing that, based on the VSA measurement, all three of the taxa are indistinguishable. The *Strongylopus* ilia could be distinguished from the *Amnirana* and *Tomopterna* specimens by both the Neck Width and Acetabular Breadth measurements, although the sample size for *Strongylopus* (n=4) is very small. Despite *Amnirana* and *Tomopterna* ilia being visually quite different, none of the three measurements resulted in a p-value less than or equal to 0.05 using either test.

Table 4.2.2. *P-values for the Mann-Whitney U tests and K-S tests on the measurements between the three genera*

Genera Tested	**Neck Width p-value (Mann-Whitney U/K-S)**	**Acetabular Breadth p-value (Mann-Whitney U/K-S)**	**VSA p-value (Mann-Whitney U/K-S)**
Amnirana (n=13) vs *Tomopterna* (n=14)	0.528/0.422	0.79/0.444	0.167/0.131
Amnirana (n=13) vs *Strongylopus* (n=4)	0.02*/0.024*	0.015*/0.01*	0.234/0.267
Strongylopus (n=4) vs *Tomopterna* (n=14)	0.029*/0.018*	0.005*/0.003*	0.08/0.123

** values that are statistically significant being ≤0.05.*

4.2.2 PCA

The loadings of the three measurements on the different principal components (PCs) are provided in Table 4.2.3. PC1 explained 99.532% of the variance, which is expected, as the VSA is one of the most varied measurements, even amongst the same taxa. PC2 and PC3 both loaded onto the two straight line measurements (Neck Width and Acetabular Breadth).

Table 4.2.3. *The loadings of the different measurements on the different PCs.*

Measurement	PC1	PC2	PC3
Neck Width (mm)	0.003	0.749	-0.661
Acetabular Breadth (mm)	0.003	0.661	0.749
VSA (°)	0.999	-0.004	-0.001

The PC plot for PC2 vs PC3 is displayed as Figure 4.2.4. As the Mann-Whitney U test and K-S test on the VSA measurements showed that this measurement seemed undiagnostic for discriminating between the genera from this sample, PC1, which mainly loaded onto the VSA, was not employed. This PC plot visualises the clustering of the genera, with *Strongylopus*, as suggested by the earlier Mann-Whitney U test and K-S test, clustering on its own with only some minor overlap with *Amnirana* on the negative side of PC2. Although there is overlap between *Tomopterna* and *Amnirana*, there is some slight separation of their respective clusters. There is also clustering within *Amnirana* with 8 specimens generally clustering near the origin of PC2 and 5 other *Amnirana* specimens clustering on the positive side of PC2.

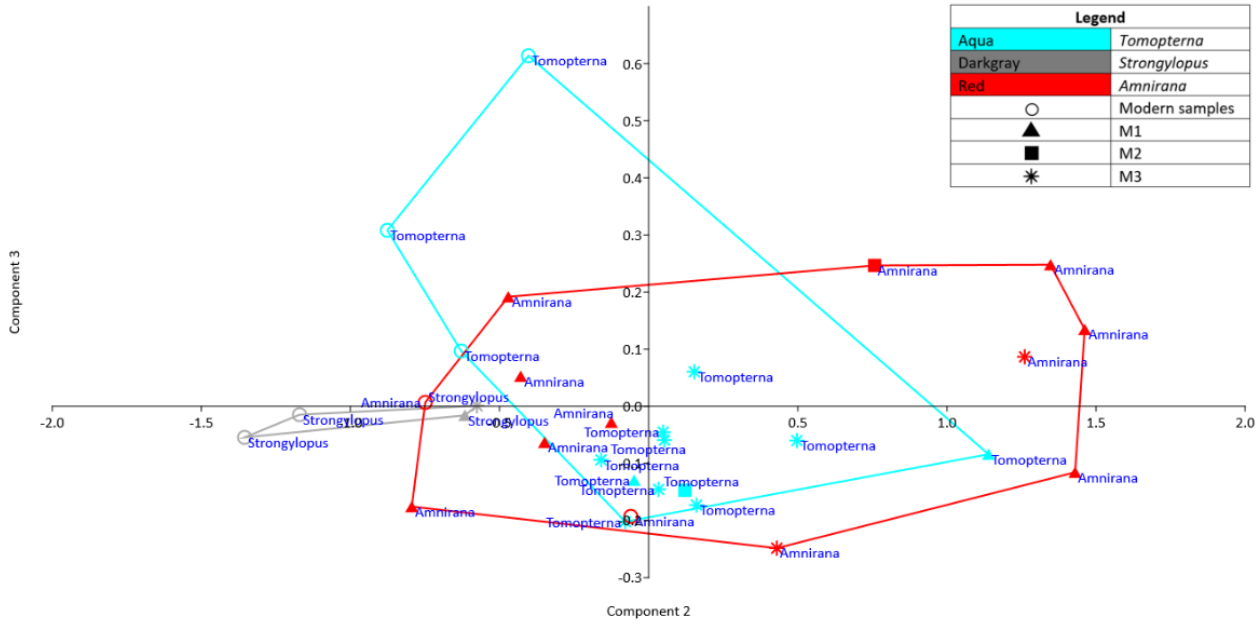

FIG. 4.2.4. *PC2 vs PC3 with convex hulls showing the distribution of the different taxa.*

These two *Amnirana* groups were subjected to two further Mann-Whitney U tests and K-S tests to determine whether there is any statistical significance to the difference in Neck Width and Acetabular Breadth within the *Amnirana* genus from this sample. The Mann-Whitney U test and K-S test on the Neck Width returned p-values of 0.006 and 0.007 respectively whilst the Mann-Whitney U test and K-S test on the Acetabular Breadth returned p-values of 0.001 and 0.004 respectively. The group of five specimens (cluster A) therefore had statistically significant larger measurements for Neck Width and Acetabular Breadth compared to the group of eight (cluster B). These size differences can also been seen in Table 4.2.4 which shows the averages of these measurements for these groups.

Table 4.2.4. *The mean ($\bar{x}$) Neck Width and Acetabular Breadth of the different Amnirana clusters and the deposits from which the specimens in each group originate.*

Mean measurements and numbers per deposit	***Amnirana* cluster of five (A)**	***Amnirana* cluster of eight (B)**
$\bar{x}$ Neck Width (mm)	3,21	2,14
$\bar{x}$ Acetabular Breadth (mm)	3,39	2,21
Number from modern material	0	2
Number from M1	3	5
Number from M2	1	0
Number from M3	1	1

4.3 Geometric Morphometrics and Interlandmark Distances

When comparing the interlandmark distances of the *Tomopterna* and the *Amnirana* specimens, only the interlandmark 5 and 7 distance was normally distributed for both taxa and none of the tests showed that they were statistically significantly different based on that distance. However, the distance of interlandmark 4 and 5 was statistically significant for both the Mann-Whitney U tests and K-S tests, and although it was only normally distributed for the *Tomopterna* specimens, the differences were also statistically significant for the t-tests and F-tests.

Table 4.3.1. *P-values for the t-tests, F-tests, Mann-Whitney U tests, and K-S tests on the interlandmark and Procrustes corrected interlandmark distances between the CT scanned Amnirana and Tomopterna specimens.*

Interlandmark distance	t-test p-value	F-test p-value	Mann-Whitney U test p-value	K-S test p-value
1 and 2	0.45	0.01*	0.78	0.23
2 and 3~	0.93	0.04*	0.71	0.23
3 and 4^	0.90	0.19	0.35	0.49
4 and 5~	<0.01*	0.02*	0.04*	0.01*
5 and 7~^	0.50	0.10	0.97	0.90
7 and 8	0.78	0.02*	0.84	0.53
8 and 9	0.53	0.20	0.44	0.45
9 and 1~	0.70	<0.01*	0.44	0.23
9 and 6	0.20	<0.01*	0.71	0.07
6 and 2	0.31	0.01*	0.84	0.23
6 and 1	0.05	<0.01*	0.35	0.07
2 and 9	0.59	<0.01*	0.97	0.23

**p-values ≤0.05 are statistically significant.*

~Indicates normal distribution for Tomopterna according to either Shapiro-Wilks, Anderson-Darling, and/or Lilliefors tests.

^Indicates normal distribution for Amnirana according to either Shapiro-Wilks, Anderson-Darling, and/or Lilliefors tests.

The Procrustes corrected interlandmark distances had no measurements that were normally distributed for both taxa. The same result was evident as in the normal interlandmark distances, in that the interlandmark 4 and 5 distance is statistically significant. Moreover, interlandmark distance 6 and 1 was also statistically significant, showing that when the size variable is removed, the depth of the acetabulum (to the acetabular rim) shows good variation between these taxa. The K-S test for interlandmark distance 9 and 6 also showed a statstically significant difference, indicating the same acetabular difference picked up by interlandmark distance 6 and 1.

Table 4.3.2. *P-values for the t-tests, F-tests, Mann-Whitney U tests, and K-S tests on the Procrustes corrected interlandmark distances between the CT scanned Amnirana and Tomopterna specimens.*

Procrustes Corrected Interlandmark distance	**t-test p-value**	**F-test p-value**	**Mann-Whitney U test p-value**	**K-S test p-value**
1 and 2	0.31	0.22	0.49	0.70
2 and 3	0.956	0.39	0.97	0.99
3 and 4	0.73	0.84	0.84	0.98
4 and 5	<0.01*	0.24	<0.01*	<0.01*
5 and 7	0.13	0.54	0.08	0.05
7 and 8	0.64	0.02*	0.27	0.20
8 and 9^	0.49	0.22	0.71	0.57
9 and 1^	0.67	0.08	0.97	0.57
9 and 6	0.02*	0.02*	0.07	0.01*

6 and 2	0.17	0.70	0.31	0.38
6 and 1~	<0.01*	0.82	<0.01*	<0.01*
2 and 9~	0.47	0.82	0.84	0.49

**p-values ≤0.05 are statistically significant.*

~Indicates normal distribution for Tomopterna according to either Shapiro-Wilks, Anderson-Darling, and/or Lilliefors tests.

^Indicates normal distribution for Amnirana according to either Shapiro-Wilks, Anderson-Darling, and/or Lilliefors tests.

None of the interlandmark distances were normally distributed for the two *Amnirana* clusters. The Mann-Whitney U tests and K-S tests however showed statistical significance for almost all the interlandmark measurements.

Table 4.3.3. *P-values for the t-tests, F-tests, Mann-Whitney U tests, and K-S tests on the interlandmark distances between the CT scanned Amnirana specimens that formed different clusters (cluster of 5 reduced to 4 specimens [A] and cluster of 8 reduced to 5 specimens [B]).*

Interlandmark distance	**t-test p-value**	**F-test p-value**	**Mann-Whitney U test p-value**	**K-S test p-value**
1 and 2	<0.01*	0.89	0.02*	<0.01*
2 and 3	0.06	0.19	0.07	0.05
3 and 4	<0.01*	0.01*	0.04*	0.05
4 and 5	<0.01*	0.18	0.02*	<0.01*
5 and 7	0.02*	0.02*	0.04*	0.05
7 and 8~	<0.01*	0.65	0.02*	<0.01*
8 and 9	0.05*	0.81	0.11	0.26

9 and 1	<0.01*	0.06	0.02*	<0.01*
9 and 6	<0.01*	0.70	0.02*	<0.01*
6 and 2	<0.01*	0.82	0.02*	<0.01*
6 and 1^	<0.01*	0.47	0.02*	<0.01*
2 and 9	<0.01*	0.06	0.02*	<0.01*

**p-values ≤0.05 are statistically significant.*

~Indicates normal distribution for Tomopterna according to either Shapiro-Wilks, Anderson-Darling, and/or Lilliefors tests.

^Indicates normal distribution for Amnirana according to either Shapiro-Wilks, Anderson-Darling, and/or Lilliefors tests.

Although almost all the interlandmark distances proved to be statistically significantly different for the *Amnirana* clusters, the Procrustes corrected interlandmark distances show no statistical significance.

Table 4.3.4. *P-values for the t-tests, F-tests, Mann-Whitney U tests, and K-S tests on the Procrustes corrected interlandmark distances between the CT scanned Amnirana specimens that formed different clusters (cluster of 5 reduced to 4 specimens [A] and cluster of 8 reduced to 5 specimens [B]).*

Interlandmark distance	**t-test p-value**	**F-test p-value**	**Mann-Whitney U test p-value**	**K-S test p-value**
1 and 2	0.24	0.95	0.18	0.26
2 and 3	0.87	0.27	0.90	0.96
3 and 4	0.71	0.18	0.90	0.96
4 and 5	0.96	0.98	0.90	0.88
5 and 7	0.99	0.29	0.90	0.96

7 and 8	0.56	0.08	0.90	0.96
8 and 9^	0.37	0.70	0.54	0.36
9 and 1	0.70	0.91	0.90	0.88
9 and 6	0.95	0.70	0.71	0.36
6 and 2	0.66	0.31	0.71	0.48
6 and 1	0.87	0.53	0.71	0.36
2 and 9	0.49	0.82	0.54	0.88

**p-values ≤0.05 are statistically significant.*

~Indicates normal distribution for Tomopterna according to either Shapiro-Wilks, Anderson-Darling, and/or Lilliefors tests.

^Indicates normal distribution for Amnirana according to either Shapiro-Wilks, Anderson-Darling, and/or Lilliefors tests.

Chapter Five: Discussion and Conclusions

5.1 The Anura Community of Swartkrans Cave and the Palaeoenvironmental Implications

The Anura community of SWK consists of a variety of taxa, with no statistically significant difference between the 2.2 Ma Oldowan (M1) and 960 ka Acheulean deposits (M3) ($F = 1.56$, $p = 0.57$). As such, there is no significant difference in the local paleoenvironment between the two periods, based on the fossil Anura community being the same. There is only a minor possible difference based on the presence of a single *Probreviceps* ilium in the Oldowan deposit. The presence of both *Phrynobatrachus* and *Bufonidae* is the least useful for an environmental reconstruction as their modern counterparts are present in a wide range of habitats. *Amietia* are only found in environments today that have running or standing water, such as ponds, streams, and rivers. Their presence indicates a higher level of ambient moisture. This is further confirmed by the presence of *Xenopus*, which is entirely aquatic and would have required at least some form of permanent waterbody nearby. *Strongylopus* can be found in a variety of environments today, such as grasslands, highlands, and around rocky outcrops, but as their common name suggests, with them being 'stream frogs,' they are generally found in riparian environments today. Although sometimes found in wetter environments, the presence of *Tomopterna* alternatively indicates a much drier environment, being predominantly found in savannahs, grasslands, and even deserts today. When considering these Anura taxa's environmental requirements and the fact that other studies (Bamford 1999; Sewell *et al*. 2019) support the notion of a region with a desiccating environment, these fossil Anura taxa suggest the presence of a perennial flowing waterbody. Presently, the size of the Blaaubank river is much reduced, but it may have been a bigger feature on the landscape in the past. This reconstruction of the environment around SWK supports the results of Pavia's (2020) study on birds from the nearby site of STK, which indicate a large waterbody not too far from the site.

The only taxon that was not present in both deposits, was *Probreviceps*, which was represented by a single ilium in the Oldowan deposit. Although it is only a single ilium, its presence suggests that there might have been a slight difference in the environments of the two deposits, despite the Anura community being statistically the same. The most likely scenario is that around the time that the Oldowan deposit was being formed, the environment may have included a thicker woodland component which supported the presence of *Probreviceps*, as that is the only environment in which this taxon is found in today. This would coincide with previous studies that specifically indicate there having been a more forested environment in the Cradle that declined from 2 Ma to 800 ka (Bamford 1999; Sewell *et al*. 2019). However, as this is a single ilium, the assemblage might not be adequately representing the entire population, with its absence in the Acheulean deposit simply being an artefact of taphonomy and/or sampling. This could be investigated with further analyses of the SWK Anura ilia. Another possibility is that earlier *Probreviceps* genera were more adaptable and flexible with regards to their habitat requirements. Assuming the first scenario, and considering the environmental reconstruction based on the other taxa, this confirms some form of woodland around SWK during the time of the formation of the Oldowan deposit, which over the next million years declined to being a mesic grassland environment.

The Cradle region generally experienced a desiccating environment from 2-1 Ma, as was occurring elsewhere in Africa during the Pleistocene. Given the results of this study at SWK, and that of Pavia's (2020) at STK, the area surrounding the Blaaubank river would have provided reprieve for fauna and flora that required higher ambient moisture. As such, it is not surprising that many Hominin fossils dating to the Oldowan and Acheulean periods are found at sites near the Blaaubank river as these are near an area that would be considered a hydro-refugium (Cuthbert *et al*. 2017; Caley *et al*. 2018). This could further assist in explaining why SWK has yielded one of the largest assemblages of *Paranthropus* fossils in the world as these

hominins managed to find reprieve around SWK, with it being one of the few areas where these hominins managed to survive before resource scarcity eventually drove them to extinction around 800 ka. This study shows that during the Pleistocene in Africa, with grasslands spreading and woodlands retracting, the area surrounding SWK is an example of one of the hydro-refugia proposed by Cuthbert *et al*. (2017).

This study has also demonstrated the usefulness of Anura as a proxy for elucidating palaeoenvironments within the greater framework of paleoenvironmental reconstruction. Anura, as well as other microfauna, serve as a proxy that allows researchers to attempt to reconstruct the smaller environments that may exist within a larger environment. Studies that seek to understand the nuanced questions about how or why early hominins and our ancestors interacted with certain parts in a greater environment can use these kinds of proxies to provide powerful insights. As such, this study demonstrated that paleoenvironmental proxies that assist with elucidating information about these micro-environments, like the use of Anura, equips Archaeologists with an additional tool to an ever-growing toolkit for answering questions about our past.

5.2 Linear and Angle Measurements

Three of the six proposed measurements in the identification guide of fossil Anura ilia in southern Africa by Matthews *et al*. (2019) were captured and evaluated on three taxa. Note that many of the results generated were based on a small sample size, i.e., *Amnirana* (N=13), *Tomopterna* (N=14), and *Strongylopus* (N=4) specimens. These results must therefore be treated as explorative rather than definitive as age and sex may result in variation in size within a species. Given the small sample of *Strongylopus* specimens in the analysed sample, the

discussion on the applicability of the measurements focuses on the results obtained for the *Amnirana* and *Tomopterna* specimens.

5.2.1 Measurements

The VSA measurement in *Tomopterna* specimens had a distribution skewed to the right, while in *Amnirana*, it was skewed to the left (Fig. 4.2.3). Despite this, there was still considerable overlap of the measurement, and it proved to be ineffective in distinguishing between the three genera. The VSA measurement relies heavily on preservation of the VAE, an area which was frequently damaged or missing. When recording the VSA measurement, subjectivity was introduced with the need to extrapolate the point to where the VAE extended, based on how large the researcher interpreted the VAE to be. Although care was taken to capture all three measurements in the same observation angle for each specimen, the VSA measurement, in particular, required the observation angle to be changed often to try and plot the points from which to measure the angle as best as possible. It proved to be a problematic measurement to deploy on this sample of ilia.

The Neck Width measurement proved more reliable and was more easily plotted and employed. The distribution plots indicate the possibility of a bimodal distribution for the *Amnirana* specimens (Fig. 4.2.1) which prompted further investigation. The *Tomopterna* distribution for this measurement is normally distributed, albeit slightly kurtotic, due to the small range observed in 8 specimens. The Neck Width measurement may be a useful measurement for distinguishing between fossil taxa as it can show consistency within taxa, as observed in the *Tomopterna* specimens, or it can assist in highlighting potential differences within taxa, as observed in the *Amnirana* specimens.

Like Neck Width, the Acetabular Breadth was easy to measure and plot. The Acetabular Breadth's distributions are also similar to those of the Neck Width (Fig. 4.2.2). However, the

bimodal distribution for the *Amnirana* specimens is further exaggerated, while the *Tomopterna* specimens show a relatively flat normal distribution. This also suggests that it may be a useful measurement for distinguishing between fossil taxa.

The resultant Mann-Whitney U test and K-S test (Table 4.2.2) showed that the VSA measurement did not distinguish between *Amnirana*, *Strongylopus*, or *Tomopterna* specimens. This is expected, given that the VSA relies heavily on the VAE, as an angle needs to be drawn to plot this. The VAE is not often preserved in fossil assemblages, as was the case in this study. As mentioned earlier, the VSA is a highly subjective measurement as the VAE exhibits a large amount of variety at the genus level. As suggested by Matthews *et al*. (2019), it is probably better employed at the species level. As the *Strongylopus* taxon is generally much smaller than the other two taxa, it is not surprising that Neck Width and Acetabular Breadth measurements differentiate it from the other two taxa. Despite being easy to differentiate visually, the size similarity is the reason that Neck Width and Acetabular Breadth measurements failed to distinguish between *Amnirana* and *Tomopterna* specimens. This study shows that running statistical tests on these measurements to differentiate between taxa provides unreliable results because of the variation in size within and amongst taxa. However, it should be noted that, Matthews *et al*. (2019), never explicitly recommends running statistical tests on these measurements. Future researchers therefore need to scrutinise the results of any statistical testing done on absolute measurements on Anura ilia, as Anura sizes vary greatly within and amongst taxa.

5.2.2 PCA

The PCA was run for two reasons. First, to visualise the variation of the most relevant measurements between the analysed genera, and secondly, to investigate the bimodal distributions observed for Neck Width (Fig. 4.2.1) and Acetabular Breadth (Fig 4.2.2)

measurements within the *Amnirana* specimens. The VSA measurement loaded strongly on PC1, with it also explaining more than 99% of the variance. As mentioned earlier, the VAE, and by extension the VSA measurement, is varied within and amongst taxa, hence, this was expected. With the focus being on the other two measurements, the PC plot (Fig. 4.2.4) aided in visualising these two measurements and exploring the clustering responsible for the bimodal distributions.

The *Tomopterna* specimens clustered relatively cohesively, with the three modern samples loading strongly onto the positive side of PC3 and the negative side of PC2. This may indicate a size difference between the modern and fossil samples but was not investigated further as the variation could be due to a large number of unknown variables. The *Amnirana* specimens showed overlap with the fossil *Tomopterna* specimens, with a cluster of five *Amnirana* specimens (cluster A) loading strongly onto the positive side of PC2, away from the other cluster of *Amnirana* specimens (cluster B). As cluster A had at least one specimen from each deposit represented, this does not seem to be the result of differences in deposit. Instead, based on the loadings, and the use of the PC plot to visualise these clusters, it is postulated that it may be the result of different sizes. The potential reason for the size differences is expanded on below.

The statistical testing shows that there was a marked difference between cluster A and cluster B. The size difference could also be observed by comparing mean Neck Width and Acetabular Breadth between the two groups, showing that cluster A was almost a 1/3rd larger in size based on these measurements. The reason(s) for this size difference are numerous, and these clusters may represent different species, differently aged individuals, or exhibit sexual dimorphism, as has been observed in *Xenopus* humeri (Herrel *et al*. 2012). Visually, other than the larger overall size, there are no obvious features that distinguish these two clusters when inspected

under a microscope. Therefore, to test whether this difference in size had some underlying shape variation not observable under microscope, a basic GM analysis was employed.

5.3 Geometric Morphometrics and Interlandmark Distances

GM allows for the analysis of shape variation and has the potential to unpack differences in shape not visible to the human eye. Moreover, GM analysis attempts to eliminate size as a variable, by transforming the plotted landmarks through a Procrustes correction. This is a promising method for attempting to identify shape differences that may be obscured by size, such as the case with *Amnirana* cluster A and cluster B, as reported on here.

To explore whether the interlandmark distances could be used to identify shape differences between the visually distinct ilia from the *Amnirana* and *Tomopterna* specimens, statistical tests were run. These were run in conjunction with tests for normality as two of the statistical tests (namely the t-test and the F-test) were parametric (Field 2018). Only one measurement, interlandmark distance 5 and 7, was normally distributed for both taxa. This lack of normal distribution across the interlandmark distances is possibly an artefact of the small sample size. As such, the results of the t-test and F-test are likely less accurate than those of the Mann-Whitney U test and K-S test, hence, the latter two were interpreted. Only interlandmark distance 4 and 5 (which relates to the width of the ilial shaft) proved to be statistically significant. This is noteworthy, as although these two taxa are visually easy to distinguish, only one of the interlandmark distances illustrates a difference. Unfortunately, the ilial shaft is not frequently preserved in fossil assemblages which potentially limits its use for this purpose. However, this study shows that where it is preserved, it may prove to be a useful feature for the identification purposes of certain taxa.

When size is controlled for using the Procrustes corrected interlandmark distances, more differences appear. Interlandmark distances 4 and 5 become more statistically significant, and

interlandmark distance 9 and 6, as well as 6 and 1 (both of which relate to the shape of the acetabulum) become statistically significant. This reinforces the need to investigate the ilial shaft as a potential feature for identification, but more importantly, it strengthens the argument for using Acetabular Breadth for identification as proposed by Matthews *et al*. (2019). However, the increased findings in statistical significance based on the Procrustes corrected interlandmark distances indicate that statistical tests on absolute measurements might be poor at differentiating between Anura taxa as these rely heavily on size, which is affected by age and/or potentially sex. As such, for future research into shape variation of Anura ilia, a focus on features like the acetabulum is recommended as well as, if possible, using a Procrustes correction to minimise the effects of size.

Moreover, the interlandmark distances between the two *Amnirana* clusters indicate major differences, as all but one interlandmark distance is statistically significant between them. As previously observed, size is the major difference between the two clusters, and the Procrustes correction presents an opportunity to test whether these differences are the result of size, or variation in shape, which may suggest taxonomic differences. However, not one of the tests on the Procrustes corrected interlandmark distances produced a statistically significant result. This is likely because the tests without the Procrustes corrections were influenced by the size difference between the clusters. However, the underlying reason for the size difference cannot be tested for using this method and falls outside of the scope of this study. Despite this, it does show that the use of GM, through the Procrustes correction, has potential for future studies on Anura ilia. It allows for the minimisation of size as a variable and can assist in focusing analyses on shape variation. This is especially true if future studies use it in conjunction with some of the reliable identification features identified in this study, such as the acetabulum (and others indicated by Matthews *et al*. [2019]).

5.4 Limitations and Future Research

One of this dissertation's aims was to test the application of the newly developed identification guide to southern African Anura ilia by Matthews *et al*. (2019). The guide has proven useful in terms of highlighting specific features to look for, and caution is advised when using other features to identify taxa. With some minor additions and changes to this guide, the process flow, developed as part of this study, assisted in identifying taxa within the SWK fossil record, and will assist with future research that involves identifying southern African Anura. However, this process flow (and by extension the taxonomic identifications in this study) is limited with regards to reliance on the preservation of multiple features, which varies between fossil assemblages with different taphonomic histories. It must also be noted that this process flow cannot account for all variations within taxa. When it is applied with the guide by Matthews *et al*. (2019), it should cover a substantial portion of southern African Anura taxa. Moreover, as Gardner and Rage (2016) caution that Anura from this region are poorly understood, there may be multiple variations within and amongst taxa for which knowledge is limited, leading to potentially incorrect identifications. Large gaps remain in our understanding of extant frog populations. For example, the poorly documented relationship between age, sex, and size, affects our ability to analyse fossil assemblages. Future research into other Anura skeletal elements, such as humeri and scapulae, will improve information on Anura from this region, but it will also play a critical role in site specific investigations, such as at SWK to improve the Anura community reconstruction of this study. Furthermore, as with any paleoenvironmental reconstruction that relies on taxonomic uniformitarianism, the ranges of environments occupied by modern Anura taxa might differ from those of their fossil counterparts. Therefore, as we learn more about Anura ilia from this region, this information will need to be refined. However, currently, this study and the resultant process flow, will serve future researchers in the identification of southern African fossil Anura ilia.

Although this study was hampered by sample sizes, insightful results were generated. Matthews *et al*. (2019) suggest recording six measurements when analysing Anura ilia. Of these measurements, two rely on the taxa being recorded possessing a dorsal crest, and another measurement relies on there being a substantial portion of the ilial shaft preserved. This latter scenario is rarely observed in fossil assemblages. Moreover, commonly found taxa in southern African Anura assemblages, like *Tomopterna*, do not have a dorsal crest, and as such, the measurements relying on these features were not assessed in this study. This presents a limitation of this study's ability to fully apply the work of Matthews *et al*. (2019) on a fossil assemblage. However, the other three measurements were recorded, and this study provides preliminary insights into their usefulness, especially regarding the use of the VSA measurement. As the two more useful straight-line measurements are absolute measurements, they are problematic in that there is frequently much size variation within and amongst taxa, and this can be attributed to the issues mentioned previously. However, using GM to run a Procrustes correction to minimise the effects of size on shape variation has proven valuable. For future researchers, this suggests that applying GM to fossil Anura ilia may produce insightful results. Researchers may not necessarily need to pursue a full GM analysis but can simply use a Procrustes correction if size is considered a variable that is influencing or obscuring other facets of their analyses. However, to assess whether there might be an association between shape variation and variables such as age and sex in Anura ilia, future researchers should consider running a full GM analysis instead.

Furthermore, due to the costs of CT scanning, the sample size of CT scanned fossils in this study was relatively small. Despite this small sample size, this explorative study generated preliminary results that could provide more insight when these methods are tested on larger sample sizes. As such, this motivates for the use of more CT scanning in future research on Anura ilia to further test and expand on the conclusions presented herein.

5.5 Conclusions

Previous reconstructions of the Cradle's environment during the Pleistocene describe a desiccating region where woodland environments retracted, and the region became increasingly covered by grasslands. This study analysed the SWK local Anura community from the Oldowan (M1, 2.2 Ma) and Acheulean (M3, 960 ka) deposits. As this palaeoenvironmental reconstruction focuses on Anura which have small home ranges, it presents a picture of the local environment. Results concur with previous studies for the region and suggest that the area around SWK included an abundance of water, possibly in the form of an enlarged Blaaubank River, and would have provided a hydro-refugium in an otherwise dry regional environment. Most of Africa was experiencing aridification and decreasing rainfall at the time, and there was a subsequent spread of grasslands, with resources becoming scarcer. These hydro-refugia, like SWK, would have been critical for the survival of many taxa, including hominins. Early *Homo* managed to endure the harsh African Pleistocene environment, eventually resulting in the rise of our species, *Homo sapiens*, possibly owing to refugia during periods of extreme resource scarcity. Other hominins, specifically *Paranthropus* which has an abundant fossil presence at SWK, would also have depended on such areas. As it has generally been assumed that *Homo* was the more adaptable lineage of hominin, the abundant presence of *Paranthropus* fossils at SWK could be attributed to it being one of the few areas where this hominin managed to survive, before resource scarcity eventually drove them to extinction.

This study shows that the guide developed by Matthews *et al*. (2019) can be successfully applied to the fossil record to identify Anura ilia to taxonomic level. Three of the six proposed measurements were omitted as these rely on the ilial shaft, which is not usually preserved in fossils, and the dorsal crest, which was observed in very few of the taxa used in this study. The evaluated measurements therefore included the VSA, Acetabular Breadth, and Neck Width. Of the three measurements, the VSA was unreliable when applied to fossil ilia. Contrastingly, the

latter two measurements provided useful results, but proved susceptible to being skewed as a consequence of variation in the relative size of specimens. This reiterates that much still remains to be established in terms of the variables affecting variation in size in extant populations. This lack of information therefore complicates interpretations of the fossil record. Due to this issue, CT scanning is suggested as a viable alternative as this enables a Procrustes correction to be performed, thus eliminating the influence of size as a variable on shape variation. In turn, this assists in differentiating taxa based on shape variation alone, and therefore has the potential for distinguishing between taxa and improving our otherwise limited understanding of southern Africa Anura.

References

Altig, R. & Johnston, G. F. 1989. Guilds of anuran larvae: relationships among developmental modes, morphologies, and habitats. *Herpetological Monographs* 3: 81–109.

Archibald, K.E., Minter, L.J., Dombrowski, D.S., O'Brien, J.L. & Lewbart, G.A. 2015. Cystic urolithiasis in captive waxy monkey frogs (*Phyllomedusa sauvagii*). *Journal of Zoo and Wildlife Medicine* 46(1): 105–112.

Asfaw, B., White, T., Lovejoy, O., Latimer, B., Simpson, S. & Suwa, G. 1999. *Australopithecus garhi*: a new species of early hominid from Ethiopia. *Science* 284(5414): 629–635.

Avery, D.M. 2001. The Plio-Pleistocene vegetation and climate of Sterkfontein and Swartkrans, South Africa, based on micromammals. *Journal of Human Evolution* 41(2): 113–132.

Avery, D.M. 2007. Micromammals as palaeoenvironmental indicators of the southern African Quaternary. *Transactions of the Royal Society of South Africa* 62(1): 17–23.

Avery, D.M. 2021. Micromammals and the Late Quaternary of southern Africa. *South African Journal of Geology* 124(4): 1073–1082.

Balter, V., Blichert-Toft, J., Braga, J., Telouk, P., Thackeray, F. & Albarède, F. 2008. U–Pb dating of fossil enamel from the Swartkrans Pleistocene hominid site, South Africa. *Earth and Planetary Science Letters* 267(1-2): 236–246.

Bamford, M. 1999. Pliocene fossil woods from an early hominid cave deposit, Sterkfontein, South Africa. *South African Journal of Science* 95(5): 231–237.

Bamford, M.K., Neumann, F.H., Pereira, L.M., Scott, L., Dirks, P.H.G.M. & Berger, L.R. 2010. Botanical remains from a coprolite from the Pleistocene hominin site of Malapa, Sterkfontein Valley, South Africa. *Palaeontologia Africana* 45: 23–28.

Beaumont, P.B. 2011. The edge: more on fire-making by about 1.7 million years ago at Wonderwerk Cave in South Africa. *Current Anthropology* 52(4): 585–595.

Blain, H.A., Agustí, J., Lordkipanidze, D., Rook, L. & Delfino, M. 2014. Paleoclimatic and paleoenvironmental context of the Early Pleistocene hominins from Dmanisi (Georgia, Lesser Caucasus) inferred from the herpetofaunal assemblage. *Quaternary Science Reviews* 105: 136–150.

Blain, H.A., Bailon, S. & Cuenca-Bescós, G. 2008. The Early–Middle Pleistocene palaeoenvironmental change based on the squamate reptile and amphibian proxies at the Gran Dolina site, Atapuerca, Spain. *Palaeogeography, Palaeoclimatology, Palaeoecology* 261(1-2): 177–192.

Blain, H.A., Fagoaga, A., Sánchez-Bandera, C., Ruiz-Sánchez, F.J., Sindaco, R. & Delfino, M. 2022. New paleoecological inferences based on the Early Pleistocene amphibian and reptile assemblage from Dmanisi (Georgia, Lesser Caucasus). *Journal of Human Evolution* 162:103117.

Blain, H.A., Gleed-Owen, C.P., López-García, J.M., Carrión, J.S., Jennings, R., Finlayson, G., Finlayson, C. & Giles-Pacheco, F. 2013. Climatic conditions for the last Neanderthals: herpetofaunal record of Gorham's Cave, Gibraltar. *Journal of Human Evolution* 64(4): 89–299.

Brophy, J.K. 2004. Preliminary report on the faunal remains and taphonomic analysis of Plover's Lake Cave, Cradle of Humankind, South Africa. Unpublished Masters thesis. Knoxville: The University of Tennessee.

Brophy, J.K., de Ruiter, D.J., Fortelius, M., Bamford, M. & Berger, L.R. 2016. Pleistocene *Bovidae* (Mammalia) from Malapa, Gauteng province, South Africa. *Palaeontologia Electronica* 19: 1–22.

Caley, T., Extier, T., Collins, J.A., Schefuß, E., Dupont, L., Malaizé, B., Rossignol, L., Souron, A., McClymont, E.L., Jimenez-Espejo, F.J. & García-Comas, C. 2018. A two-million-year-long hydroclimatic context for hominin evolution in southeastern Africa. *Nature* 560(7716): 76–79.

Campisano, C.J. 2012. Milankovitch cycles, paleoclimatic change, and hominin evolution. *Nature Education and Knowledge* 4(3): 5

Carruthers, V. 2019. Cradle of Life: *The Story of the Magaliesberg and the Cradle of Humankind*. South Africa: Struik.

Carruthers, V. & Du Preez, L. 2017. *Frogs of Southern Africa – A Complete Guide*. South Africa: Penguin Random House.

Cerling, T.E., Wynn, J.G., Andanje, S.A., Bird, M.I., Korir, D.K., Levin, N.E., Mace, W., Macharia, A.N., Quade, J. & Remien, C.H. 2011. Woody cover and hominin environments in the past 6 million years. *Nature* 476(7358): 51–56.

Channing, A. 2011. Distribution and conservation status of the desert rain frog *Breviceps macrops*. *African Journal of Herpetology* 60(2): 101–112.

Channing, A. & Rödel, M.O. 2019. *Field Guide to the Frogs & Other Amphibians of Africa*. South Africa: Penguin Random House.

Chase, B.M., Meadows, M.E., Scott, L., Thomas, D.S.G., Marais, E., Sealy, J. & Reimer, P.J. 2009. A record of rapid Holocene climate change preserved in hyrax middens from southwestern Africa. *Geology* 37(8): 703–706.

Churchill, S.E., Green, D.J., Feuerriegel, E.M., Macias, M.E., Mathews, S., Carlson, K.J., Schmid, P. & Berger, L. 2018. The shoulder, arm, and forearm of *Australopithecus sediba*. *PaleoAnthropology* 2018: 234–281.

Comay, O. & Dayan, T. 2018. From micromammals to paleoenvironments. *Archaeological and Anthropological Sciences* 10(8): 2159–2171.

Constantino, P.J., Borrero-Lopez, O. & Lawn, B.R. 2018. Mechanisms of tooth damage and *Paranthropus* dietary reconstruction. *Biosurface and Biotribology* 4(3): 73–78.

Crump, M. L. 2015. Anuran reproductive modes: evolving perspectives. *Journal of Herpetology*, 49(1): 1–16.

Cruz-Uribe, K., Klein, R.G., Avery, G., Avery, M., Halkett, D., Hart, T., Milo, R.G., Sampson, C.G. & Volman, T.P. 2003. Excavation of buried late Acheulean (Mid-Quaternary) land surfaces at Duinefontein 2, Western Cape province, South Africa. *Journal of Archaeological Science* 30(5): 559–575.

Cuthbert, M.O., Gleeson, T., Reynolds, S.C., Bennett, M.R., Newton, A.C., McCormack, C.J. & Ashley, G.M. 2017. Modelling the role of groundwater hydro-refugia in East African hominin evolution and dispersal. *Nature Communications* 8(1): 1–11

DeGusta, D. & Vrba, E. 2003. A method for inferring paleohabitats from the functional morphology of bovid astragali. *Journal of Archaeological Science* 30(8): 1009–1022.

Delfino, M. 2020. Early Pliocene anuran fossils from Kanapoi, Kenya, and the first fossil record for the African burrowing frog *Hemisus* (Neobatrachia: *Hemisotidae*). *Journal of Human Evolution* 140:102353.

Domínguez-Rodrigo, M. & Musiba, C.M. 2010. How accurate are paleoecological reconstructions of early paleontological and archaeological sites? *Evolutionary Biology* 37(2): 128–140.

Donges, J.F., Donner, R.V., Trauth, M.H., Marwan, N., Schellnhuber, H.J. & Kurths, J. 2011. Nonlinear detection of paleoclimate-variability transitions possibly related to human evolution. *Proceedings of the National Academy of Sciences* 108(51): 20422–20427.

Drewry, G. E. & Jones, K. L. 1976. A new ovoviviparous frog, *Eleutherodactylus jasperi* (Amphibia, Anura, *Leptodactylidae*), from Puerto Rico. *Journal of Herpetology* 10(3): 161–165.

Faith, J.T., Chase, B.M. & Avery, D.M. 2019. Late Quaternary micromammals and the precipitation history of the southern Cape, South Africa. *Quaternary Research* 91(2): 848–860.

Faith, J.T. & Behrensmeyer, A.K. 2013. Climate change and faunal turnover: testing the mechanics of the turnover-pulse hypothesis with South African fossil data. *Paleobiology* 39(4): 609–627.

Ferring, R., Oms, O., Agustí, J., Berna, F., Nioradze, M., Shelia, T., Tappen, M., Vekua, A., Zhvania, D. & Lordkipanidze, D. 2011. Earliest human occupations at Dmanisi (Georgian Caucasus) dated to 1.85–1.78 Ma. *Proceedings of the National Academy of Sciences* 108(26):10432–10436.

Field, A. 2018. *Discovering Statistics Using IBM SPSS Statistics*. London: SAGE.

Franz-Odendaal, T.A., Lee-Thorp, J.A. & Chinsamy, A. 2002. New evidence for the lack of C4 grassland expansions during the early Pliocene at Langebaanweg, South Africa. *Paleobiology* 28(3): 378–388.

Frost, D. 2022. Amphibian species of the world 6.0, viewed November 2022, from *http://research.amnh.org/vz/herpetology/amphibia*

Gardner, J. D. & Rage, J. C. 2016. The fossil record of lissamphibians from Africa, Madagascar, and the Arabian Plate. *Palaeobiodiversity and Palaeoenvironments* 96(1): 169–220.

Gervasi, S. S. & Foufopoulos, J. 2008. Costs of plasticity: responses to desiccation decrease post-metamorphic immune function in a pond-breeding amphibian. *Functional Ecology* 22: 100–108.

Gibbon, R.J., Pickering, T.R., Sutton, M.B., Heaton, J.L., Kuman, K., Clarke, R.J., Brain, C.K. & Granger, D.E. 2014. Cosmogenic nuclide burial dating of hominin-bearing Pleistocene cave deposits at Swartkrans, South Africa. *Quaternary Geochronology* 24: 10–15.

Gómez, R.O. & Turazzini, G.F. 2016. An overview of the ilium of anurans (Lissamphibia, Salientia), with a critical appraisal of the terminology and primary homology of main ilial features. *Journal of Vertebrate Paleontology* 36(1): 1030023.

Gornitz, V. 2009. Paleoclimate Proxies, An Introduction. In: Gornitz, V. (ed) *Encyclopedia of Paleoclimatology and Ancient Environments. Encyclopedia of Earth Sciences Series*: 716–721. Netherlands: Springer.

Granger, D.E., Gibbon, R.J., Kuman, K., Clarke, R.J., Bruxelles, L. & Caffee, M.W. 2015. New cosmogenic burial ages for Sterkfontein member 2 Australopithecus and member 5 Oldowan. *Nature* 522(7554): 85–88.

Grine, F.E. & Susman, R.L. 1991. Radius of *Paranthropus robustus* from member 1, Swartkrans formation, South Africa. *American Journal of Physical Anthropology* 84(3): 229–248.

Heatwole, H., Cameron, E. & Webb, G.J. 1971. Studies on anuran water balance: II. Desiccation in the Australian frog, *Notaden bennetti*. *Herpetologica* 27(4):365–378.

Herrel A., Gonwouo L.N., Fokam E.B., Ngundu, W.I. & Bonneaud, C. 2012. Intersexual differences in body shape and locomotor performance in the aquatic frog, *Xenopus tropicalis*. *Journal of Zoology.* 287(4): 311–316.

Herries, A.I., Martin, J.M., Leece, A.B., Adams, J.W., Boschian, G., Joannes-Boyau, R., Edwards, T.R., Mallett, T., Massey, J., Murszewski, A. & Neubauer, S. 2020. Contemporaneity of *Australopithecus, Paranthropus*, and early *Homo erectus* in South Africa. *Science* 368(6486): eaaw7293.

Herries, A. I. R. & Shaw, J. 2011. Palaeomagnetic analysis of the Sterkfontein palaeocave deposits: implications for the age of the hominin fossils and stone tool industries. *Journal of Human Evol*ution 60: 523–539.

Holland, M. & Witthüser, K.T. 2009. Geochemical characterization of karst groundwater in the Cradle of Humankind World Heritage Site, South Africa. *Environmental Geology* 57(3): 513–524.

Hopley, P., Vermeesch, P., Parrish, R. & Latham, A. 2021. Clusters of flowstone ages are not supported by statistical evidence. *Nature* 594(7863): E10.

Iskandar, D. T., Evans, B. J. & McGuire, J. A. 2014. Novel reproductive mode in frogs: a new species of fanged frog with internal fertilization and birth of tadpoles. *PLoS One* 9(12): e115884.

Jacobs, Z., Jones, B.G., Cawthra, H.C., Henshilwood, C.S. & Roberts, R.G. 2020. The chronological, sedimentary and environmental context for the archaeological deposits at Blombos Cave, South Africa. *Quaternary Science Reviews* 235:105850.

Kivell, T.L., Kibii, J.M., Churchill, S.E., Schmid, P. & Berger, L.R. 2011. *Australopithecus sediba* hand demonstrates mosaic evolution of locomotor and manipulative abilities. *Science* 333(6048): 1411–1417.

Klein, R.G. 1976. A preliminary report on the 'Middle Stone Age' open-air site of Duinefontein 2 [Melkbosstrand, South-Western Cape province, South Africa]. *The South African Archaeological Bulletin* 31(121-122): 12–20.

Klein, R.G., Avery, G., Cruz-Uribe, K., Halkett, D., Hart, T., Milo, R.G. & Volman, T.P. 1999. Duinefontein 2: an Acheulean site in the Western Cape province of South Africa. *Journal of Human Evolution* 37(2): 153–190.

Kramers, J. D. & Dirks, P. H. G. M. 2017. The age of fossil StW573 ('Little Foot'): an alternative interpretation of 26Al/10Be burial data. *South African. Journal of Sci*ence 113(3-4): 1–8.

Kuman, K., Granger, D.E., Gibbon, R.J., Pickering, T.R., Caruana, M.V., Bruxelles, L., Clarke, R.J., Heaton, J.L., Stratford, D. & Brain, C.K. 2021. A new absolute date from Swartkrans Cave for the oldest occurrences of *Paranthropus robustus* and Oldowan stone tools in South Africa. *Journal of Human Evolution* 156:103000.

Lee-Thorp, J., Thackeray, J.F. & Van der Merwe, N. 2000. The hunters and the hunted revisited. *Journal of Human Evolution* 39(6):565–576.

Lee-Thorp, J.A., Sponheimer, M. & Luyt, J. 2007. Tracking changing environments using stable carbon isotopes in fossil tooth enamel: an example from the South African hominin sites. *Journal of Human Evolution* 53(5): 595–601.

Lee-Thorp, J.A., Van der Merwe, N.J. & Brain, C.K. 1994. Diet of *Australopithecus robustus* at Swartkrans from stable carbon isotopic analysis. *Journal of Human Evolution* 27(4): 361–372.

Leichliter, J., Sandberg, P., Passey, B., Codron, D., Avenant, N.L., Paine, O.C., Codron, J., de Ruiter, D. & Sponheimer, M. 2017. Stable carbon isotope ecology of small mammals from the Sterkfontein Valley: implications for habitat reconstruction. *Palaeogeography, Palaeoclimatology, Palaeoecology* 485: 57–67.

Linnaeus, C. 1758. *Systema Naturae.* Stockholm: Laurentii Salvii.

Lycett, S.J. & Gowlett, J.A. 2008. On questions surrounding the Acheulean 'tradition'. *World Archaeology* 40(3): 295–315.

Marean, C.W., Cowling, R.M. & Franklin, J. 2020. The Palaeo-Agulhas Plain: temporal and spatial variation in an extraordinary extinct ecosystem of the Pleistocene of the Cape Floristic Region. *Quaternary Science Reviews* 235: 106161

Matthews, T., Curtis, C.W. & Cleghorn, N. 2020. Past and present distributions and community evolution of *Muridae* and *Soricidae* from MIS 9 to MIS 1 on the edge of the Palaeo-Agulhas Plain, south coast, South Africa. *Quaternary Science Reviews* 235: 105774

Matthews, T., John Measey, G. & Roberts, D.L. 2016. Implications of summer breeding frogs from Langebaanweg, South Africa: regional climate evolution at 5.1 mya. *South African Journal of Science* 112(9-10): 1–7.

Matthews, T., Keeffe, R. & Blackburn, D. C. 2019. An identification guide to fossil frog assemblages of southern Africa based on ilia of extant taxa. *Zoologischer Anzeiger* 283: 46–57.

Matthews, T., Rector, A., Jacobs, Z., Herries, A.I. & Marean, C.W. 2011. Environmental implications of micromammals accumulated close to the MIS 6 to MIS 5 transition at Pinnacle Point cave 9 (Mossel Bay, Western Cape province, South Africa). *Palaeogeography, Palaeoclimatology, Palaeoecology* 302(3-4): 213–229.

Matthews, T., van Dijk, E., Roberts, D.L. & Smith, R.M. 2015. An early Pliocene (5.1 Ma) fossil frog community from Langebaanweg, south-western Cape, South Africa. *African Journal of Herpetology* 64(1): 39–53.

Meadows, M.E., Chase, B.M. & Seliane, M. 2010. Holocene palaeoenvironments of the Cederberg and Swartruggens mountains, Western Cape, South Africa: pollen and stable isotope evidence from hyrax dung middens. *Journal of Arid Environments* 74(7): 786–793.

Merceron, G., Zazzo, A., Spassov, N., Geraads, D. & Kovachev, D. 2006. Bovid paleoecology and paleoenvironments from the Late Miocene of Bulgaria: evidence from dental microwear and stable isotopes. *Palaeogeography, Palaeoclimatology, Palaeoecology* 241(3-4): 637–654.

Minter, L.R. 1999. Aspects of the reproductive biology of *Breviceps*. Unpublished PhD thesis. Johannesburg: University of the Witwatersrand.

Mörs, T., Reguero, M. & Vasilyan, D. 2020. First fossil frog from Antarctica: implications for Eocene high latitude climate conditions and Gondwanan cosmopolitanism of Australobatrachia. *Scientific Reports* 10(1): 1–11.

Nel, T.H., Wurz, S. & Henshilwood, C.S. 2018. Small mammals from marine isotope stage 5 at Klasies River, South Africa–reconstructing the local palaeoenvironment. *Quaternary International* 471: 6–20.

Nowacki, A. 2017. Chi-square and Fisher's exact tests. *Cleveland Clinic Journal of Medicine* 84(2): e20.

Olson, S.L. & Rasmussen, D.T. 1986. Paleoenvironment of the earliest hominoids: new evidence from the Oligocene avifauna of Egypt. *Science* 233(4769): 1202–1204.

Özçomak, M.S., Kartal, M., Senger, Ö. & Çelik, A.K. 2013. Comparison of the powers of the Kolmogorov-Smirnov two-sample test and the Mann-Whitney test for different kurtosis and skewness coefficients using the Monte Carlo simulation method. *Journal of Statistical and Econometric Methods* 2(4): 81–98.

Partridge, T.C. 1978. Re-appraisal of lithostratigraphy of Sterkfontein hominid site. *Nature* 275(5678): 282–287.

Pavia, M. 2020. Palaeoenvironmental reconstruction of the Cradle of Humankind during the Plio-Pleistocene transition, inferred from the analysis of fossil birds from member 2 of the hominin-bearing site of Kromdraai (Gauteng, South Africa). *Quaternary Science Reviews* 248: 106532.

Peter, B.D. 2004. African climate change and faunal evolution during the Pliocene–Pleistocene. *Earth and Planetary Science Letters* 220(1-2): 3–24.

Peterson, A., Abella, E.F., Grine, F.E., Teaford, M.F. & Ungar, P.S. 2018. Microwear textures of *Australopithecus africanus* and *Paranthropus robustus* molars in relation to paleoenvironment and diet. *Journal of Human Evolution* 119: 42–63.

Philander, S.G. & Fedorov, A.V. 2003. Role of tropics in changing the response to Milankovich forcing some three million years ago. *Paleoceanography* 18(2): 1045.

Pickering, R., Herries, A.I., Woodhead, J.D., Hellstrom, J.C., Green, H.E., Paul, B., Ritzman, T., Strait, D.S., Schoville, B.J. & Hancox, P.J. 2019. U–Pb-dated flowstones restrict South African early hominin record to dry climate phases. *Nature* 565(7738): 226–229.

Pickering, R. & Herries, A.I. 2020. A New Multidisciplinary Age of 2.61-2.07 Ma for the Sterkfontein Member 4 Australopiths. In: Richmond, B.G., Ward, C.V. & Zipfel, B. (eds) *Hominin Postcranial Remains from Sterkfontein, South Africa 1936–1995*: 21–30. USA: Oxford University Press.

Pickering, R., Herries, A.I., Woodhead, J.D., Hellstrom, J.C., Green, H.E., Paul, B., Ritzman, T., Strait, D.S., Schoville, B.J. & Hancox, J. 2021. Reply to: clusters of flowstone ages are not supported by statistical evidence. *Nature* 594(7863): E11.

Pickering, R., Kramers, J.D., Hancox, P.J., de Ruiter, D.J. & Woodhead, J.D. 2011. Contemporary flowstone development links early hominin bearing cave deposits in South Africa. *Earth and Planetary Science Letters* 306(1-2): 23–32.

Potts, R. 2013. Hominin evolution in settings of strong environmental variability. *Quaternary Science Reviews* 73: 1–13.

Reed, K.E. 1998. Using large mammal communities to examine ecological and taxonomic structure and predict vegetation in extant and extinct assemblages. *Paleobiology* 24(3): 384–408.

Reynolds, S.C. & Kibii, J.M. 2011. Sterkfontein at 75: review of paleoenvironments, fauna, dating and archaeology from the hominin site of Sterkfontein (Gauteng province, South Africa). *Palaeontologia Africana* 46: 59–88.

Roelants, K., Haas, A. & Bossuyt, F. 2011. Anuran radiations and the evolution of tadpole morphospace. *Proceedings of the National Academy of Sciences* 108(21): 8731–8736.

Rossouw, L., Stynder, D.D. & Haarhof, P. 2009. Evidence for opal phytolith preservation in the Langebaanweg 'E' Quarry Varswater formation and its potential for palaeohabitat reconstruction. *South African Journal of Science* 105(5-6): 223–227.

Ryan, T.M., Carlson, K.J., Gordon, A.D., Jablonski, N., Shaw, C.N. & Stock, J.T. 2018. Human-like hip joint loading in *Australopithecus africanus* and *Paranthropus robustus*. *Journal of Human Evolution* 121: 12–24.

Sampson, C.G. 2003. Amphibians from the Acheulean site at Duinefontein 2 (Western Cape, South Africa). *Journal of Archaeological Science* 30(5): 547–557.

Sánchez-Bandera, C., Oms, O., Blain, H.A., Lozano-Fernández, I., Bisbal-Chinesta, J.F., Agustí, J., Saarinen, J., Fortelius, M., Titton, S., Serrano-Ramos, A. & Luzón, C. 2020. New stratigraphically constrained palaeoenvironmental reconstructions for the first human settlement in Western Europe: the Early Pleistocene herpetofaunal assemblages from Barranco León and Fuente Nueva 3 (Granada, SE Spain). *Quaternary Science Reviews* 243: 106466.

Sandberger, L., Hillers, A., Doumbia, J., Loua, N.S., Brede, C. & Roedel, M.O. 2010. Rediscovery of the Liberian Nimba toad, *Nimbaphrynoides liberiensis* (Xavier, 1978) (Amphibia: Anura: *Bufonidae*), and reassessment of its taxonomic status. *Zootaxa* 2355(1): 56–68.

Savriama, Y. 2018. A step-by-step guide for geometric morphometrics of floral symmetry. *Frontiers in Plant Science* 9: 1433.

Schick, K. & Toth, N. 2006. An Overview of the Oldowan Industrial Complex: The Sites and the Nature of Their Evidence. In: Schick, K. & Toth, N. (eds) *The Oldowan: Case Studies into the Earliest Stone Age*: 3–42. USA: Stone Age Institute Press.

Schoeninger, M.J., Reeser, H. & Hallin, K. 2003. Paleoenvironment of *Australopithecus anamensis* at Allia Bay, East Turkana, Kenya: evidence from mammalian herbivore enamel stable isotopes. *Journal of Anthropological Archaeology* 22(3): 200–207.

Semprebon, G.M. & Rivals, F. 2007. Was grass more prevalent in the pronghorn past? An assessment of the dietary adaptations of Miocene to recent *Antilocapridae* (Mammalia: Artiodactyla). *Palaeogeography, Palaeoclimatology, Palaeoecology* 253(3-4): 332–347.

Sewell, L. 2019. Using a multiproxy analysis of springbok fossils to track 2 million years of vegetation changes experienced by hominins in southern Africa. Unpublished PhD thesis. Bournemouth: Bournemouth University.

Sobol, M.K., Chazan, M., Scott, L. & Finkelstein, S.A. 2022. Characterizing the Meghalayan stage in southern Africa: a multiproxy record of paleoenvironmental change at the southern margin of the Kalahari. *Quaternary International* 614: 98–110.

Sponheimer, M., Reed, K.E. & Lee-Thorp, J.A. 1999. Combining isotopic and ecomorphological data to refine bovid paleodietary reconstruction: a case study from the Makapansgat Limeworks hominin locality. *Journal of Human Evolution* 36(6): 705–718.

Sponheimer, M., Passey, B.H., De Ruiter, D.J., Guatelli-Steinberg, D., Cerling, T.E. & Lee-Thorp, J.A. 2006. Isotopic evidence for dietary variability in the early hominin *Paranthropus robustus*. *Science* 314(5801): 980–982.

Steininger, C.M. 2011. The dietary behaviour of early Pleistocene bovids from Cooper's Cave and Swartkrans, South Africa. Unpublished PhD thesis. Johannesburg: University of the Witwatersrand.

Stratford, D., Bruxelles, L., Francis Thackeray, J., Pickering, T.R. & Verheyden, S. 2020. Comments on 'U-Pb dated flowstones restrict South African early hominin record to dry climate phases' (Pickering *et al*. Nature 2018; 565: 226-229). *South African Journal of Science* 116(3-4): 1–2.

Strobel, P., Bliedtner, M., Carr, A.S., Frenzel, P., Klaes, B., Salazar, G., Struck, J., Szidat, S., Zech, R. & Haberzettl, T. 2021. Holocene sea level and environmental change at the southern Cape – an 8.5 kyr multi-proxy paleoclimate record from lake Voëlvlei, South Africa. *Climate of the Past* 17(4): 1567–1586.

Stringer, C. 2012. What makes a modern human. *Nature* 485(7396): 33–35.

Stynder, D.D. 2011. Fossil bovid diets indicate a scarcity of grass in the Langebaanweg E Quarry (South Africa) late Miocene/early Pliocene environment. *Paleobiology* 37(1): 126–139.

Tattersall, I. 2007. *Homo ergaster* and its contemporaries. *Handbook of Paleoanthropology* 3: 1633–53.

Tracy, C. R., Christian, K. A. & Tracy, C. R. 2010. Not just small, wet, and cold: effects of body size and skin resistance on thermoregulation and arboreality of frogs. *Ecology* 91(5): 1477–1484.

Trauth, M.H., Maslin, M.A., Deino, A.L., Strecker, M.R., Bergner, A.G. & Dühnforth, M. 2007. High-and low-latitude forcing of Plio-Pleistocene East African climate and human evolution. *Journal of Human Evolution* 53(5): 475–486.

Vaks, A., Bar-Matthews, M., Ayalon, A., Matthews, A., Frumkin, A., Dayan, U., Halicz, L., Almogi-Labin, A. & Schilman, B. 2006. Paleoclimate and location of the border

between Mediterranean climate region and the Saharo–Arabian Desert as revealed by speleothems from the northern Negev Desert, Israel. *Earth and Planetary Science Letters* 249(3-4): 384–399.

Vincent, T. 2021. A multi-proxy palaeoenvironmental reconstruction of the Homa Peninsula, Western Kenya. Unpublished PhD thesis. Liverpool: Liverpool John Moores University.

Vrba, E.S. 1974. Chronological and ecological implications of the fossil *Bovidae* at the Sterkfontein Australopithecine site. *Nature* 250(5461): 19–23.

Vrba, E.S. 1975. Some evidence of chronology and palaeoecology of Sterkfontein, Swartkrans and Kromdraai from the fossil *Bovidae*. *Nature* 254(5498): 301–304.

Vrba, E.S. 1985. Ecological and Adaptive Changes Associated with Early Hominid Evolution. In: Delson, E. (ed) *Ancestors: The Hard Evidence*: 63–71. USA: Alan R. Liss.

Vrba, E.S.1993. Turnover-pulses, the Red Queen, and related topics. *American Journal of Science* 293(A):418–452.

Wake, M. H. 1980. The reproductive biology of *Nectophrynoides malcolmi* (Amphibia: *Bufonidae*), with comments on the evolution of reproductive modes in the genus *Nectophrynoides*. *Copeia* 1980(2): 193–209.

Wang, Y., Kromhout, E., Zhang, C., Xu, Y., Parker, W., Deng, T. & Qiu, Z. 2008. Stable isotopic variations in modern herbivore tooth enamel, plants and water on the Tibetan Plateau: implications for paleoclimate and paleoelevation reconstructions. *Palaeogeography, Palaeoclimatology, Palaeoecology* 260(3-4): 359–374.

Williams, H.M., Lee-Thorp, J.A., Matthews, T. & Marean, C.W. 2020. Micromammal and macromammal stable isotopes from a MIS 6 fossil hyena den (Pinnacle Point site 30, south coast, South Africa) reveal differences in relative contribution of C4 grasses to local and regional palaeovegetation on the Palaeo-Agulhas Plain. *Quaternary Science Reviews* 235: 106201.

Wood, B. & Baker, J. 2011. Evolution in the genus Homo. *Annual Review of Ecology, Evolution, and Systematics* 42: 47–69.

Wood, B. & Constantino, P. 2007. *Paranthropus boisei*: fifty years of evidence and analysis. *American Journal of Physical Anthropology* 134(S45): 106–132.

Wurz, S., Bentsen, S.E., Reynard, J., Van Pletzen-Vos, L., Brenner, M., Mentzer, S., Pickering, R. & Green, H. 2018. Connections, culture and environments around 100 000 years ago at Klasies River main site. *Quaternary International* 495: 102–115.

Yetman, C.A. & Ferguson, J.W.H. 2011. Spawning and non-breeding activity of adult giant bullfrogs (*Pyxicephalus adspersus*). *African Journal of Herpetology* 60(1): 13–29.

Zhang, P., Liang, D., Mao, R. L., Hillis, D. M., Wake, D. B. & Cannatella, D. C. 2013. Efficient sequencing of anuran mtDNAs and a mitogenomic exploration of the phylogeny and evolution of frogs. *Molecular Biology and Evolution* 30(8): 1899–1915.

Zhu, Z., Dennell, R., Huang, W., Wu, Y., Qiu, S., Yang, S., Rao, Z., Hou, Y., Xie, J., Han, J. & Ouyang, T. 2018. Hominin occupation of the Chinese Loess Plateau since about 2.1 million years ago. *Nature* 559(7715): 608–612.

Appendices

Appendix A

Images shared by Dr Thalassa Matthews showing the distinct morphologies of the five genera that do not require the process flow to identify as they have unique acetabula morphologies. Note that these are not to scale and the purpose of this is to assist with a simple visual distinction between these five genera:

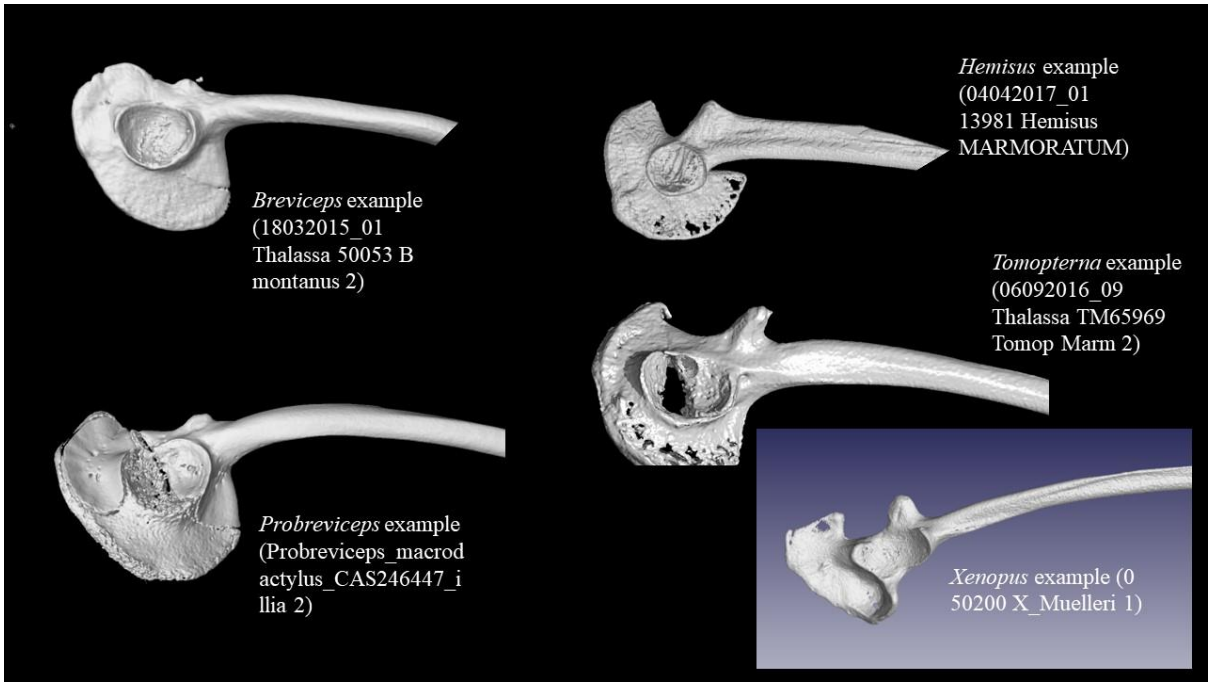

FIG. A1. *The five genera that are morphologically unique and can easily be distinguished based on the shape of their acetabula (not to scale), shared by Dr Thalassa Matthews.*

Appendix B

Table B1. *The Taxonomic Identifications of the Wits Sample**

*with the TJCD Sample omitted as the researchers who shared this data did not want it published yet

**all of these were sided for the MNI counts in Table 4.1.1

Short Specimen code (bag #-# from bag)	**Long Specimen Code**	**Sample Origin**	**Bag Number**	**CT scanned?**	**Side (if CT scanned)****	**Family**	**Genus**	**Species**	**Deposit**
01-IO1	SWK_M101-IO1	Wits Sample	1	No	NA	*Pyxicephalidae*	*Tomopterna*	*tandyi*	M1
01-IO2	SWK_M101-IO2	Wits Sample	1	No	NA	*Pyxicephalidae*	*Tomopterna*	*indet.*	M1
06-IO1	SWK_M106-IO1	Wits Sample	6	No	NA	*Ranidae*	*Amnirana*	*indet.*	M1
07-IO1	SWK_M107-IO1	Wits Sample	7	Yes	Left	*Ranidae*	*Amnirana*	*indet.*	M1
07-IO2	SWK_M107-IO2	Wits Sample	7	No	NA	*Ranidae*	*Amnirana*	*indet.*	M1
08-IO1	SWK_M108-IO1	Wits Sample	8	No	NA	*Pipidae*	*Xenopus*	*indet.*	M1
09-IO1	SWK_M109-IO1	Wits Sample	9	Yes	Left	*Pyxicephalidae*	*Tomopterna*	*tandyi*	M1
12-IO1	SWK_M112-IO1	Wits Sample	12	No	Right	*Pyxicephalidae*	*Tomopterna*	*delalandii*	M1
17-IO1	SWK_M117-IO1	Wits Sample	17	Yes	Right	*Ranidae*	*Amnirana*	*indet.*	M1
18-IO1	SWK_M118-IO1	Wits Sample	18	No	Left	*Pyxicephalidae*	*Amietia*	*indet.*	M1
22-IO1	SWK_M122-IO1	Wits Sample	22	Yes	Left	*Ranidae*	*Amnirana*	*indet.*	M1
22-IO2	SWK_M122-IO2	Wits Sample	22	Yes	Right	*Pipidae*	*Xenopus*	*indet.*	M1
23-IO1	SWK_M123-IO1	Wits Sample	23	Yes	Right	*Ranidae*	*Amnirana*	*indet.*	M1
26-IO1	SWK_M126-IO1	Wits Sample	26	Yes	Left	*Ranidae*	*Amnirana*	*indet.*	M1
26-IO2	SWK_M126-IO2	Wits Sample	26	No	NA	*Pyxicephalidae*	*Tomopterna*	*indet.*	M1
26-IO3	SWK_M126-IO3	Wits Sample	26	No	NA	*Pyxicephalidae*	*Tomopterna*	*indet.*	M1
27-IO1	SWK_M127-IO1	Wits Sample	27	No	NA	*Ranidae*	*Amnirana*	*indet.*	M1
28-IO1	SWK_M128-IO1	Wits Sample	28	Yes	Left	*Ranidae*	*Amnirana*	*indet.*	M1
32-IO1	SWK_M132-IO1	Wits Sample	32	No	NA	*Ranidae*	*Amnirana*	*indet.*	M1
38-IO1	SWK_M138-IO1	Wits Sample	38	No	NA	*Pyxicephalidae*	*Tomopterna*	*tandyi*	M1
41-IO1	SWK_M141-IO1	Wits Sample	41	Yes	Left	*Pipidae*	*Xenopus*	*indet.*	M1
43-IO1	SWK_M143-IO1	Wits Sample	43	No	NA	*Pipidae*	*Xenopus*	*indet.*	M1
43-IO2	SWK_M143-IO2	Wits Sample	43	No	NA	*Pipidae*	*Xenopus*	*indet.*	M1
45-IO1	SWK_M145-IO1	Wits Sample	45	No	NA	*Ranidae*	*Amnirana*	*indet.*	M1
45-IO2	SWK_M145-IO2	Wits Sample	45	No	NA	*Ranidae*	*Amnirana*	*indet.*	M1
45-IO3	SWK_M145-IO3	Wits Sample	45	No	NA	*Pipidae*	*Xenopus*	*indet.*	M1
45-IO4	SWK_M145-IO4	Wits Sample	45	No	NA	*Pyxicephalidae*	*Tomopterna*	*indet.*	M1
51-IO2	SWK_M151-IO2	Wits Sample	51	Yes	Left	*Pyxicephalidae*	*Tomopterna*	*tandyi*	M1
57-IO1	SWK_M157-IO1	Wits Sample	57	No	NA	*Ranidae*	*Amnirana*	*indet.*	M1
58-IO1	SWK_M158-IO1	Wits Sample	58	Yes	Left	*Pyxicephalidae*	*Strongylopus*	*indet.*	M1

58-IO2	SWK_M1 58-IO2	Wits Sample	58	No	NA	*Bufonidae*	*Indet.*	*indet.*	M1
60-IO1	SWK_M1 60-IO1	Wits Sample	60	No	NA	*Pyxicephalidae*	*Amietia*	*indet.*	M1
61-IO1	SWK_M1 61-IO1	Wits Sample	61	Yes	Right	*Pipidae*	*Xenopus*	*indet.*	M1
61-IO2	SWK_M1 61-IO2	Wits Sample	61	No	NA	*Ranidae*	*Amnirana*	*indet.*	M1
61-IO3	SWK_M1 61-IO3	Wits Sample	61	No	NA	*Ranidae*	*Amnirana*	*indet.*	M1
63-IO1	SWK_M1 63-IO1	Wits Sample	63	No	NA	*Pyxicephalidae*	*Strongylopus*	*indet.*	M1
63-IO2	SWK_M1 63-IO2	Wits Sample	63	No	NA	*Pipidae*	*Xenopus*	*indet.*	M1
88-IO1	SWK_M1 88-IO1	Wits Sample	88	Yes	Left	*Ranidae*	*Amnirana*	*indet.*	M1
90-IO1	SWK_M1 90-IO1	Wits Sample	90	Yes	Right	*Ranidae*	*Amnirana*	*indet.*	M1
90-IO2	SWK_M1 90-IO2	Wits Sample	90	No	NA	*Ranidae*	*Amnirana*	*indet.*	M1
64-IO1	SWK_M2 64-IO1	Wits Sample	64	Yes	Right	*Pyxicephalidae*	*Tomopterna*	*tandyi*	M2
66-IO1	SWK_M2 66-IO1	Wits Sample	66	Yes	Right	*Ranidae*	*Amnirana*	*indet.*	M2
66-IO2	SWK_M2 66-IO2	Wits Sample	66	No	NA	*Pyxicephalidae*	*Tomopterna*	*indet.*	M2
66-IO3	SWK_M2 66-IO3	Wits Sample	66	Yes	Left	*Pipidae*	*Xenopus*	*indet.*	M2
66-IO4	SWK_M2 66-IO4	Wits Sample	66	No	NA	*Breviceptidae*	*Probreviceps*	*indet.*	M2
67-IO1	SWK_M3 67-IO1	Wits Sample	67	Yes	Right	*Pyxicephalidae*	*Strongylopus*	*indet.*	M3
67-IO2	SWK_M3 67-IO2	Wits Sample	67	Yes	Right	*Pyxicephalidae*	*Tomopterna*	*tandyi*	M3
68-IO1	SWK_M3 68-IO1	Wits Sample	68	No	NA	*Pyxicephalidae*	*Tomopterna*	*tandyi*	M3
68-IO2	SWK_M3 68-IO2	Wits Sample	68	No	NA	*Ranidae*	*Amnirana*	*indet.*	M3
68-IO3	SWK_M3 68-IO3	Wits Sample	68	Yes	Left	*Pyxicephalidae*	*Tomopterna*	*tandyi*	M3
68-IO4	SWK_M3 68-IO4	Wits Sample	68	No	NA	*Pyxicephalidae*	*Tomopterna*	*indet.*	M3
69-IO1	SWK_M3 69-IO1	Wits Sample	69	Yes	Right	*Pyxicephalidae*	*Tomopterna*	*tandyi*	M3
69-IO2	SWK_M3 69-IO2	Wits Sample	69	No	NA	*Pyxicephalidae*	*Amietia*	*indet.*	M3
70-IO1	SWK_M3 70-IO1	Wits Sample	70	No	NA	*Pyxicephalidae*	*Tomopterna*	*indet.*	M3
71-IO2	SWK_M3 71-IO2	Wits Sample	71	Yes	Left	*Pipidae*	*Xenopus*	*indet.*	M3
73-IO1	SWK_M3 73-IO1	Wits Sample	73	No	NA	*Pipidae*	*Xenopus*	*indet.*	M3
73-IO2	SWK_M3 73-IO2	Wits Sample	73	No	NA	*Pyxicephalidae*	*Tomopterna*	*indet.*	M3
74-IO1	SWK_M3 74-IO1	Wits Sample	74	No	NA	*Pyxicephalidae*	*Tomopterna*	*krugerensis*	M3
74-IO2	SWK_M3 74-IO2	Wits Sample	74	No	NA	*Pyxicephalidae*	*Tomopterna*	*indet.*	M3
75-IO1	SWK_M3 75-IO1	Wits Sample	75	No	NA	*Pyxicephalidae*	*Tomopterna*	*delalandii*	M3
75-IO2	SWK_M3 75-IO2	Wits Sample	75	Yes	Left	*Pyxicephalidae*	*Tomopterna*	*tandyi*	M3
76-IO1	SWK_M3 76-IO1	Wits Sample	76	No	NA	*Pyxicephalidae*	*Tomopterna*	*tandyi*	M3
76-IO2	SWK_M3 76-IO2	Wits Sample	76	No	NA	*Pyxicephalidae*	*Tomopterna*	*tandyi*	M3
76-IO3	SWK_M3 76-IO3	Wits Sample	76	No	NA	*Pyxicephalidae*	*Tomopterna*	*indet.*	M3
77-IO1	SWK_M3 77-IO1	Wits Sample	77	No	NA	*Pyxicephalidae*	*Tomopterna*	*indet.*	M3
77-IO2	SWK_M3 77-IO2	Wits Sample	77	Yes	Right	*Pyxicephalidae*	*Tomopterna*	*tandyi*	M3

77-IO3	SWK_M3 77-IO3	Wits Sample	77	No	NA	*Ranidae*	*Amnirana*	*indet.*	M3
77-IO4	SWK_M3 77-IO4	Wits Sample	77	No	NA	*Pyxicephalidae*	*Tomopterna*	*tandyi*	M3
77-IO5	SWK_M3 77-IO5	Wits Sample	77	Yes	Left	*Pyxicephalidae*	*Tomopterna*	*delalandii*	M3
77-IO6	SWK_M3 77-IO6	Wits Sample	77	No	NA	*Ranidae*	*Amnirana*	*indet.*	M3
77-IO7	SWK_M3 77-IO7	Wits Sample	77	No	NA	*Pyxicephalidae*	*Tomopterna*	*indet.*	M3
80-IO1	SWK_M3 80-IO1	Wits Sample	80	No	NA	*Pyxicephalidae*	*Strongylopus*	*indet.*	M3
80-IO2	SWK_M3 80-IO2	Wits Sample	80	No	NA	*Ranidae*	*Amnirana*	*indet.*	M3
80-IO3	SWK_M3 80-IO3	Wits Sample	80	Yes	Right	*Pyxicephalidae*	*Tomopterna*	*delalandii*	M3
80-IO4	SWK_M3 80-IO4	Wits Sample	80	No	NA	*Pyxicephalidae*	*Tomopterna*	*tandyi*	M3
82-IO1	SWK_M3 82-IO1	Wits Sample	82	Yes	Right	*Pipidae*	*Xenopus*	*indet.*	M3
83-IO1	SWK_M3 83-IO1	Wits Sample	83	No	NA	*Ranidae*	*Amnirana*	*indet.*	M3
84-IO1	SWK_M3 84-IO1	Wits Sample	84	Yes	Right	*Ranidae*	*Amnirana*	*indet.*	M3
86-IO1	SWK_M3 86-IO1	Wits Sample	86	No	NA	*Pyxicephalidae*	*Tomopterna*	*indet.*	M3
87-I10	SWK_M3 87-I10	Wits Sample	87	No	NA	*Pyxicephalidae*	*Tomopterna*	*indet.*	M3
87-IO1	SWK_M3 87-IO1	Wits Sample	87	No	NA	*Pyxicephalidae*	*Tomopterna*	*tandyi*	M3
87-IO2	SWK_M3 87-IO2	Wits Sample	87	Yes	Right	*Ranidae*	*Amnirana*	*indet.*	M3
87-IO3	SWK_M3 87-IO3	Wits Sample	87	No	NA	*Pyxicephalidae*	*Tomopterna*	*indet.*	M3
87-IO4	SWK_M3 87-IO4	Wits Sample	87	No	NA	*Pyxicephalidae*	*Tomopterna*	*indet.*	M3
87-IO5	SWK_M3 87-IO5	Wits Sample	87	No	NA	*Pyxicephalidae*	*Tomopterna*	*indet.*	M3
87-IO6	SWK_M3 87-IO6	Wits Sample	87	No	NA	*Ranidae*	*Amnirana*	*indet.*	M3
87-IO8	SWK_M3 87-IO8	Wits Sample	87	Yes	Left	*Pyxicephalidae*	*Tomopterna*	*tandyi*	M3

Appendix C

Table C1. *Results of the Measurements of Neck Width, Acetabular Breadth, and VSA*

Family	Genus	Species	Specimen number	Neck width (mm)	Acetabular Breadth (mm)	VSA (°)	Source of Data
Pyxicephalidae	*Strongylopus*	*Strongylopus springbokensis*	TM66787	1,41	1,57	138,08	Matthews *et al.* (2019)
Pyxicephalidae	*Tomopterna*	*Tomopterna delalandii*	ZM046810	1,45	2,08	110,42	Matthews *et al.* (2019)
Pyxicephalidae	*Strongylopus*	*Strongylopus grayii*	CAS211614	1,5	1,7	130,4	Dr Thalassa Matthews
Pyxicephalidae	*Tomopterna*	*Tomopterna tandyi*	ZM052343	1,61	2,63	113,16	Matthews *et al.* (2019)
Ranidae	*Amnirana*	*Amnirana albolabris*	CAS202204	1,76368	1,95718	117,0719	Matthews *et al.* (2019)
Pyxicephalidae	*Tomopterna*	*Tomopterna krugerensis*	TM061058	1,81	2,12	122,58	Matthews *et al.* (2019)
Ranidae	*Amnirana*	*Amnirana indet.*	SWK_M1 26-IO1	1,87	1,81	123,9	This study
Pyxicephalidae	*Strongylopus*	*Strongylopus indet.*	SWK_M1 58-IO1	1,89	2,04	121,2	This study
Ranidae	*Amnirana*	*Amnirana indet.*	SWK_M1 28-IO1	1,9	2,33	134,7	This study
Pyxicephalidae	*Strongylopus*	*Strongylopus indet.*	SWK_M3 67-IO1	1,94	2,11	131,9	This study
Ranidae	*Amnirana*	*Amnirana indet.*	SWK_M1 17-IO1	2,01	2,24	130	This study
Ranidae	*Amnirana*	*Amnirana indet.*	SWK_M1 88-IO1	2,1	2,16	113,6	This study
Ranidae	*Amnirana*	*Amnirana indet.*	SWK_M1 07-IO1	2,2	2,29	98	This study
Pyxicephalidae	*Tomopterna*	*Tomopterna tandyi*	SWK_M3 68-IO3	2,24	2,24	105,8	This study
Pyxicephalidae	*Tomopterna*	*Tomopterna tandyi*	SWK_M1 09-IO1	2,36	2,3	110,5	This study
Pyxicephalidae	*Tomopterna*	*Tomopterna tandyi*	SWK_M3 67-IO2	2,43	2,62	126	This study
Pyxicephalidae	*Tomopterna*	*Tomopterna delalandii*	SWK_M3 80-IO3	2,44	2,47	128,1	This study
Pyxicephalidae	*Tomopterna*	*Tomopterna tandyi*	SWK_M3 87-IO8	2,44	2,35	113,2	This study
Ranidae	*Amnirana*	*Amnirana darlingi*	ZM18179	2,44979	2,30117	130,2137	Matthews *et al.* (2019)
Pyxicephalidae	*Tomopterna*	*Tomopterna delalandii*	SWK_M3 77-IO5	2,45	2,29	133	This study
Pyxicephalidae	*Tomopterna*	*Tomopterna tandyi*	SWK_M2 64-IO1	2,48	2,38	103,6	This study
Pyxicephalidae	*Tomopterna*	*Tomopterna tandyi*	SWK_M3 77-IO2	2,48	2,53	146,5	This study
Pyxicephalidae	*Tomopterna*	*Tomopterna tandyi*	SWK_M3 69-IO1	2,58	2,44	122,5	This study
Pyxicephalidae	*Tomopterna*	*Tomopterna tandyi*	SWK_M3 75-IO2	2,73	2,72	112,8	This study

Ranidae	*Amnirana*	*Amnirana indet.*	SWK_M2 66-IO1	2,73	3,13	115,5	This study
Ranidae	*Amnirana*	*Amnirana indet.*	SWK_M3 84-IO1	2,84	2,57	125,4	This study
Ranidae	*Amnirana*	*Amnirana indet.*	SWK_M1 23-IO1	3,22	3,57	132,7	This study
Ranidae	*Amnirana*	*Amnirana indet.*	SWK_M3 87-IO2	3,24	3,37	125	This study
Pyxicephalidae	*Tomopterna*	*Tomopterna tandyi*	SWK_M1 51-IO2	3,25	3,15	120,8	This study
Ranidae	*Amnirana*	*Amnirana indet.*	SWK_M1 22-IO1	3,4	3,58	139,4	This study
Ranidae	*Amnirana*	*Amnirana indet.*	SWK_M1 90-IO1	3,47	3,3	114,3	This study

Appendix D

Table D1. *Interlandmark Distances Measurements*

Family	Genus	Species	Specimen Tag	Distance 1 to 2	Distance 2 to 3	Distance 3 to 4	Distance 4 to 5	Distance 5 to 7	Distance 7 to 8	Distance 8 to 9	Distance 9 to 1	Distance 9 to 6	Distance 6 to 2	Distance 6 to 1	Distance 2 to 9
Ranidae	*Amnirana*	*Amnirana indet.*	SWK_M1 17-IO1	0,962615463	1,270637226	1,810958814	0,769499638	2,076457591	1,506160718	1,260297615	0,866487516	1,374566053	1,638761571	1,246850824	1,796870286
Ranidae	*Amnirana*	*Amnirana indet.*	SWK_M1 22-IO1	1,588335252	2,763474342	3,008250098	1,32626336	3,651689965	2,131052551	1,529719178	1,747804215	3,002361278	2,502019246	2,393572827	3,265896564
Ranidae	*Amnirana*	*Amnirana indet.*	SWK_M1 23-IO1	1,847138984	1,447948095	3,811183551	1,560809517	4,884439411	2,027808067	1,137291828	1,69273444	3,0508471	2,149523875	2,371887237	3,35445386
Ranidae	*Amnirana*	*Amnirana indet.*	SWK_M1 26-IO1	0,841765628	0,955276292	1,861925745	0,683666195	2,31337218	1,066230724	0,607936862	0,818984661	1,324661492	1,292843639	1,132961864	1,630938395
Ranidae	*Amnirana*	*Amnirana indet.*	SWK_M1 28-IO1	1,129910644	1,254971262	1,924442701	0,650337968	2,13291928	1,368042477	0,671456195	1,297780695	1,642986766	1,376972112	1,274242214	2,260374564
Ranidae	*Amnirana*	*Amnirana indet.*	SWK_M1 07-IO1	1,225404027	1,727098974	1,945440098	0,894596162	2,357021791	1,478150146	0,743466996	1,426251237	2,189193086	1,533863541	1,668089143	2,464868675
Ranidae	*Amnirana*	*Amnirana indet.*	SWK_M2 66-IO1	1,488080596	1,85072547	2,004560678	1,075023277	2,509903094	2,66815711	1,858825478	1,777311199	2,553482221	2,339258611	2,015193222	3,128869975
Ranidae	*Amnirana*	*Amnirana indet.*	SWK_M1 88-IO1	0,994998928	1,263039491	2,213363308	0,739103293	2,646749608	1,708440514	1,384989243	0,991496104	1,413853582	1,456692225	1,173234815	1,935008072
Ranidae	*Amnirana*	*Amnirana indet.*	SWK_M1 90-IO1	1,726495286	1,709329906	2,762784236	1,343259299	3,574717456	2,084040738	1,358892945	1,605675524	2,544361701	2,253901622	1,735795923	3,248188413
Pyxicephalidae	*Tomopterna*	*Tomopterna tandyi*	SWK_M2 64-IO1	1,242512888	1,666701709	1,932756425	1,385995754	2,481119648	1,699767531	1,16493514	1,294732455	1,804152073	1,857787601	1,362707415	2,482880179
Pyxicephalidae	*Tomopterna*	*Tomopterna tandyi*	SWK_M3 67-IO2	1,403712274	1,530331951	2,305433312	1,387887452	2,542969923	1,925680893	1,089089478	1,249760207	1,823147794	1,568910623	1,410700857	2,519980165
Pyxicephalidae	*Tomopterna*	*Tomopterna tandyi*	SWK_M3 68-IO3	0,978123995	1,569339033	3,059442291	1,212631583	3,313972573	1,965379437	1,104504798	1,240225246	1,721021553	1,396765991	1,129840382	2,063811627
Pyxicephalidae	*Tomopterna*	*Tomopterna tandyi*	SWK_M3 69-IO1	1,004704725	1,364259443	2,530347042	1,33856618	2,635018125	2,026840141	1,04918968	1,527985533	1,916741548	1,706181286	1,303561482	2,495591198
Pyxicephalidae	*Tomopterna*	*Tomopterna tandyi*	SWK_M3 75-IO2	1,311644823	1,620478845	3,22706125	1,434231873	3,865520511	2,171552551	1,547028566	1,366729645	2,045709002	1,642995224	1,325217975	2,630514899
Pyxicephalidae	*Tomopterna*	*Tomopterna tandyi*	SWK_M3 77-IO2	1,175115156	1,496508791	1,952950127	1,277271803	2,281789807	1,87407899	1,311801369	1,214170525	1,717749684	1,601932361	1,440677405	2,273930121
Pyxicephalidae	*Tomopterna*	*Tomopterna delalandii*	SWK_M3 77-IO5	1,286953707	1,327052289	2,24882436	1,236087551	2,483690099	1,595890197	0,986610711	1,263603062	1,651677917	1,701117661	1,217535737	2,4766293
Pyxicephalidae	*Tomopterna*	*Tomopterna delalandii*	SWK_M3 80-IO3	1,20386759	1,592013591	2,190115862	1,243747561	2,134352554	1,750727677	1,122552212	1,22622059	1,747811315	1,805625734	1,35180351	2,377714062
Pyxicephalidae	*Tomopterna*	*Tomopterna tandyi*	SWK_M1 09-IO1	1,116004466	1,307442517	2,406990486	1,330977668	2,408852382	1,474105719	0,698287274	1,166437377	1,770425732	1,404047113	1,272707872	2,215551783
Pyxicephalidae	*Tomopterna*	*Tomopterna tandyi*	SWK_M1 51-IO2	1,427156852	2,186947289	2,195912281	1,701916894	2,529166139	1,815323711	0,611822006	1,524006394	2,036062575	2,001949415	1,492538659	2,842835517

Appendix E

Table E1. *Procrustes Corrected Interlandmark Distances Measurements*

Family	Genus	Species	Specimen Tag	Distance 1 to 2	Distance 2 to 3	Distance 3 to 4	Distance 4 to 5	Distance 5 to 7	Distance 7 to 8	Distance 8 to 9	Distance 9 to 1	Distance 9 to 6	Distance 6 to 2	Distance 6 to 1	Distance 2 to 9
Ranidae	*Amnirana*	*Amnirana indet.*	SWK_M1 07-IO1	0,250872101	0,353236649	0,399213709	0,183839741	0,48331735	0,3034801	0,153045	0,291818419	0,44768	0,314604	0,341064	0,504797
Ranidae	*Amnirana*	*Amnirana indet.*	SWK_M2 66-IO1	0,248474196	0,308770633	0,33855547	0,181140081	0,42238306	0,4426946	0,307565	0,29576401	0,42514	0,389335	0,335087	0,521699
Ranidae	*Amnirana*	*Amnirana indet.*	SWK_M1 17-IO1	0,227204349	0,299702078	0,427418051	0,182094695	0,490033289	0,3551801	0,295971	0,205016903	0,324746	0,385908	0,293901	0,424524
Ranidae	*Amnirana*	*Amnirana indet.*	SWK_M1 22-IO1	0,214703719	0,371375024	0,40644192	0,179675171	0,49281586	0,2884349	0,20622	0,236049426	0,404367	0,337304	0,322044	0,441206
Ranidae	*Amnirana*	*Amnirana indet.*	SWK_M1 23-IO1	0,232690656	0,186515887	0,477545722	0,197588217	0,61094986	0,2589166	0,145473	0,214660041	0,383714	0,273147	0,297839	0,424405
Ranidae	*Amnirana*	*Amnirana indet.*	SWK_M1 26-IO1	0,215577049	0,245292959	0,474631759	0,175609041	0,58872822	0,2736401	0,155956	0,210190719	0,338892	0,330348	0,289106	0,418024
Ranidae	*Amnirana*	*Amnirana indet.*	SWK_M1 28-IO1	0,260900209	0,290040483	0,444714449	0,150849571	0,4929888	0,3163747	0,155562	0,299558556	0,379619	0,318332	0,294357	0,522032
Ranidae	*Amnirana*	*Amnirana indet.*	SWK_M1 88-IO1	0,206447764	0,261988327	0,458018496	0,153946567	0,5473775	0,3536024	0,28559	0,205925325	0,293735	0,302056	0,243372	0,401663
Ranidae	*Amnirana*	*Amnirana indet.*	SWK_M1 90-IO1	0,258544186	0,256581502	0,414311411	0,201516407	0,53543367	0,3126451	0,203668	0,240742843	0,381217	0,337771	0,260307	0,486715
Pyxicephalidae	*Tomopterna*	*Tomopterna tandyi*	SWK_M2 64-IO1	0,235876118	0,316281988	0,367334115	0,262870507	0,47119445	0,3228008	0,221075	0,245829691	0,342649	0,352571	0,258801	0,471366
Pyxicephalidae	*Tomopterna*	*Tomopterna tandyi*	SWK_M1 51-IO2	0,246511141	0,376630138	0,380527195	0,292930697	0,43830109	0,3142511	0,107554	0,263249588	0,352252	0,345815	0,258343	0,491118
Pyxicephalidae	*Tomopterna*	*Tomopterna tandyi*	SWK_M1 09-IO1	0,224921383	0,263649461	0,484355053	0,267605662	0,48534607	0,2973483	0,141326	0,235126332	0,356706	0,28333	0,256536	0,446568
Pyxicephalidae	*Tomopterna*	*Tomopterna tandyi*	SWK_M3 67-IO2	0,255867795	0,279282839	0,420780558	0,25295511	0,46428364	0,3512737	0,198791	0,228221078	0,332915	0,286566	0,257538	0,459856
Pyxicephalidae	*Tomopterna*	*Tomopterna tandyi*	SWK_M3 68-IO3	0,165600581	0,263437519	0,510421419	0,203572724	0,55362292	0,3294872	0,185535	0,208749064	0,290289	0,236494	0,191467	0,348967
Pyxicephalidae	*Tomopterna*	*Tomopterna tandyi*	SWK_M3 69-IO1	0,178003652	0,241543032	0,44734769	0,236585812	0,46612574	0,3582654	0,185657	0,270053529	0,339084	0,301877	0,230753	0,441459
Pyxicephalidae	*Tomopterna*	*Tomopterna tandyi*	SWK_M3 75-IO2	0,193289252	0,238899905	0,473119043	0,210755604	0,56640237	0,3192084	0,226836	0,201496555	0,301439	0,242755	0,195898	0,387654
Pyxicephalidae	*Tomopterna*	*Tomopterna tandyi*	SWK_M3 77-IO2	0,231749167	0,295128685	0,385385218	0,251738985	0,45021959	0,3694469	0,258454	0,239486237	0,338876	0,315989	0,284064	0,448553
Pyxicephalidae	*Tomopterna*	*delalandii*	SWK_M3 77-IO5	0,25291437	0,261050239	0,442062422	0,242891498	0,48830851	0,3138669	0,194022	0,24841743	0,324891	0,334399	0,239529	0,486802
Pyxicephalidae	*Tomopterna*	*Tomopterna delalandii*	SWK_M3 80-IO3	0,235611426	0,311456769	0,426685976	0,243252313	0,41836416	0,3426534	0,219614	0,240082315	0,34227	0,353243	0,264663	0,465418

Appendix F

The below is a summary of the Normality Test Results for the Interlandmark and Procrustes Corrected Interlandmark Distances that had $p \leq 0.05$

Tomopterna interlandmark (n=10):

Distance 2 to 3: Shapiro Wilk (W=0.82, p=0.03)

Distance 4 to 5: Shapiro Wilk (W=0.84, p=0.04)

Distance 5 to 7: Shapiro Wilk (W=0.79, p=0.01), Anderson-Darling (A=1.02, p=0.006), Lilliefors (L=0.32, p=0.003)

Distance 9 to 1: Shapiro Wilk (W=0.83, p=0.04), Anderson-Darling (A=0.76, p=0.03)

Amnirana interlandmark (n=9):

Distance 3 to 4: Shapiro Wilk (W=0.81, p=0.03), Anderson-Darling (A=0.76, p=0.03)

Distance 5 to 7: Shapiro Wilk (W=0.83, p=0.04), Anderson-Darling (A=0.68, p=0.05), Lilliefors (L=0.27, p=0.05)

Tomopterna Procrustes Corrected interlandmark (n=10):

Distance 6 to 1: Lilliefors (L=0.27, p=0.05)

Distance 2 to 9: Lilliefors (L=0.27, p=0.04)

Amnirana Procrustes Corrected interlandmark (n=9):

Distance 8 to 9: Shapiro Wilk (W=0.83, p=0.04), Anderson-Darling (A=0.69, p=0.05)

Distance 9 to 1: Shapiro Wilk (W=0.82, p=0.03), Anderson-Darling (A=0.7, p=0.04)